UNCLASSIFIED

AD NUMBER

ADB955538

NEW LIMITATION CHANGE

TO

Approved for public release, distribution unlimited

FROM

Distribution limited to DoD only; Critical Technology; 26 Mar 84. Other requests must be referred to Naval Research Lab., Code 1221, Washington, DC 20375.

AUTHORITY

Naval Research Laboratory, Technical Library, Research Reports Section Notice, dtd October 10, 2000.

THIS PAGE IS UNCLASSIFIED

ATI 4267

UNANNOUNCED

AD B955588

NAVAL RESEARCH LABORATORY
REPORT NO. R-3030

UPPER ATMOSPHERE RESEARCH REPORT No. II

By

H. E. Newell, Jr. and J. W. Siry

DTIC
ELECTE
APR 13 1984
S D
A

DTIC FILE COPY

NAVY DEPARTMENT
OFFICE OF NAVAL RESEARCH
NAVAL RESEARCH LABORATORY
WASHINGTON 20, D. C.

84 04 12 056

Navy Department - Office of Naval Research

NAVAL RESEARCH LABORATORY
Washington, D. C. 20375
Code 1221

* * * * * * * * *

RADIO DIVISION I
ROCKET-SONDE RESEARCH SECTION

30 December 1946

DISTRIBUTION STATEMENT E: Distribution limited to DoD only: Other requests must be referred to: CT. 26 MAR 1984

UPPER ATMOSPHERE RESEARCH REPORT NO. II

The report consists of a series of articles by various authors on research connected with the second cycle of V-2 firings.

Report R-3030

DTIC ELECTE APR 13 1984 S D A

Compiled and Edited by

H. E. Newell, Jr. and J. W. Siry

* * * * * * * * *

Approved by:

Dr. E. H. Krause, Head
Rocket-Sonde Research Section
Dr. J. M. Miller, Superintendent
Radio Division I

Commodore H. A. Schade, USN
Director, Naval Research Laboratory

Preliminary Pages . . .	a-j
Numbered Pages.	149
Number of Figures . . .	72
Distribution.	k-o

TABLE OF CONTENTS

	PAGE
ABSTRACT	j
INTRODUCTION	1
CHAPTER I. THE SECOND CYCLE OF V-2 FIRINGS - H. E. Newell, Jr.	3
CHAPTER II. INSTALLATIONS FOR THE OCTOBER 10 FIRING	10
A. General Description of Installations in the V-2 - J. T. Mengel	10
1. Introduction.	10
2. Instrumentation	11
3. Locations of Installations	12
4. Miscellaneous Installations	13
B. The Program Timer - C. C. Rockwood	22
CHAPTER III. TELEMETERING FROM THE V-2 - C. H. Hoeppner, J. R. Kauke, R. E. Taylor, and K. M. Uglow . .	26
A. Improvements in the V-2 Telemetering System . . .	26
1. Introduction.	26
2. Overall Improvements in the Telemetering System	26
3. Improvements in the Transmitter	28
4. The Transmitting Antennas	28
5. Receiving Antennas	37
6. Telemetering Receivers	40
B. The Study of Rocket Performance through the Use of Telemetering	42
CHAPTER IV. UPPER ATMOSPHERE EXPERIMENTS CONDUCTED IN THE V-2	44
A. Solar Spectroscopy - F. S. Johnson, J. J. Oberly, C. V. Strain and R. Tousey	44
1. Introduction.	44
2. Relocation of the Spectrograph	44
3. Changes in the Spectrograph	49
4. Calibration of the Spectrograph	53

TABLE OF CONTENTS (Cont'd)

	PAGE
5. Electrical Circuits	53
6. Preparation for Flight	53
7. Flight and Recovery	55
8. Time and Altitude Data	55
9. Film Development	55
10. Preliminary Results	55
Solar Ultraviolet Spectrum to 88 Kilometers - W. A. Baum, F. S. Johnson, J. J. Oberly, C. C. Rockwood, C. V. Strain, and R. Tousey	56
11. Acknowledgment	57
B. Pressure and Temperature Measurements at High Altitudes - N. R. Best, E. Durand and R. J. Havens .	58
1. Introduction.	58
2. General Procedures	58
3. Gage Locations.	60
4. Pressure Measurements	60
5. General Discussion of the Pressure Data from the October 10 Experiments	69
C. The Cosmic Ray Experiment - S. E. Golian, E. H. Krause, and G. J. Perlow	79
Additional Cosmic Ray Measurements With the V-2 Rocket	79
D. The Cosmic Ray Auxiliary Electronics and Recorder - B. Howland and M. L. Kuder	82
E. The Ionosphere Experiment - J. F. Clark, T. M. Moore, and J. C. Seddon	91
F. The Ejection and Recovery of Instruments - T. A. Bergstralh, M. W. Rosen, and C. H. Smith. .	100
G. The Biological Experiments - T. M. Moore	112
CHAPTER V. THEORETICAL DISCUSSIONS.	117
A. Determination of Ambient Temperatures and Pressures in the Atmosphere from Pressure Measurements Made at Various Points on the Surface of a Rocket - M. A. Garstens	117

TABLE OF CONTENTS (Cont'd)

	PAGE
B. Geometric Factors Underlying Coincidence Counting with Geiger Counters - Homer E. Newell, Jr. and Eleanor Pressly	130
1. Introduction	130
2. The Case of Identical Counters	130
3. Counters of Different Sizes.	137
4. Counting Rates in a Single Counter . . .	141
5. Summary	141
CHAPTER VI. FUTURE RESEARCH - E. H. Krause	145
APPENDIX. TABLE OF CRITICAL VALUES	148

Accession For
NTIS GRA&I
DTIC TAB
Unannounced
Justification
Letter on file
Distribution/
Availability Codes
Avail and/or
Dist Special
E-4

DTIC COPY INSPECTED 3

LIST OF FIGURES

CHAPTER I

Page

1. 10 October trajectory information deduced from experimental data. 8
2. Warhead recovered from the October 10 flight. 9

CHAPTER II

Section A

1. V-2 equipped for upper atmosphere research. 14
2. Cosmic ray counter telescope installed in warhead 15
3. Warhead installation showing cosmic ray electronics (top), Atmospheric physics commutator, and ionosphere transmitter (bottom). 16
4. Cosmic ray auxiliary electronics and dynamotors 17
5. Ionosphere antenna tuning box installation. 18
6. Overall rocket wiring diagram 19
7. Warhead showing base counterweight. 20
8. Warhead showing counterweight and storage battery mounts. . . 21

Section B

1. The program timer 23
2. Timer circuits. 25

CHAPTER III

Section A

1. Dipole transmitting antenna 31
2. Production model of dipole and mount. 33
3. Three phase circularly polarized transmitting antenna 34
4. Three phase circularly polarized transmitting antenna mounted in bakelite section of V-2 fin. 35
5. Circuit diagram of three phase circularly polarized transmitting antenna. 36
6. Ground station antenna assembly 39

CHAPTER IV

Section A

1. Spectrograph fairing shield 46

LIST OF FIGURES (Cont'd)

Ch. IV, Sect. A (Cont'd)

		Page
2.	Spectrograph mounted in fin.	47
3.	V-2 tail assembly showing spectrograph fairing shield and balancing fairing shield	48
4.	Spectrograms obtained in the October 10 firing	50
5.	Spectrograph housing as seen from the extension of fin II. .	51
6.	Reflectivity of polished quarts crystal and evaporated aluminum	52
7.	Spectrograph after recovery.	54

Section B

1.	Pressure and temperature gauge locations	61
2.	Bellows gauge.	62
3.	Pressure vs. altitude as measured by bellows gauge	64
4.	Nose chamber gauges.	65
5.	Tail section gauges.	66
6.	Tungsten Pirani gauge, tail mount	68
7.	Pressure vs. altitude as measured by tail tungsten pirani gauge.	70
8.	Pressure vs. altitude as measured by nose tungsten pirani gauge.	71
9.	Nose cone temperature gauge.	72
10.	Platinum resistance temperature gauge.	73
11.	Thermistor mount	75

Section C

1.	Cosmic ray intensity vs. altitude.	81

Section D

1.	The 10 channel recorder assembled.	83
2.	The 10 channel recorder showing the neon lamps and housing .	85
3.	The 10 channel recorder with light covers removed.	86
4.	Optical system of 16 mm. recorder (10 channel)	87
5.	Sample 16 mm. film record taken with 10 channel recorder . .	88
6.	Electronic intelligence translating circuit.	90

Section E

1.	Cameras mounted around the venturi as seen from outside the V-2.	94
2.	Cameras mounted around the venturi opening as seen from inside the V-2 before assembly	95
3.	Midsection camera.	96

LIST OF FIGURES (Cont'd)

Ch. IV, Sect. E (Cont'd)

		Page
4.	Venturi camera installation showing plastic camera motor covers.	97
5.	Tail ring as found after impact	98
6.	Two tail ring cameras after impact.	99

Section F

1.	Recovery container.	101
2.	Recovery container partially disassembled showing the two parachutes and the breakaway cover.	102
3.	Timer chassis	104
4.	Ejection well and solenoid attached to door of control chamber	105
5.	Recovery apparatus installed in the October 10 rocket	106
6.	Velocity vs. time calculated for a 30.5 cm. (1 ft.) cube weighing 18.1 kg. (40 lbs.) assuming supersonic and subsonic drag coefficients of 2.0 and 1.2 respectively	107
7.	Velocity vs. time calculated for a 30.5 cm. (1 ft.) cube weighing 18.1 kg. (40 lbs.) assuming supersonic and subsonic drag coefficients of 4.0 and 2.4 respectively	108
8.	Altitude vs. time calculated for a 30.5 cm. (1 ft.) cube weighing 18.1 kg. (40 lbs.) assuming supersonic and subsonic drag coefficients of 2.0 and 1.2 respectively	110

Section G

1.	After portion of the V-2 as found in the impact area.	113
2.	Various types of seed container	114
3.	Locations of seed containers.	116

CHAPTER V

Section A

1.	Comparison of the calculated surface pressures with the wind tunnel observations	118
2.	Plot of $\frac{P_1}{P_g}$ versus temperature in °K for 30° cone	120
3.	Pressure distribution along the V-2	122
4.	Pressure distribution along the V-2	123
5.	Ratios of the pressure at 2 and 6 calibres and at 2 and 3.5 calibres from the nose of the V-2 versus ambient temperature	124

LIST OF FIGURES (Cont'd)

Ch. V, Sect. A (Cont'd)

		Page
6.	Ratio of the pressure at the nose and at 6 calibres from the nose of the V-2 versus ambient temperature.	125
7.	Mach number versus altitude and time for 10 October firing. .	127

Section B

1.	Orthogonal projections of the counter arrays for the special case considered in the text	131
2.	Schematic drawing of tube cross section	133
3.	Figure showing the relation between the parameters α and β and spherical polar coordinates	133
4.	Drawing for obtaining the sine of the polar angle ϕ in terms of the parameters α and β	135
5.	Orthogonal projections of the counter arrays for the general case considered in the text	138

LIST OF TABLES

CHAPTER I

		Page
I.	Summary of the Second Cycle of V-2 Firings, 10 October through 21 November 1946	6
II.	October 10 Flight Data	7

CHAPTER IV

SECTION B.

Table of Gages Used on the October 10 Flight. 76

CHAPTER V

Section A.

I. Relative Error Tolerable in Measured Nose Pressure and Measured Surface Pressure to Attain Indicated Accuracy in Computed Ambient Pressure. 129

II. Relative Error Tolerable in Measured Surface Pressure to Attain Indicated Accuracies in Computed Ambient Temperatures 129

APPENDIX

Table of Critical Values. 149

ABSTRACT

This report continues the description of the upper atmosphere research conducted by the Naval Research Laboratory in connection with the V-2 firings being carried out by the Army at its White Sands Proving Ground. The discussions are primarily concerned with the second cycle of V-2 firings; but some of the articles have as their subject general considerations applying to the Rocket-Sonde Program as a whole. A review of the second cycle of V-2 firings, and in particular of the October 10 flight, is provided. The installations for that flight, and the improvements incorporated into the telemetering system, are described in detail. The results obtained in solar spectroscopy and in the pressure-temperature and cosmic ray experiments, are given. The cosmic ray auxiliary systems and the ionosphere, biological and recovery experiments are discussed. General theoretical discussions pertinent to the program and an outline of plans for future research are included.

UPPER ATMOSPHERE RESEARCH
REPORT NO. II

INTRODUCTION

On 10 October 1946, at the White Sands Proving Ground in New Mexico, the second V-2 to be instrumented by the Naval Research Laboratory for high altitude research, the 12th fired there by the Army, rose to a height in excess of 160 kilometers (100 miles) in what was a very successful flight. The experiments performed during the flight have provided an abundance of data on the upper atmosphere, on cosmic rays, and in solar spectroscopy. The following pages contain descriptions of the various experiments and rocket installations together with whatever information has been derived to date from analyses of the data. Analysis of the data continues and any further information will appear in later reports of this series.

The principal emphasis in the present report falls naturally upon the results of the October 10 firing, but there are also discussions of a general nature applying to the rocket sonde program as a whole. The history of the program was given in some detail in the first report*. The part of the Naval Research Laboratory in upper atmosphere research in general, and particularly in the V-2 program, was outlined there, along with a discussion of the V-2 Panel and its functions. Reference may be made to that report for such information.

Many features of the experimentation associated with the October 10 rocket are quite similar to those of the experiments performed on June 28. Advantage is taken of this fact to shorten the discussions of the present report by referring when convenient to the descriptions set forth in the first report, and outlining significant changes made for the October 10 flight.

The various chapters of this report contain a series of articles which cover the different fields and aspects of the high altitude research program. Chapter I provides a review of what may be referred to as the second cycle of V-2 firings, along with a detailed description of the October 10 flight. A general description of the rocket installations for October 10 appears in Chapter II. Telemetering is discussed in Chapter III. Section A of Chapter IV is on solar spectroscopy; Section B reviews the temperature and pressure measurements made from the V-2 on October 10; Sections C and D are given over to the cosmic ray experimentation; Section E covers the ionosphere experiment; Section F is devoted to a discussion of the ejection and recovery of instruments;

---

* Naval Research Laboratory Report No. R-2955 (1 October 1946).

and Section G contains a brief description of the biological experiments conducted for Harvard. Theoretical discussions appertaining to the upper atmosphere program appear in Chapter V, of which Section A is devoted to aerodynamic theory considerations underlying temperature and pressure measurements from a rocket, while Section B deals with some of the geometric factors involved in coincidence counting with Geiger counters. Plans for the future are reviewed in Chapter VI. Finally, the appendix contains a table of information which has been found useful.

CHAPTER I

THE SECOND CYCLE OF V-2 FIRINGS

by

H. E. Newell, Jr.

The V-2 missiles 12 through 15 comprise what may be referred to as the second cycle of firings at White Sands. The first eleven of the rockets were fired during the period from 15 March 1946 to 22 August 1946, with varying degrees of success and failure. The essential characteristics of the flights in the first cycle were tabulated in the first of this series of reports*. A similar tabulation for the second cycle appears in Table I at the end of this chapter. As indicated there, the Naval Research Laboratory was directly involved in the first of the four firings listed.

A glance at page 12 of the first report shows that of the last four firings in the first cycle, three were failures. For this reason, unusual care was taken by the General Electric Company in preparing the October 10 rocket. At the same time the Naval Research Laboratory was correspondingly careful in the construction, calibration, installation, and checking of equipment and instruments for the various upper atmosphere experiments. All of this painstaking prior to the flight apparently bore fruit. From many points of view, the October 10 firing was the best to date. The telemetering record from one station was unusually good. The maximum altitude of the rocket exceeded 160 kilometers (100 miles). Most of the experimental equipment functioned properly. A breakup of the missile occurred before impact, and many of the parts were found in only slightly damaged condition. The spectrograph, which was mounted in the tail, was recovered in good enough condition to be used again on a later flight, should that seem desirable. At the same time the spectrographic film was recovered, and upon development yielded good solar spectrograms for various altitudes up to 88.5 kilometers (55 miles). A number of the cameras which were attached to the rocket were found in fairly good shape, although, apparently due to violent shaking, turbulence, and shock waves, the film records obtained from the cameras were of little real value.

Along with the considerable success which attended the October 10 firing, there were, as one might expect in such an extensive undertaking, also some failures. The most unfortunate feature of the flight is the lack of good tracking information. For various reasons both the radio and optical tracking systems failed to provide adequate information about the rocket's trajectory and aspect. The lack of such data

---

* Naval Research Laboratory Report No. R-2955, pp. 11-12.

hampers considerably the analysis and interpretation of the data obtained from the various upper atmosphere experiments. In many cases it is impossible to make best use of the research data without adequate tracking information.

It has long been known that one source of difficulty in the performance of the ionosphere experiment is antenna failure. The design and development of efficient antennas specifically for the ionosphere are being pushed. In the meantime, attempts to make the most of available antennas continue. For the purpose of determining whether or not the failure of trailing wire antennas could be ascribed to their becoming interentangled, cameras were installed at various points on the tail and side of the October 10 rocket. Unfortunately, as the rocket rose, the longer (4.272Mc) antenna caught on the launching platform and was torn off. Until that time signals from both antennas were strong. Even with the one antenna missing, photographs of the whip motion of the remaining antenna might have furnished enough information to decide whether or not tangling of antennas was a probable cause of the signal failure experienced in previous attempts to carry through the ionosphere experiment. But, as mentioned earlier, the camera records revealed nothing.

The rocket, which was fired at about 3 minutes after the scheduled take off time of 11:00 A.M., MST, followed a steeper trajectory than usual. The customary 11° tilt program during the burning period was replaced by a 5° program, and indications are that the actual tilt was even smaller, not more than 3.5°. As a result of the unusual tilt program, the impact point was within 27 kilometers (17 miles) of the launching site.

Brennschluss appears to have occurred at 68 seconds after takeoff, when the rocket's altitude was about 40 kilometers (25 miles). At this time the V-2 had moved only 1.6 kilometers (1 mile) horizontally.

Estimates of the maximum altitude given by the optical and radar stations respectively are 164 and 171 kilometers (102 and 106 miles). There are, however, some indications from data provided by various of the upper atmosphere experiments that the peak of the trajectory was at an even greater altitude, perhaps as high as 187 kilometers (116 miles). These points are discussed in the ionosphere and the temperature-pressure articles below. The warhead blowoff was set on the timer for 330 seconds after launching. The radio control for blowoff was applied at about 335 seconds. All evidence indicates, however, that the actual breakup of the missile did not occur before 410 seconds after takeoff. Apparently the explosive fired at some time between 330 and 335 seconds after the beginning of flight, weakening the missile structure, and complete breakup occurred when the air forces became sufficiently great.

Due to the missile breakup the total time of flight was unusually long, apparently between 9 and 11 minutes.

An estimate of the trajectory based on these facts is shown in Fig. 1. The various parts of the missile were found strewn over a range of from 19 to 27 kilometers (12 to 17 miles) along a line running from the launching site at an angle of about 10.5° east of north.

The warhead was recovered. It had landed base down, and, therefore, did not bury itself in the sand. This is shown in Fig. 2. The venturi ring was found with five of the originally six attached cameras intact. It appears in Fig. 5 of Chapter IV, Section E. Most of the rocket engine was found in somewhat damaged condition as shown in Fig. 1 of Chapter IV, Section G. Portions of the tail fins were recovered, including that one which bore the spectrograph, which, as mentioned before, was almost entirely undamaged. The Daughter ejection container, which was set for release at 190 seconds after takeoff, and which contained seeds, cosmic ray film, half exposed film and a camera, was reported seen in descent, but to date has not been found. Some observers claim to have seen the Naval Research Laboratory's parachute ejection device falling, but as yet this also has not been recovered.

Table II summarizes the essential details of the October 10 flight.

TABLE I

SUMMARY OF THE SECOND CYCLE OF V-2 FIRINGS
10 OCTOBER THROUGH 21 NOVEMBER 1946.

Firing	Date	Research Agencies	Best Estimate of Altitude (kilometers)	Best Estimate of Altitude (miles)	Range (kilometers)	Range (miles)	Remarks
12	10 October 1946	Naval Research Laboratory	174	108	19-27	12-17	Except for poor tracking, the best flight to date.
13	24 October 1946	Applied Physics Laboratory	105	65	29	18	Short burning time (59 sec). Missile tumbled while falling.
14	7 November 1946	Princeton University.	0.39	0.24	8	5	Emergency cutoff applied at 39 sec. because missile headed in wrong direction. Cause of failure undetermined.
15	21 November 1946	Watson Laboraries University of Michigan.	101	63	19	12	Low altitude attributed to low motor efficiency.

TABLE II

OCTOBER 10 FLIGHT DATA

	According to tracking data (T) or calculations based on tracking data (C)	According to deductions from data obtained in various upper atmosphere experiments.
Maximum altitude	167 ± 3 kilometers (104 ± 2 miles) (T)	174 ± 3 kilometers (108 ± 2 miles) (pressure-temperature and ionosphere data).
Horizontal range	19 to 27 kilometers (12 to 17 miles)	
Total flight time	9 to 11 minutes (T)	
Time of flight until breakup		412 ± 3 seconds (pressure-temperature, ionosphere data, and telemetering).
Altitude at time of breakup		35 kilometers (22 miles) (approx.) (pressure-temperature, ionosphere, and telemetering).
Cutoff time	68 seconds (T)	
Cutoff altitude	40 kilometers (25 miles) (approx.) (T)	39.5 kilometers (24.5 miles) (approx.) (Pressure-temperature data).
Cutoff velocity	15.95 meters (5234 feet) per second (T)	1591 meters (5220 feet) per second (pressure-temperature data).
Tilt at cutoff	3.5° or less (T)	
Time of flight until peak was reached	227 seconds (C)	238 ± 2 seconds (pressure-temperature and ionosphere data).
Roll period		59 seconds (approx.) (ionosphere data) or 66 seconds (photocell data) or perhaps twice these figures.

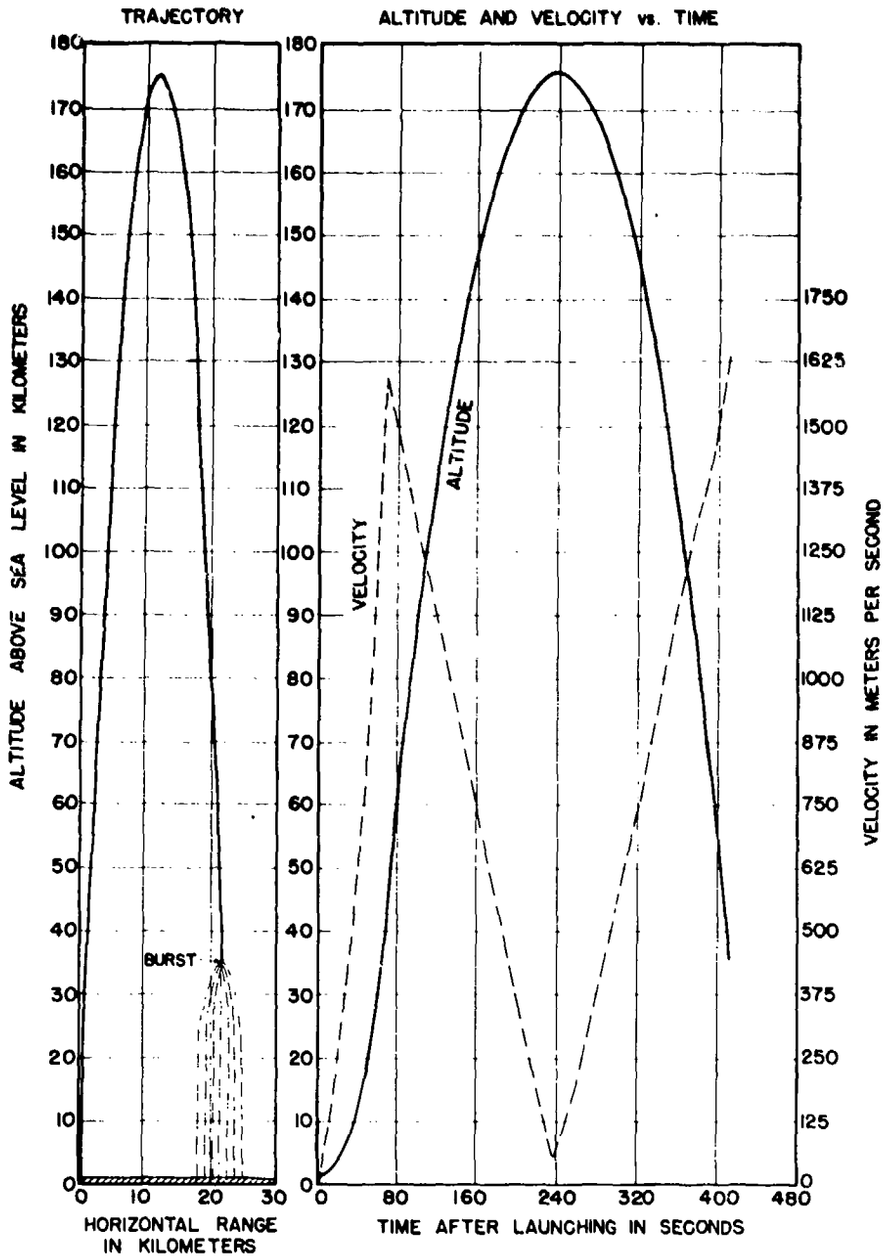

10 OCTOBER TRAJECTORY INFORMATION DEDUCED FROM EXPERIMENTAL DATA

CH. I FIG. 1

WARHEAD RECOVERED FROM THE OCTOBER 10 FLIGHT

CHAPTER II

INSTALLATIONS FOR THE OCTOBER 10 FIRING

A. General Description of Installations in the V-2

by

J. T. Mengel

1. Introduction. The Naval Research Laboratory's V-2 installation for the October 10 firing was similar to that for the June 28 firing described in Naval Research Laboratory Report R-2955. For an overall picture reference may be made to the earlier report. Certain alterations, additions, and refinements which were incorporated into the October 10 flight, should, however, be noted. The more important of these are the following:

(a) Storage batteries plus dynamotors were utilized for all plate power supplies in order to simplify control, decrease weight and volume, and to obtain a source of power, the exact power reserve of which was known. Dry batteries were used only for high voltage, low drain supplies requiring exceptionally close voltage regulation.

(b) All equipments, the recovery of which was essential for obtaining data, were mounted in the tail section. This change was prompted by the flight of July 30 for which the warhead was blown successfully with the result that the tail section came to earth slowly enough to allow recovery of suitably mounted apparatus.

(c) A photo-cell aspect indicator was included in the warhead in order to determine the attitude of the missile with reference to the sun and by this means to determine the rolling of the missile after power cut-off as a function of time.

(d) There was a camera recording unit consisting of ten 1/4 watt neon bulbs mounted by means of prisms in the field of a 16 mm gunsight camera so as to record the cosmic ray output pulses and two pressure-temperature outputs, the latter by means of voltage to frequency circuits. This unit was mounted in a block which was ejected from the missile at the top of its trajectory.

(e) Eight 16 mm gunsight cameras set to run consecutively in pairs for over five minutes were included for photographing the action of the trailing wire antennas during the ascent of the rocket.

(f) A consolidated timer unit consisting of a constant speed DC motor and multisection cams to actuate contacts was used to initiate the operation of the ejection mechanism, the successive starting of the 16 mm cameras, the film wind-up in the spectrograph, and the detonation of explosives at the base of the warhead.

(g) Two tail switches consisting of push-to-open double pole single throw switches were mounted in the tail fins so as to remain open while the missile was on the launching platform, but to close at takeoff.

(h) The small access door at the top of the warhead was altered to 3.2 mm (1/8 inch) thick cold rolled steel instead of 6.4 mm (1/4 inch) or thicker as originally cast.

2. Instrumentation. The following equipments were carried in the October 10 missile:

(a) Cosmic ray equipment, consisting of a ten counter telescope, main electronics, dynamotor, auxiliary electronics for driving the indicators in the recording camera, the recording camera, the photocell aspect indicator and high voltage battery. See Figs. 2 through 4.

(b) Ionosphere study equipment, consisting of a two frequency transmitter, two trailing wire antennas, and two tuning boxes for the antennas. The transmitter appears at the bottom of Fig. 3 and a tuning box installation is shown in Fig. 5.

(c) Pressure-temperature equipment, consisting of a mechanical commutator to divide each of two telemetering channels into 12 subchannels plus two calibration subchannels, and 12 temperature and 6 pressure measuring elements. The pressure-temperature installations appear in Fig. 1 of Chapter IV, Section B.

(d) Equipment for solar spectroscopy, consisting of a solar spectrograph capable of recording into the far ultraviolet region. See Fig. 2 of Chapter IV, Section A.

(e) An ejection mechanism, consisting of a 30.5 mm (1 foot) cube including the cosmic ray recording camera unit and

a special double parachute with time release for slowing the rate of the fall. This mechanism is illustrated in Figs. 1-5 of Chapter IV, Section F.

3. Locations of Installations. The locations of the experimental equipment in the missile were as follows:

(a) The nose tip contained two pressure measuring elements plus a platinum plated cone, which was in fact the extreme tip of the nose, for temperature measurements.

(b) The nose section, which housed the solar spectrograph on June 28, contained an element for measuring skin temperature.

(c) The top half of the warhead enclosed the cosmic ray telescope and aspect indicating device. The cosmic ray main electronics was mounted beneath the telescope at about the top level of the two large access doors.

(d) In the warhead between the large access doors were the ionosphere transmitter and the pressure-temperature commutator unit.

(e) At the base of the warhead there were the cosmic ray auxiliary electronics, a high voltage battery, a dynamotor, and three AN-3152 storage batteries.

(f) In quadrant I of the control chamber were located the telemetering junction box, telemetering transmitter, and doppler unit; quadrant IV contained an ejection mechanism, telemetering storage batteries, and the program timer; on doors of quadrants I and III there were six skin temperature measuring elements.

(g) At the midsection of the rocket were mounted two 16 mm gunsight cameras. One of these is shown in Fig. 3 of Chapter IV, Section E.

(h) The tail section held the spectrograph in fin II; one temperature and three pressure measuring elements just forward of fin I; six 16 mm gunsight cameras around the venturi ring as shown in Figs. 1, 2, and 4 of Chapter IV, Section E; two trailing wire antenna supports and two antenna tuning boxes one set on fin I, one set on fin III; two push-to-open switches on fin II for initiation of recorders and cameras at take-off and lock-in of the main power relays.

4. Miscellaneous Installations. The overall rocket wiring is shown in Fig. 6. This diagram shows the wiring through the midsection which was installed by the Army at White Sands, according to Naval Research Laboratory requirements. The diagram also shows the control chamber and tail section wiring required between all units.

Figs. 7 and 8 show the two counterweights added to the October 10 missile at White Sands. The base counterweight, made up of 39 mm (1.5 inch) of lead plus 13 mm (.5 inch) of steel as shown in Fig. 7, weighed 186 kilograms (410 pounds); the lead counterweight added inside the warhead weighed 41 kilograms (90 pounds). This brought the total weight of the warhead to about 900 kilograms (1,980 pounds), placing its center of gravity at about 38 cm (15 inches) from the base.

Explosives were attached to each of the four structural members holding the warhead mounting ring. A total of eight pounds of TNT was used, fused by primer cord from a single detonator timed from the Naval Research Laboratory program timer to go off at 330 seconds. The explosive could also be detonated by means of the ARW-17 emergency cutoff receiver and during the October 10 flight a detonation signal was transmitted to this receiver 335 seconds after takeoff. The rocket broke up at 410 seconds after takeoff; but, it is not known whether the detonation was initiated by the emergency cutoff receiver or the program timer.

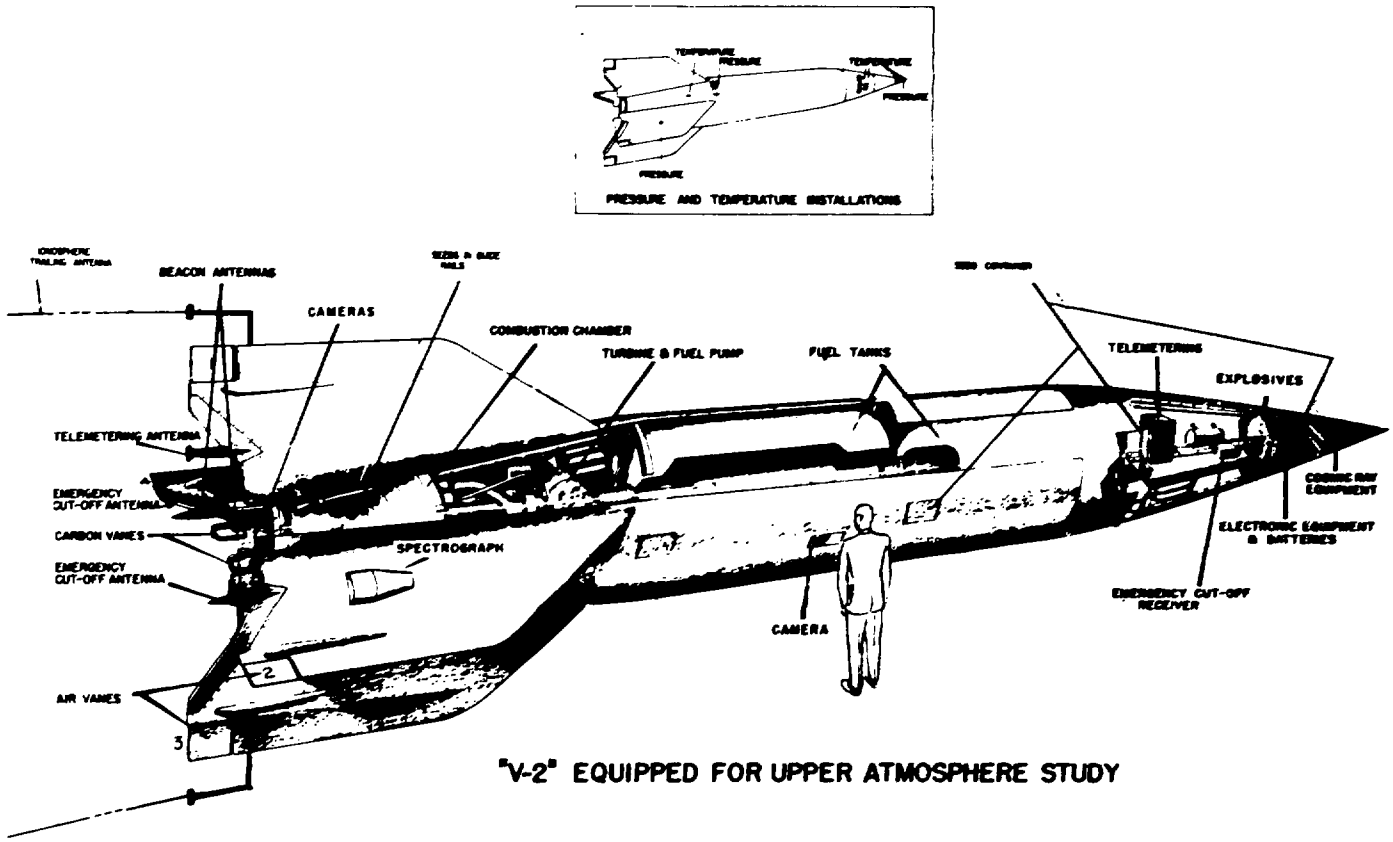

"V-2" EQUIPPED FOR UPPER ATMOSPHERE STUDY

CH. II SEC. A FIG 1

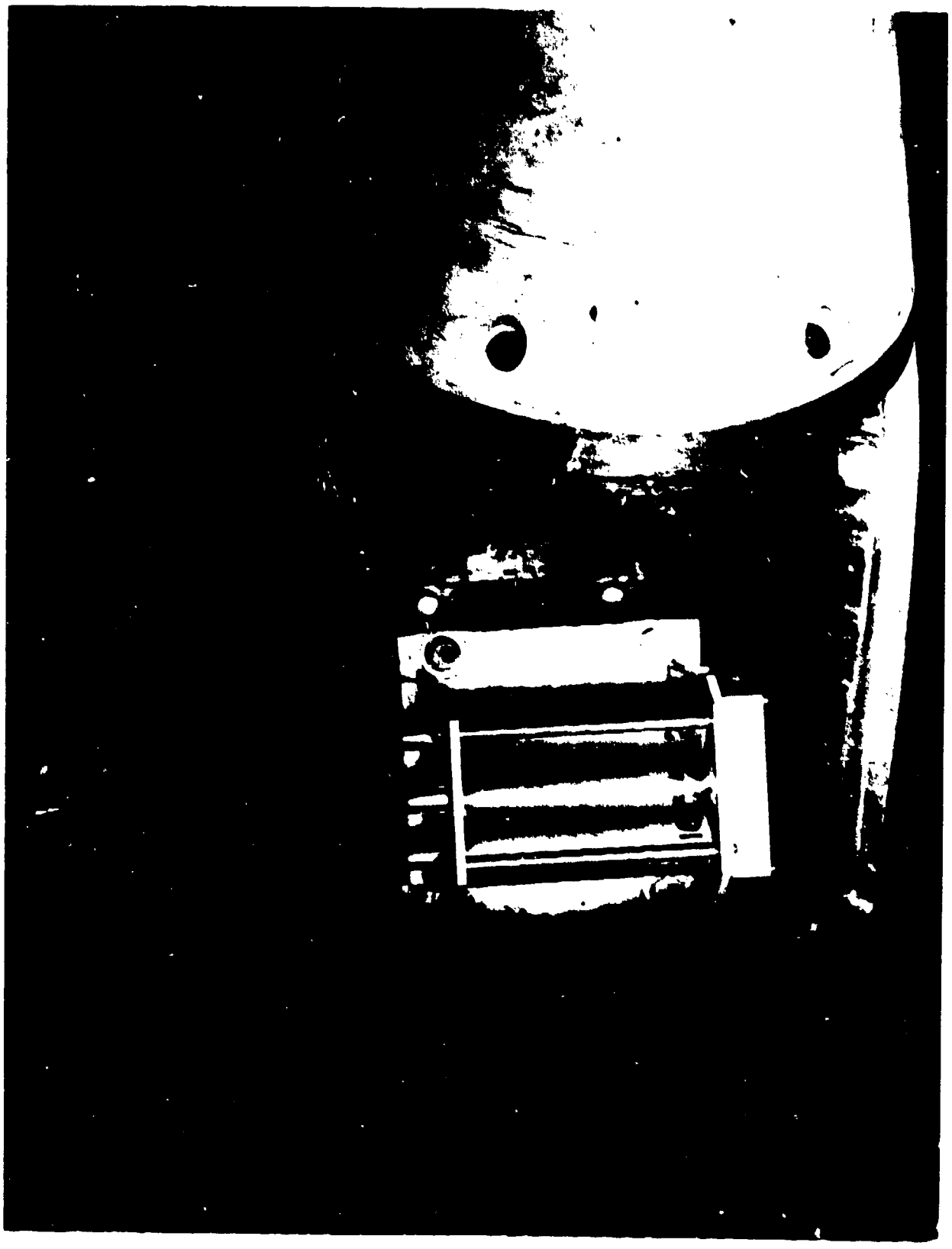

COSMIC RAY COUNTER TELESCOPE INSTALLED IN WARHEAD

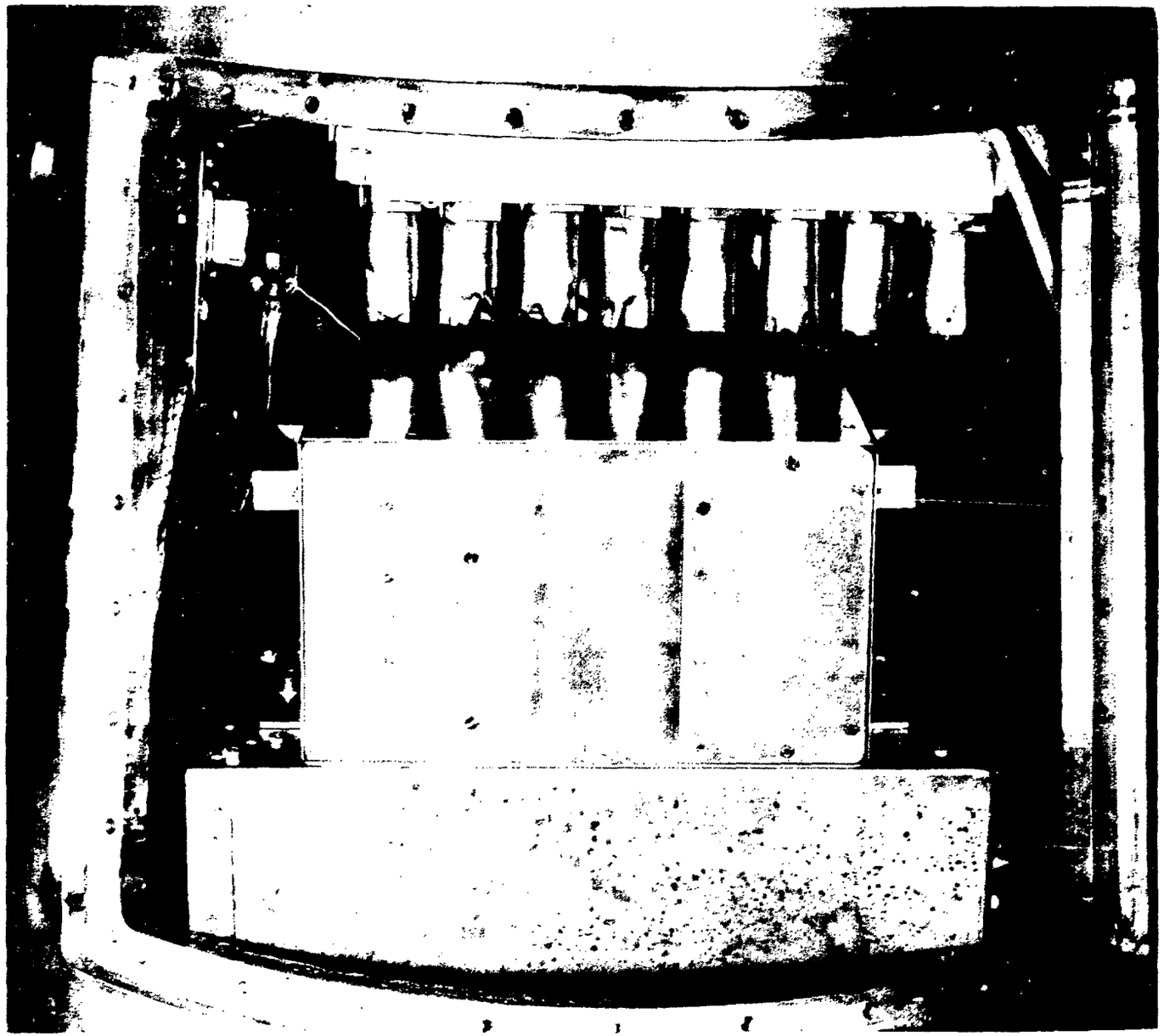

WARHEAD INSTALLATION SHOWING COSMIC RAY ELECTRONICS (TOP)
ATMOSPHERIC PHYSICS COMMUTATOR AND IONOSPHERE TRANSMITTER (BOTTOM

ELECTRONICS AND DYNAMOTORS COSMIC RAY AUXILIARY

FIG. 4

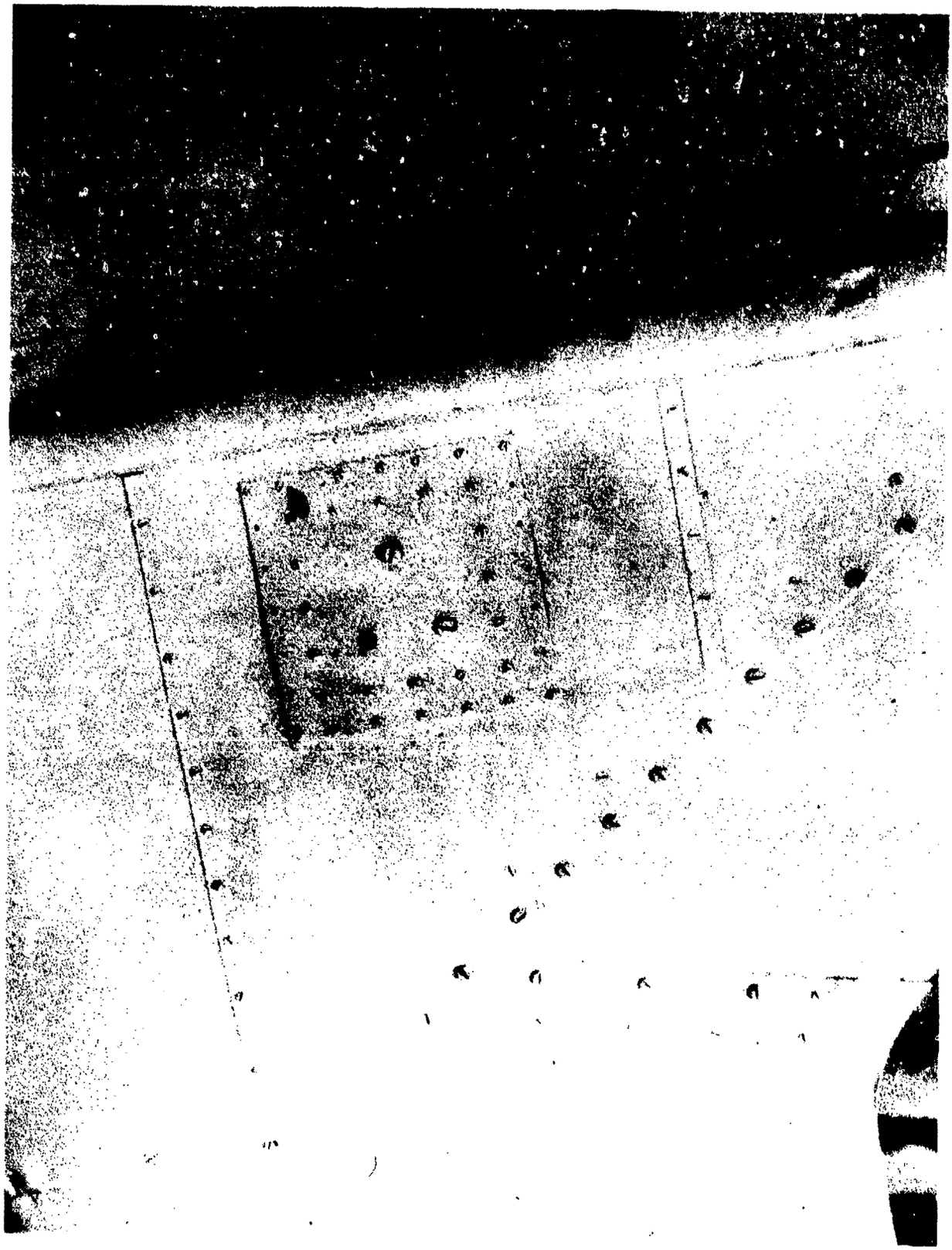

IONOSPHERE ANTENNA TUNING BOX INSTALLATION

CH. II SEC. A FIG. 5

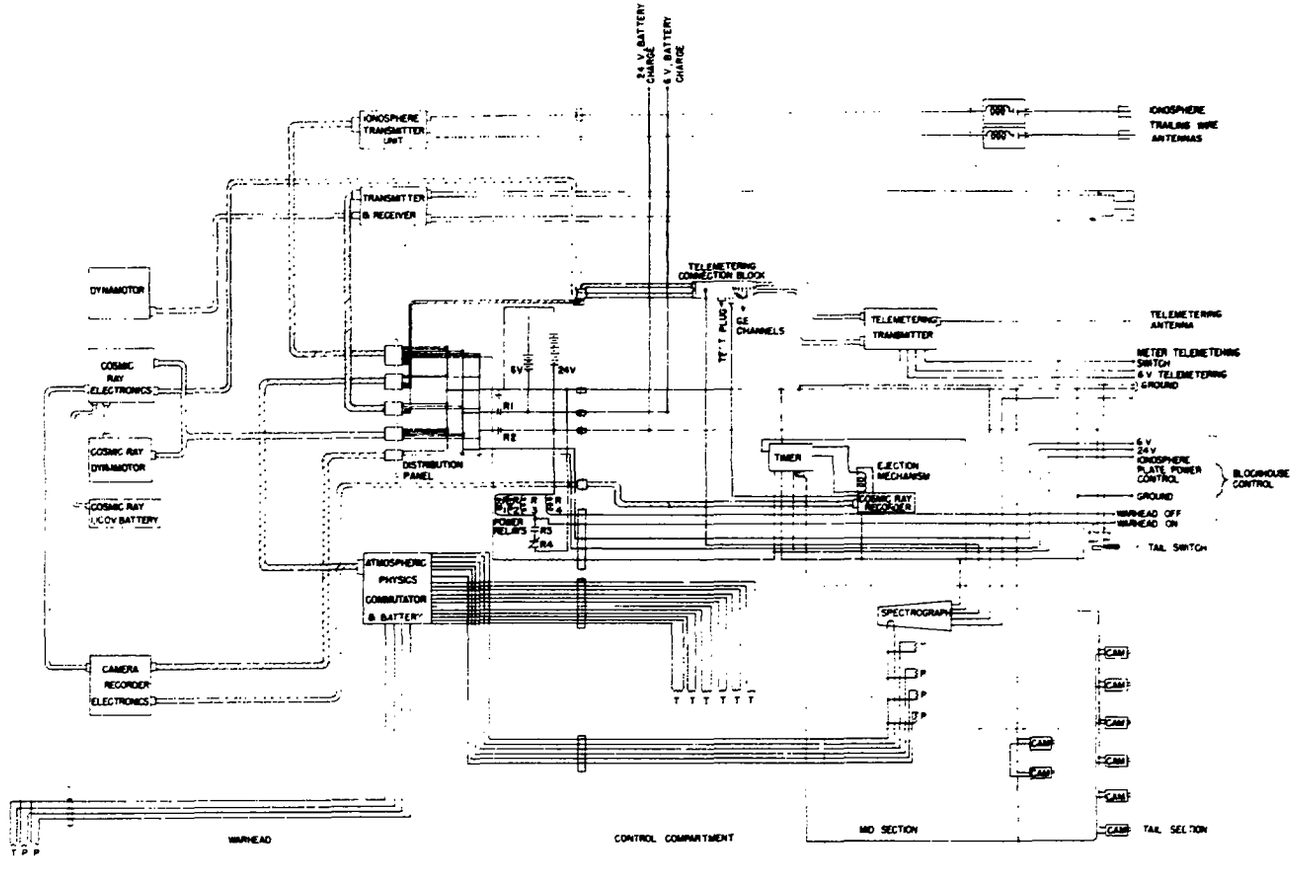

OVERALL ROCKET WIRING DIAGRAM

CH. II SEC. A FIG. 6

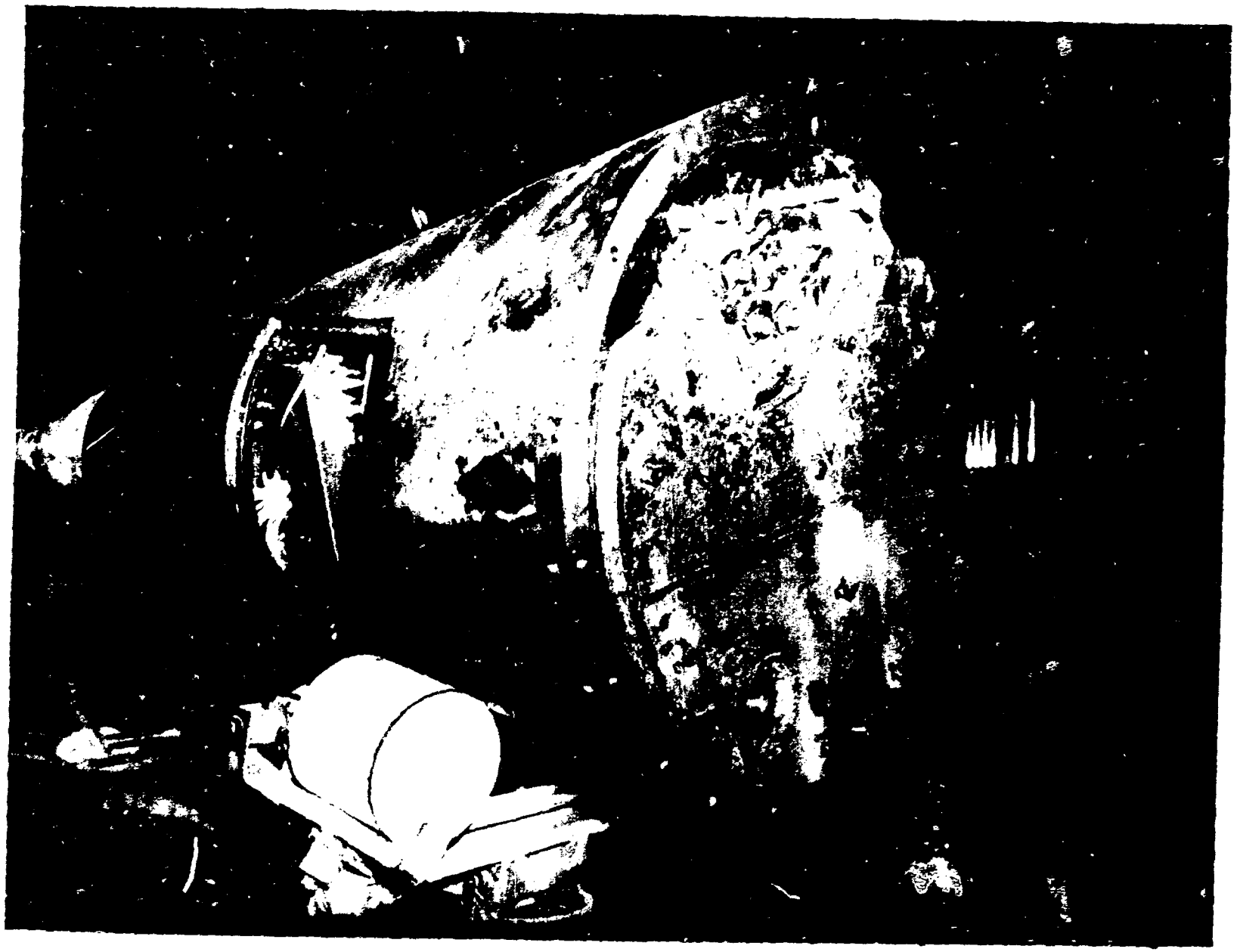

WARHEAD SHOWING BASE COUNTERWEIGHT

CHAPTER II

INSTALLATIONS FOR THE OCTOBER 10 FIRING

B. The Program Timer

by

C. C. Rockwood

A timer was installed in the October 10 V-2 rocket originally for the purpose of detonating explosive charges in the control chamber. The timing equipment is described below in some detail. As pointed out, the equipment was finally used for various other purposes in addition to that of firing the explosives behind the warhead.

The timer which appears in Fig. 1 was constructed from parts of a device originally designed to detonate delayed action mines. It consisted essentially of five cams mounted on a shaft which completed one revolution in approximately 400 seconds. Each cam actuated a double pole single throw switch. One pole of each switch provided a signal to some circuit within the rocket while the other provided a telemetering indication of the operation of the associated cam.

A schematic diagram of the timer circuit appears in Fig. 2. Cam No. 1 provided a zero position for the timer. The second cam operated the parachute ejection mechanism. Cam No. 3 operated a solenoid which allowed any length of spectrograph film remaining after all desired exposures have been made, to be taken up very rapidly. This was done in order to insure that all of the film had been wound onto the receiving spool before the explosive charge was detonated by cam 4. Cam 5 operated the tail ring and midsection cameras which were discussed in the preceding section. The intervals during which these switches were closed are as follows. Time is measured from takeoff, in seconds.

Cam	Time
1	0 - 10
2	240 - 250
3	310 - 325
4	325 - 335
5	60 - 180

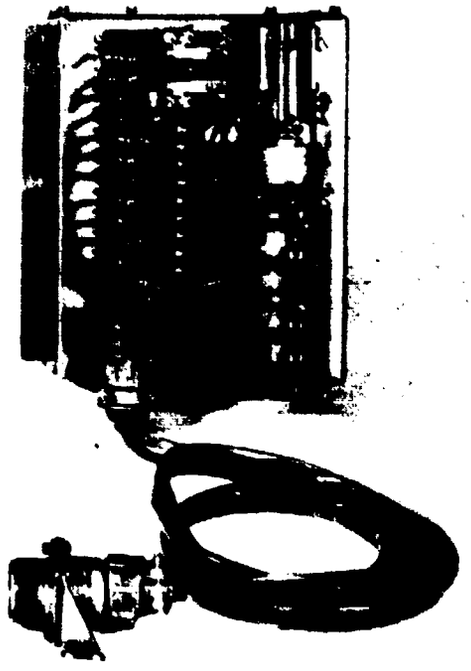

THE PROGRAM TIMER

The cam was driven through a gear train by a 4000 rpm Oster motor. Power was supplied to the motor by two 6 volt dry batteries in series. These occupied slightly more than half of the timer housing space of 15 cm x 15 cm x 20 cm (6 in. x 6 in. x 8 in.).

Setting, testing, etc., of the timer was accomplished by means of a specially constructed timer test box.

For the October 10 flight, precautions were taken both to ensure that the explosive charge would not detonate prematurely, and to ensure that it would explode at the desired instant. The explosive charges were not armed until ten minutes before scheduled takeoff time. The detonation circuit was also held open by a push-to-open safety switch in the tail of the missile which closed as the rocket began to rise.

In case the timer failed to operate for any reason, provision was made to detonate the charges remotely. Two channels of the emergency fuel cutoff system were assigned for this purpose. The two channels were connected so that both had to be energized simultaneously in order to cause detonation. This arrangement was resorted to in order to prevent random noise, or interference, from causing an accidental explosion of the charges. The signal was transmitted on this circuit to the ARW-17 receiver in the V-2, 335 seconds after takeoff.

As stated in Chapter I, indications are that the rocket broke up during the latter part of the flight, some 75 seconds after the radio signal for detonation of the explosives in the warhead. It is not known whether the detonation was initiated by the timer or the radio control.

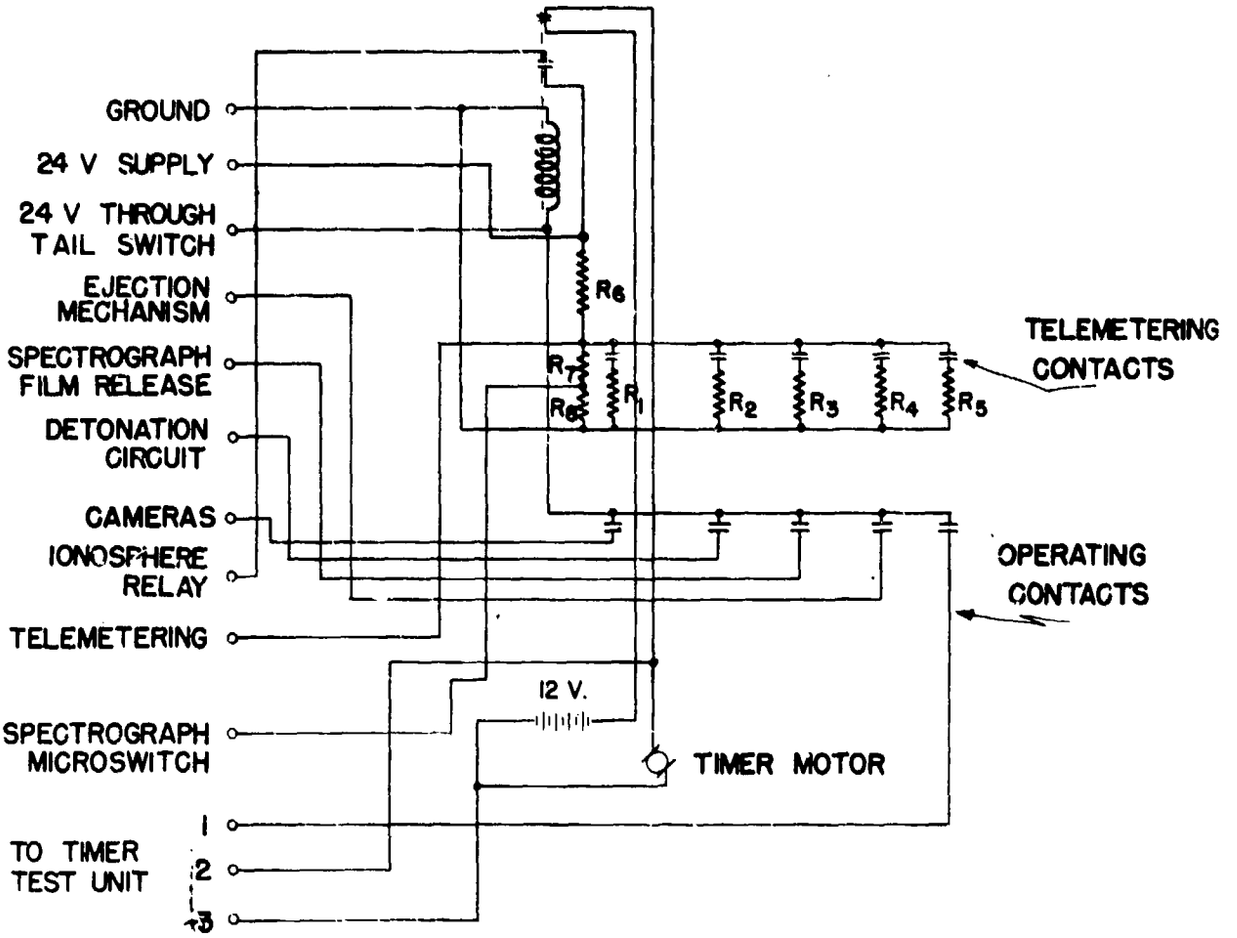

TIMER CIRCUITS

CH. II SEC. B FIG. 2

CHAPTER III

TELEMETERING FROM THE V-2

by

C. H. Hoeppner, J. R. Kauke,
R. E. Taylor, and K. M. Uglow

A. Improvements in the V-2 Telemetering System

1. Introduction. To date, twelve V-2 rockets have been fired at White Sands Proving Ground, each containing a telemetering transmitter of the type described in the first report of this series.* In addition to the data which has been obtained by means of telemetering, valuable experience in the general techniques involved has been gained. As rapidly as possible the lessons of this experience have been applied toward improving the overall system. In general, the performance of the system has been good, and the telemetering transmitter has proved to be one of the most reliable of the electronic equipments in the V-2.

2. Overall Improvements in the Telemetering System: Major Problems. There are two principal difficulties which have been encountered in telemetering. First, because of the complexity of the system, and multiplicity of data recording schemes in each of several complete receiving stations, completely automatic operation is not obtainable and the number of operators required is somewhat larger than is desirable. Secondly, it has been found that the signal strength obtained with the original equipment is not adequate for 100 percent reliability of data transmission.

The Operating Problem. The operating problem is being resolved in several ways. A permanent building containing two complete ground stations, as well as shop facilities, has been constructed. A simulated telemetering signal is to be provided so that a partial system check can be obtained between firings. These things will lessen the amount of readjustment necessary prior to each firing, will allow duplicate equipment for the two stations to be operated by a single person in some instances, and will expedite construction, repair, experimental, and calibration work between firings. With both receiving antennas close together, for instance, only one man will be required for tracking the

---

* The Naval Research Laboratory Report R-2955, Chapter II, Section C.

rocket, both antennas being controlled from the same electrical information. Furthermore, duplicate communication facilities will not be required for the two stations.

Improvements in Signal Strength. The problem of insufficient signal strength is also under attack and already several modifications have been made in the system. The transmitter power output has been increased and made to remain more nearly constant during flight. The power loss in the transmitting antenna feed cable has been reduced by substituting RG-17/U cable for the RG-9/U used originally. Dielectric losses present in the original transmitting antenna have been reduced. Signal fading due to change in wave polarization has been eliminated, and that due to motion of the transmitting antenna radiation pattern is to be reduced. The power gain of the directional receiving antenna has been increased. Receivers having nearly the maximum performance obtainable under the present state of the art are to be developed. With all of these improvements and others which appear advisable in future work, a good telemetering record should be obtained throughout all of the interesting portion of the rocket's flight. These improvements are discussed in detail below.

Telemetering Before Takeoff. The transmitting antenna, located at the rear of the rocket, does not by itself produce a receivable signal at the ground station location while the rocket rests on the launching platform. However, a "relay" antenna system has been put in use, which provides a strong signal at the ground station for pre-flight tuning, ground checks, and calibration. The scheme consists of picking up about 25% of the radiated power by placing a small dipole quite close to the transmitting antenna, and re-radiating this power from another dipole mounted atop a 40 foot pole nearby. The pick-up dipole is firmly attached to the launching platform and remains there after takeoff. Although the location is quite hot prior to takeoff, one of these dipoles containing bakelite insulation survived four firings.

Recording of a Time Reference. In addition to the changes aimed at increasing signal strength, an improved system has been devised for indicating, on the telemetering record, the instant of takeoff of the rocket. The original system utilized a timing signal generated in the blockhouse and transmitted over the amplitude-modulated communications equipment. The signal consisted of pulses each half second on a 100 cycle background. This system has not proven entirely satisfactory because of interference and variations in signal strength. The method now used telemeters the takeoff time from the rocket itself, by superimposing on one channel a d.c. voltage which passes through one of the pull-away connectors at the base of the rocket. As the rocket rises the circuit is opened and for the remainder of the flight the channel may be used for telemetering other data. It is intended in the near future to install a time mark generator at the telemetering building for timing during the flight.

3. Improvements in the Transmitter. The peak power output of the transmitter is being increased by several means. A deficiency in filament voltage has been corrected, a heavier plate supply has been added, and the modulator driver stage output is to be increased. Although originally 6.3 volts was provided by the batteries in the transmitter, the circuit resistance, including that of the control switch contacts, allowed a drop of 0.5 volt. It is now standard practice to begin with eight volts of filament battery mounted outside the pressurized case with lead resistance adjusted so that exactly 6.3 volts appears at the tubes. In addition to increasing the power output, the use of proper filament voltage is essential to maintaining proper duration of the temporary states of the premodulator multivibrators.* A channel calibrated so that, with filament voltage at 6.3 volts, the temporary state time is 50 microseconds for a zero data voltage and 200 microseconds for a five volt level, exhibits durations of less than 50 and 200 microseconds for the zero and five volt levels when the filament voltage drops below 6.3 volts.

In the space previously occupied by the filament batteries inside the case a second set of plate batteries supplying current to the premodulator is installed and connected in parallel with the set already in the transmitter. The current drain on these batteries is quite high and, since all the plate batteries are in series, this parallel set aids in maintaining higher voltage on all circuits. The output level of the system is also improved by the addition of a relay in the transmitter which permits an external plate supply to be switched in while the transmitter is being used during preflight tests. Thus the internal batteries are conserved for the flight alone.

4. The Transmitting Antennas: The General Problem. The transmitting antenna problems are mainly those of obtaining satisfactory radiation patterns, prevention of power loss due to arc over, location and design of mountings, and designing antennas with satisfactory aerodynamic properties and resistance to heat.

Radiation Pattern Requirements. The desirable radiation pattern depends largely on the attitude taken by the rocket during flight. There is evidence that during flight the rocket rolls, pitches, and yaws. The most troublesome motion is the roll, which requires that the antenna be placed where it will not be shadowed by the rocket. Apparently the pitch and yaw do not exceed 90 degrees to the vertical over most of the flight, so that a tail mounted antenna with hemispherical coverage to the rear should suffice. Although this requires a long run of cable to the available transmitter location, the attenuation in the large solid dielectric coaxial cable used is not excessive. With the original dipole transmitting antenna, signal fading has been experienced, even

---

* Cf. op. cit.

though a circularly polarized receiving antenna is used, which seems to indicate that due to pitch and yaw of the rocket a null in the dipole pattern approaches the receiving location. Work is progressing on an antenna with more uniform coverage.

A Proposed Antenna. A Turnstile design is near completion which will give a fairly uniform pattern in the plane of its elements, and circular polarization of the same amplitude in a direction normal to this plane, which is the most probable direction of transmission. It can be shown that in order to obtain efficient transmission between two circularly polarized antennas, the sense of rotation must be the same for both. In the present case counter-clockwise rotation is to be used. Viewed from the nose of the rocket the rotation would be clockwise, but that this aspect of the rocket should ever be presented to the ground station seems improbable.

The Interim Antenna. An interim antenna has been designed, using the three phase feed element from the circularly polarized receiving antenna, which is superior to a dipole. It has a symmetric three lobed pattern in the plane transverse to the rocket axis, with minima 7 db. down from the maxima. The polarization is nearly circular to the rear of the rocket.

Arc Over Problems. Bell jar tests indicate that glow discharge can occur externally to the antenna even when a heavy dielectric cover is used, but that such discharge does not absorb nearly as much power as does arc over in the feed line. Internal arc over is prevented by constructing the antenna to withstand the transmitter power at atmospheric pressure, and then maintaining such a pressure during flight within the antenna feed system.

It is expected that external glow is less likely with the high air speeds encountered in the V-2, and that even if it does occur at lower altitudes, it is extinguished at the higher altitudes. It is not known whether any of the antennas employed suffered glow discharge during flight. In any event, signals have been received from all altitudes attained by the V-2.

The Mounting of the Antenna. The antenna must be designed so that aerodynamic drag does not require excessive strength in the mounting. It should be light enough so that vibrational accelerations encountered do not damage the antenna assembly. The mounting used to date fastens to a protrusion from the insulating section of one of the fins, which was provided in the original German design for another type of antenna.

The First Telemetering Antenna for the V-2. The dipole antenna originally used in the V-2 was not entirely satisfactory. As pointed out above certain features of the radiated pattern render the antenna inadequate except perhaps for a rocket which maintains nearly constant

attitude during flight.

The construction of the antenna is illustrated in Fig. 1. For lack of parts made from high temperature dielectric the dipole pictured in the previous report* of this series was enclosed in bakelite. The power loss incurred, however, was about 2 db., so that as soon as was practicable high temperature low loss dielectric of relatively high permittivity was substituted. This material served two purposes: first to shorten the physical length of the half wave dipole; and secondly, to pressurize the radiating elements, as well as the end of the coaxial transmission line terminated by the elements. The length of the dipole was reduced by a factor of approximately the inverse square root of the relative permittivity of the surrounding material, and the radiation resistance was reduced in the same ratio. The cone shape of the dielectric covering served to lower wind resistance. The dipole was pressurized with rubber washers, and by sealing with Sauereisen Insalute, a high temperature cement.

A shorted, quarter wave detuning sleeve, or "Balun", was used to keep antenna currents from flowing down the outside of the 50 ohm feeder. The sleeve was placed around the feeder with the open end near the antenna feed point. The space within the sleeve was filled with a dielectric material in order to decrease the length required. The dielectric material used to cover the radiating elements, and to fill the detuning sleeve was Grade "A" Lava** with a dielectric constant of 5.0. This material withstands quite high temperatures without damage.

A series coaxial transformer was used to match the antenna impedance to the 50 ohm characteristic impedance of the feeder. The matching transformer, with a characteristic impedance of 25 ohms, was filled with polystyrene. Variations in dielectric constant of the other dielectrics tried caused prohibitive corresponding variations in input impedances. As the terminal impedance of the radiating elements was not purely resistive, the transformer length was somewhat different from a quarter wave, actually 0.305 wavelength at 1040 megacycles. The transformed impedance gave a voltage standing wave ratio on a 50 ohm line of better than 2:1 from 1000 to 1090 megacycles, and better than 1.25:1 over the operating frequency range of 1020 to 1040 megacycles.

The radiation pattern of the antenna, when measured in free space was essentially the same as that of a half wave free space dipole.

---

* Cf. op. cit.

** Provided by the American Lava Company, Chattanooga, Tenn.

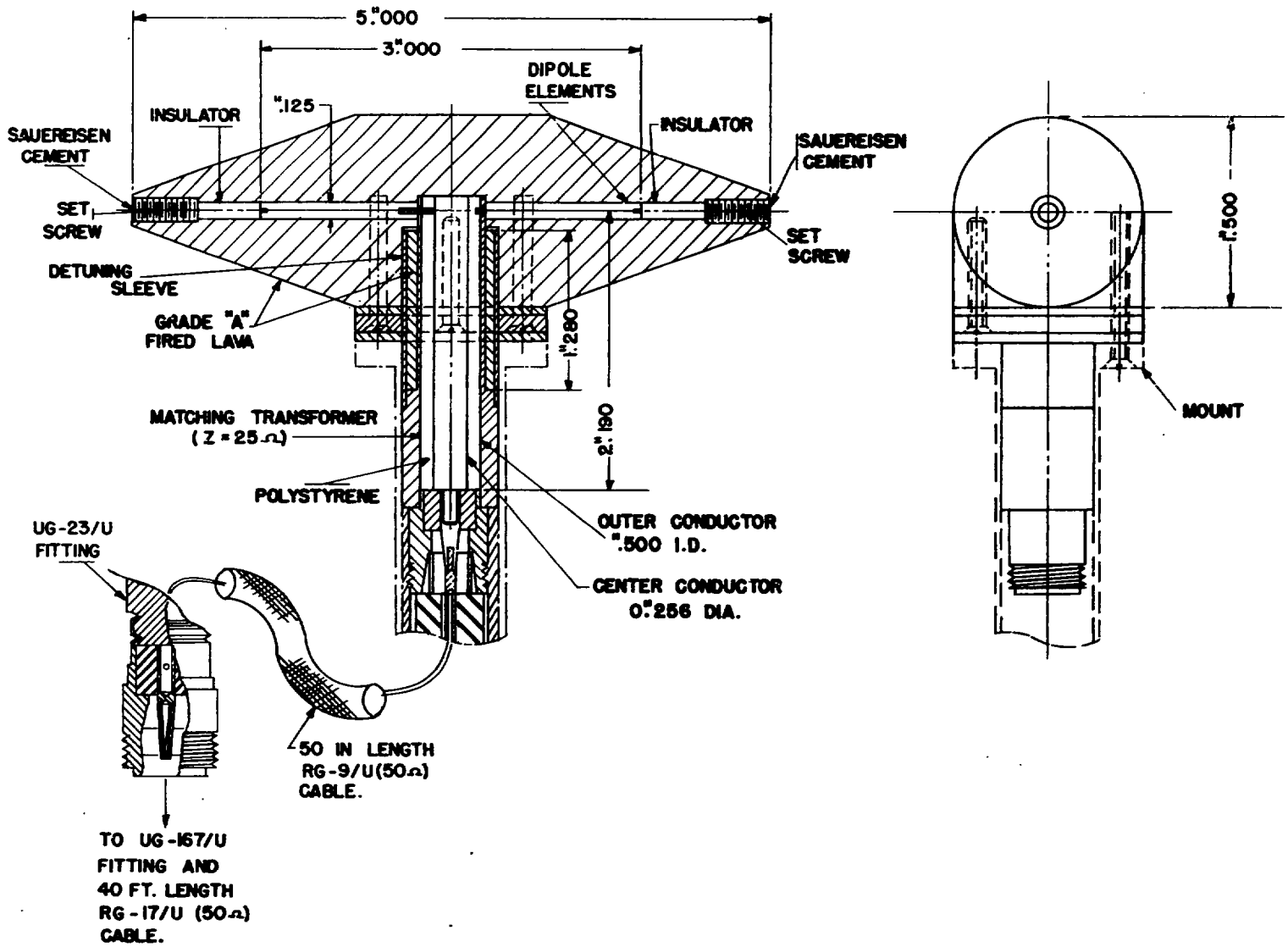

DIPOLE TRANSMITTING ANTENNA
(LAVA COVERED)

A production model of the Lava covered dipole with its mount is ullustrated in Fig. 2.

A Detailed Description of the Interim Antenna. The three phase circularly polarized transmitting antenna presently in use, is shown in Figs. 3 and 4. The eccentricity of the polarization in a direction normal to the plane of the elements is less than 3 db. from 1000 to 1100 megacycles. The impedance match to a 50 ohm line is better than 1.20 VSWR over the same frequency range. The plane polarized pattern in the plane of the elements has three symmetrically spaced lobes, with 7 db. minima between lobes. The measured radiation pattern checks the pattern computed using the assumption that the radiation phase center of each element is 0.1 wavelength from the center of the array.

All insulating parts are made from Lava or Poly F-1114 to withstand high temperatures. Cracks and joints are sealed with either silver solder or Sauereisen high temperature cement. The assembly is quite rugged, so that no damage should result from aerodynamic or vibrational forces.

The Three Phase Feed System. If the antenna be considered as three identical symmetrically spaced elements, then its equivalent circuit can be represented by the circuits of Fig. 5(a) and 5(b), where A, B. and C are the terminals of the elements, and the impedances Z_1 and Z_2 are in general complex. The equivalent circuit of the feed system is shown in Fig. 5(c) and the current vector relations in Fig. 5(d). By means of reactances X_B and X_C, which consist of shorted and open-circuited lines inside of elements B and C respectively, the currents into these terminals are made to lead and lag, by 60 degrees each, the fictitious voltage vector E_{DN}, and to be equal in magnitude. Since $I_A = -(I_B + I_C)$ its phase is spaced 120 degrees from both I_B and I_C. Point A is connected to the outer conductor of the coaxial feed line, and point D to the inner conductor. An RF choke ("Balun") around the outer conductor prevents the flow of currents on the outside of the feed line, and therefore insures the relation $I_A + I_B + I_C = 0$. The advantage of this type of feed system is that the current relations can be adjusted by means of the variable reactances, without exact predesign of all dimensions.

It can be shown that such an arrangement of current elements spaced by 120 degrees in time phase and space will produce circular polarization in a direction normal to the plane of the elements, and uniform coverage in the plane of the elements, provided that the radiation phase front centers of each element be at the center of the array. Actually, however, the phase center of each element is displaced outward along the element, so that a three lobed pattern results.

PRODUCTION MODEL OF DIPOLE AND MOUNT

CH. III SEC. A FIG. 2

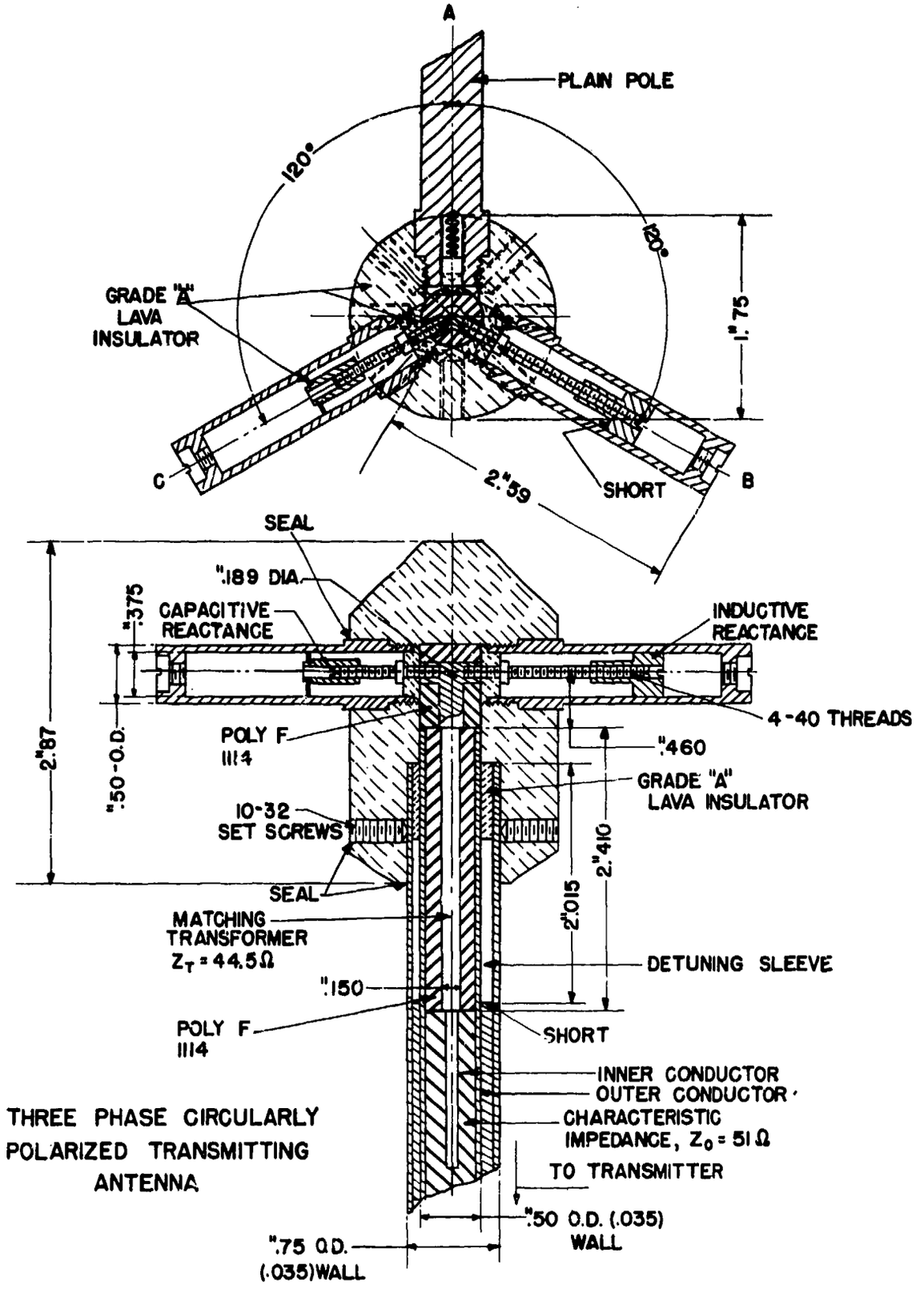

THREE PHASE CIRCULARLY POLARIZED TRANSMITTING ANTENNA

CH. III SEC. A FIG. 3

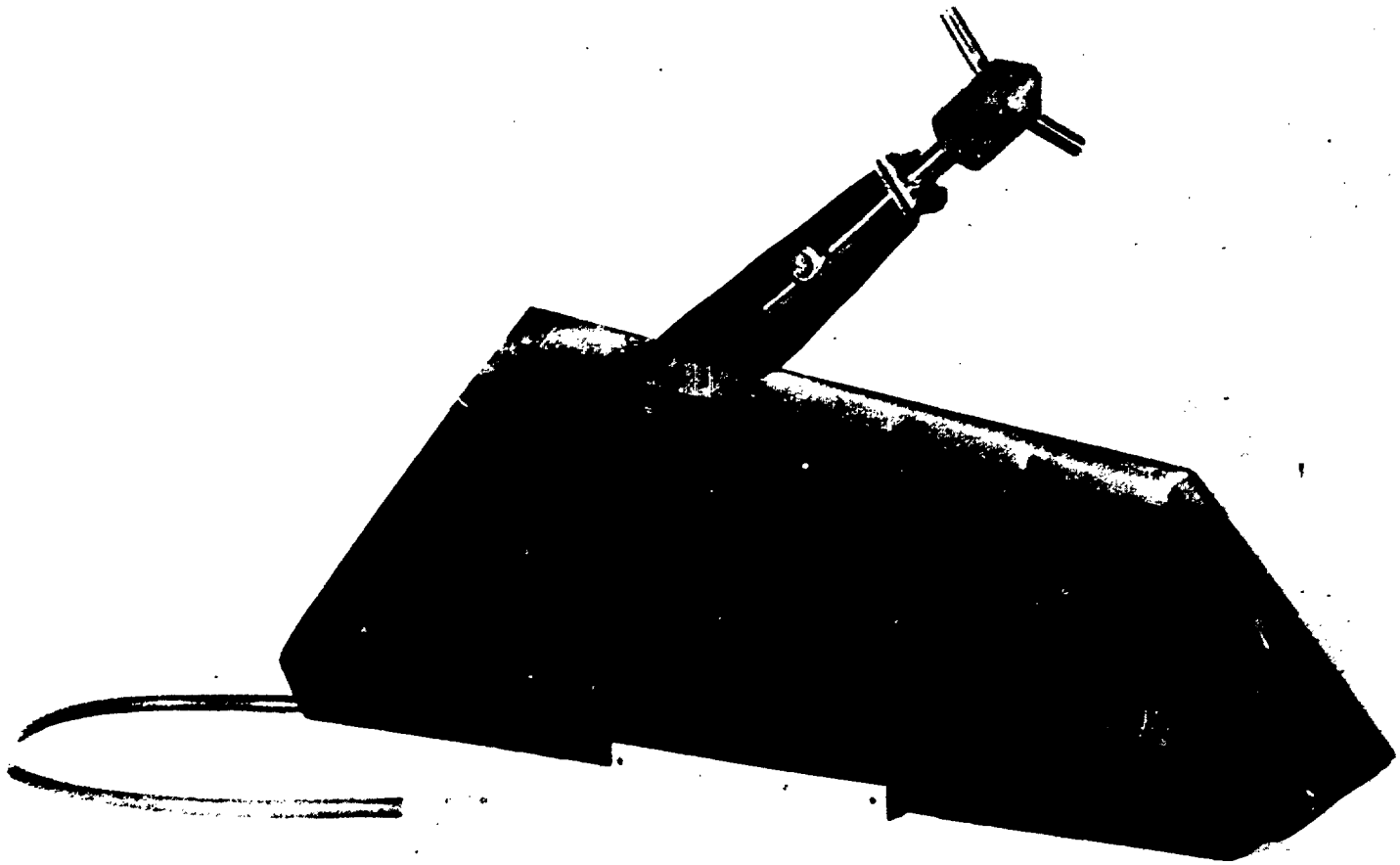

THREE PHASE CIRCULARLY POLARIZED TRANSMITTING ANTENNA MOUNT ED IN BAKELITE SECTION OF V-2 FIN

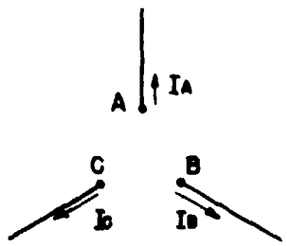

FIG. 5 a

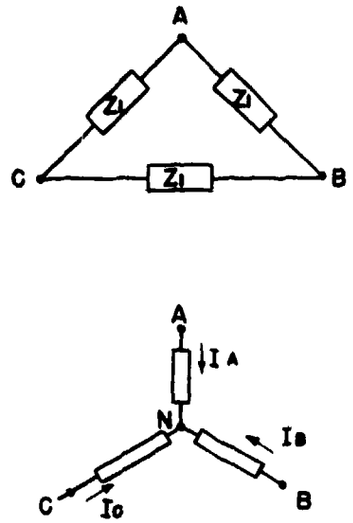

FIG. 5 b

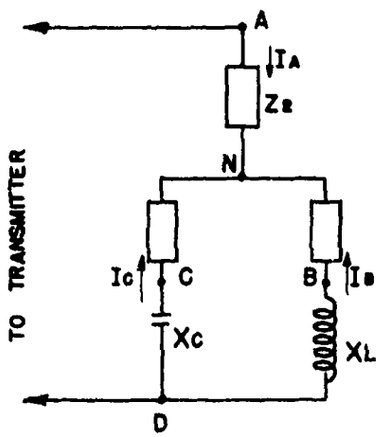

FIG. 5 c

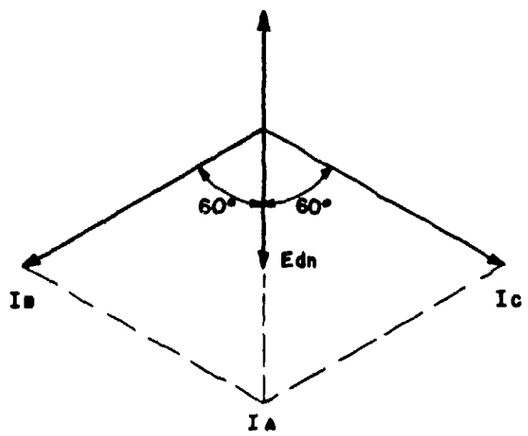

FIG. 5 d

CIRCUIT DIAGRAM OF THREE PHASE CIRCULARLY POLARIZED TRANSMITTING ANTENNA

CH. III SEC. A FIG. 5

5. Receiving Antennas: The General Problem. The receiving antenna originally chosen for telemetering appeared at first to be adequate. It was horizontally polarized when pointed at the horizon, had an azimuth beam width of 50 degrees, and an elevation beam width of 30 degrees. Since the receiving station was located beneath the rocket's expected trajectory, the antenna was arranged for elevation tracking only, and the azimuth was preset. Several inadequacies, however, soon became apparent.

First, as mentioned previously, the received signal was insufficient for 100 percent reliability. Secondly, experience showed that some of the rockets varied sufficiently from the prescribed trajectory to make azimuth control highly desirable. Such control is absolutely necessary for telemetering in the case of an unsuccessful flight in which the missile departs widely from the intended trajectory. For such cases telemetering is of considerable value in providing information relative to the cause of the rocket's behavior. Lastly, when the rocket began to roll at fuel cutoff, the direction of polarization of the received radiation rotated so that the signal faded periodically. The resultant fading has actually been correlated with the roll period as determined from gyro data telemetered in an early flight. This feature was, perhaps, the antenna's most serious deficiency, and it appeared desirable to eliminate such a characteristic by the use of circular polarization. Since even circularly polarized antenna systems possess very definite directional characteristics, the use of such a system on the rocket alone could not be expected to eliminate the polarization fading. On the other hand, the ground antenna can be directed by appropriate tracking of the rocket so that the missile remains essentially on the principal axis of the antenna during the entire flight. For this reason circular polarization could be used to advantage in the ground station antenna. Suitable circularly polarized antennas have actually been constructed and are in use at the White Sands telemetering stations.

Another less serious problem involves directing the receiving antenna properly. So far this has been accomplished by knowing roughly the rocket's location and by maximizing aurally the received signal. This was partially successful with the original receiving antenna, but the introduction of azimuth control and narrowed beam widths has rendered the operation more difficult. The aural method is actually an off beam method which necessarily results in signal fluctuations.

The possibility of using lobe switching direction finding on the received signalhas been examined, but so far the need for such a system has not been considered sufficiently great to undertake its development. Serious consideration is, however, being given to the use of optical tracking with the receiving antennas servo driven, using information from synchros geared to the optical equipment. With such

a system, suitable precautions must be taken to avoid loss of the very small image of the rocket as it passes overhead, at which time the tracking instrument must be rotated through 180 degrees in azimuth. Perhaps the optical and aural methods should be combined.

The Present Receiving Antenna. The receiving antenna now in use at White Sands consists of a paraboloidal reflector, with a three phase circularly polarized feed, similar to the three phase transmitting antenna. A two axis servo driven mount is employed. A photograph of the antenna assembly appears in Fig. 6. The mount is of lightweight construction, using fabricated and cast aluminum alloys wherever practicable. It is easily broken down into subassemblies, each light enough for two men to handle. The antenna was originally designed to be mounted on the ground station trailers, but is now in use in the permanent installation.

The feed assembly is a three phase radiator, covered by a weatherproof housing, which also serves to support an aluminum reflector plate which shapes the primary pattern. The reflector is a 48 inch paraboloid of 14 1/2 inch focal length. It is perforated to reduce the load on the drive motors due to wind, and has a dark grey finish to prevent reflected sunlight from damaging the feed assembly. The beam width of the antenna is 20 degrees in azimuth and elevation. The eccentricity of polarization is less than 3 db. over a frequency range of 40 megacycles, which is narrower than the bandpass of the three phase transmitting antenna because of the proximities of reflector plate and paraboloid.

The antenna is driven in azimuth and elevation by two phase, 50 watt output, low inertia servo motors. Handwheel driven, or remotely located, synchro generators supply position information to synchro control transformers in the antenna mount, which in turn supply error signals to 60 cycle amplifiers capable of delivering 100 watts at 115 volts to one phase of each driving motor. The other phase is connected to the 115 volt line which is also the source of synchro excitation voltage. The error signal is phase shifted by 90 degrees in passing through the amplifier. A band rejection filter is used to stabilize the servo system by "envelope differentiation". The synchro system is a one speed system, since the required accuracy is not great.

The elevation driving system is arranged for 180 degrees rotation, so that rockets passing overhead can be tracked without changing the azimuth by 180 degrees. As the antenna is elevated past 90 degrees, a cam operated switch causes the proper one of two azimuth dials to be illuminated to indicate true azimuth at all times. Elevation limit switches are provided to remove the motor voltages whenever the antenna points below the horizon. A phase detecting circuit is used to re-energize the motor when the synchro error signal becomes of the proper polarity

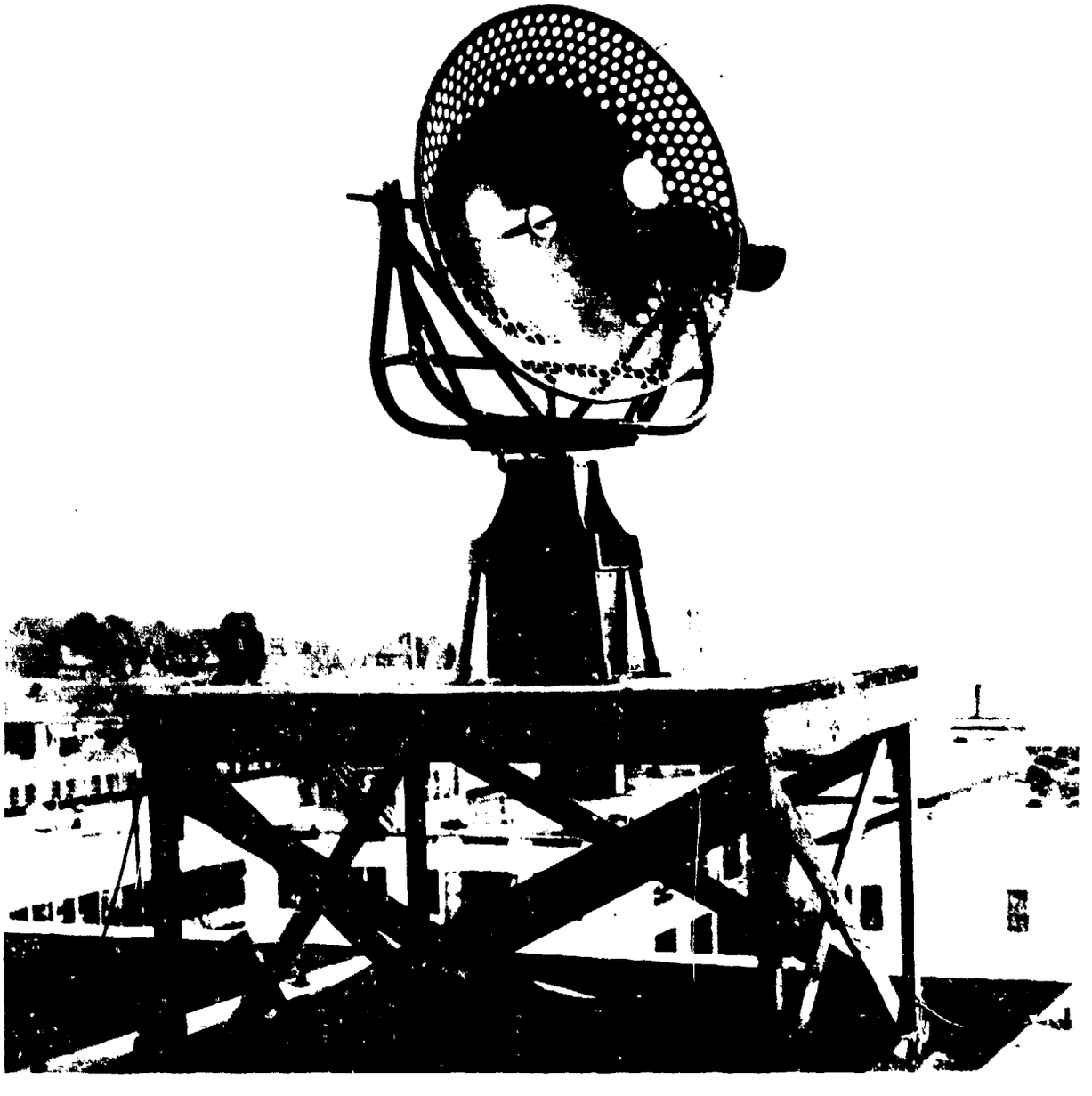

GROUND STATION ANTENNA ASSEMBLY

to cause the motor to drive the antenna upward from the horizon.

6. Telemetering Receivers. To achieve optimum system performance and maximum reliability of operation, for a given size and weight of transmitting equipment, it is essential that the receiver employed have the best possible characteristics, and that it should require a minimum of attention in operation. The receiver used at present for telemetering was chosen primarily because it was available in quantity at the beginning of the V-2 program. It is well designed from the standpoint of reliability but has the following major shortcomings:

(a) I.F. and video bandwidth are not appropriate.

(b) The I.F. amplifier alignment is largely dependent on individual tube characteristics, and no adjustments are provided. In some units there are several serious dips within the pass band.

(c) Some of the components are not easily accessible for replacement.

(d) The R.F. input was designed for a three to one frequency range, and is accordingly badly mismatched at the frequencies being used. This necessitates the use of a stub tuner on the input.

(e) The overall receiver noise figure is far from that obtainable using the most recent developments in receiver design.

(f) No R.F. selectivity is provided, so that interference is experienced even from signals the frequencies of which are far removed from the operating frequency.

(g) No automatic gain control is provided.

Development is under way on a receiver which does not possess the shortcomings listed above. It is to cover a range of at least 1000 to 1100 megacycles. The R.F., I.F., and video band pass filters are to be sufficient to pass a square 1.0 microsecond pulse with a rise time of no more than 0.2 microsecond. This requires an effective overall bandpass of about 4 megacycles, which is consistent with the band pass required by transmitter drift and frequency pulling due to the relay pickup antenna. Selective cavity resonators will be used in the R.F. input circuit to discriminate against pulse interference. The insertion loss to be expected from a cavity resonator of the required bandwidth can be less than 1 db. Using recent improvements in I.F. amplifier design and the best mixer crystals available, an overall noise figure under 10 db.

can be achieved, giving a sensitivity of about 2.5 microvolts on a 50 ohm line.

An automatic gain control will be provided, to insure proper operation of the pulse length discriminator* and to insure good system accuracy by preventing strong signal saturation which results in pulse lengthening and trailing edge undershoot in the video circuits. This will also reduce the level of noise and interference whenever the telemetering signal level is high. If desired, the AGC voltage developed can be used, with proper calibration, to record the received signal strength during a flight. A tuning indicator will be provided for rapidly maximizing the signal strength. Audio output will also be provided, to be used when needed for tracking, searching for signal, etc. The use of the audio output has the advantage over the use of oscilloscopes for these purposes that no synchronization is required to obtain an indication. The audio output is to be obtained by pulse stretching the video waveform in order to strengthen its fundamental, or repetition frequency, component. All I.F. tuned circuits will be designed so that proper alignment is possible without a sweep generator or tedious point-by-point band pass measurements.

---

* Cf. op. cit.

CHAPTER III

TELEMETERING FROM THE V-2

B. The Study of Rocket Performance through the Use of Telemetering.

The Naval Research Laboratory telemetering system has proved to be of great value as an aid in the analysis of rocket performance. This is particularly true in cases where trouble develops during flight. Four of the first twelve flights were marked by malperformance of the rocket. In three of these cases the attempt to determine the cause of failure was materially aided by a study of the telemetering record.

Six telemetering channels are normally assigned to the General Electric Company for such a study of rocket performance. The quantities measured are the angular position of each of the four carbon vanes in the jet stream, the combustion pressure, and the speed of the turbine which drives the fuel pumps.

On 19 July 1946 the rocket exploded above a cloud layer 27 seconds after take-off. The telemetering record showed that the combustion pressure and turbine speed were normal and revealed no malfunctioning of the jet vanes until the explosion occurred. This information eliminated several possible causes of the explosion. Subsequent examination of the wreckage showed that an overheated bearing in the oxygen pump caused the explosion.

Shortly after take-off on 15 August 1946 the rocket began to rotate around its axis so violently that the stabilizer fins were torn off. The fuel was immediately cut off by means of the emergency cutoff system described in the first report* and the rocket crashed to earth. An examination of the telemetering record of this firing showed that one of the carbon vanes suddenly turned to one of its extreme positions and remained there. The rocket thereupon began to spin, and at the same time, according to the record, the position of the other three vanes changed in such a way as to compensate for the spin. By determining from the telemetering record the rate of angular motion of the faulty vane, a German engineer familiar with the control system was able to estimate the probable origin of trouble in the rocket. In this case, the same vane had not functioned properly when the rocket was originally to have been fired a week previously. The trouble was apparently due to an intermittent break in one of the cables joining the computer and servomotor which actuated the vane.

---

* Naval Research Laboratory Report R-2955, Chapter II, Section B.

During the firing one week later the rocket rose about 100 meters and then started to fly horizontally over the heads of a group of spectators. The fuel was cut off when it was considered that the rocket was at a safe distance. The telemetering record in this instance showed that two of the vanes moved together in the same direction at a slow rate, while the other two vanes moved so as to correct for this misdirection. It was therefore concluded that the trouble lay within the computer.

The use of the telemetering system to monitor rocket performance is continuing.

CHAPTER IV

UPPER ATMOSPHERE EXPERIMENTS CONDUCTED IN THE V-2

A. Solar Spectroscopy

by

F. S. Johnson*, J. J. Oberly,
C. V. Strain and R. Tousey*

1. Introduction. The solar spectroscopic experiment conducted in the V-2 rocket fired at White Sands, New Mexico on 10 October 1946 was similar to the one attempted on June 28. The objectives of the astrophysics program of the Naval Research Laboratory and the design and performance of the solar spectrograph used on June 28, were fully described in the first of these reports**. For the second firing a spectrograph similar to the first except for a few details was constructed and mounted in fin II of the rocket. The spectrograph was recovered successfully after a flight to an altitude of more than 160 kilometers. When developed, the recovered film revealed a series of ultraviolet solar spectrograms taken at altitudes ranging from about 1 to 88 kilometers above sea level.

2. Relocation of the Spectrograph: Reason for the Change. The experience of the June 28 flight showed recovery of spectrograph film to be highly unlikely should the rocket remain intact until striking the earth. On the other hand, during the firing of July 30 the warhead of the V-2 was successfully separated from the rest of the rocket in mid air by means of explosive charges; and, as a result, the after body of the rocket with tail fins still attached, struck the earth at a moderate speed and was not greatly damaged. It was quickly located by search planes, whereas the warhead was never found although great effort was expended in searching for it. It was decided, therefore, that the chance of recovering the spectrograph film would be increased if the spectrograph were installed in the after part of the rocket instead of in the warhead.

The Fin Location. The solar spectrograph was designed originally for the nose section of the warhead and was approximately conical in shape. Sunlight was allowed to enter through either of two apertures on opposite sides of the cone. Each aperture consisted of a small sphere or bead of

---

* Members of the Optics Division at the Naval Research Laboratory. The experiments on solar spectroscopy have been carried on as a joint project by the Micron Waves Section, R. Tousey, Head, of the Optics Division, E.O.Hulburt, Superintendent; and the Rocket Sonde Research Section, E.H.Krause, Head, of the Radio Division I, J.M.Miller, Superintendent.

** Naval Research Laboratory Report R-2955, Chapter III, Section H.

lithium fluoride which served in place of the usual spectrographic slit. Each bead accepted sunlight over a cone of 140° vertex angle with axis at 45° to the axis of the spectrograph. The most favorable location for such an instrument, in view of its shape and optical characteristics, appeared to be fin II or IV. This would place one aperture on each side of the fin directed north and south respectively at launching, and for a firing after 9 A.M. would insure full illumination by the sun of one side of the spectrograph until Brennschluss. The angular field of view was necessarily reduced somewhat as compared to that obtained by use of the warhead position; but actually the portions obscured by the rocket itself and the adjacent fins were near the margin of the field and the reduction was not serious. The parts of the rocket in the field of view were painted black to reduce stray light.

A new light weight housing of 1/16 inch sheet steel was constructed for the spectrograph. This enclosure was light tight except for the two apertures for the beads. Fin II was strengthened and a well was formed inside. Four brackets were welded to the housing and the spectrograph was fastened in the well by means of them. Two fairing shields were constructed and one was fastened permanently over one side of the well as shown in Fig. 1. The other shield was screwed in place after final installation of the spectrograph. Fig. 2 shows the spectrograph in place without the second shield.

In order to balance the drag on fin II due to the bulges caused by the spectrograph two sheet metal shields similar to the fairing shields were attached in corresponding positions to the opposite fin. One of these is shown in Fig. 3.

To prevent stray light from entering around the bead mounting and to improve the fairing, two small cover plates with rubber gaskets were attached outside the fairing shields and fastened with screws into the spectrograph housing.

Since a port for evacuation opening directly to the outside was not permitted in the tail fin installation, the spectrograph was evacuated through a channel provided with blackened baffles and leading from the base of the spectrograph housing into the hollow fin. The fin in turn, was evacuated by means of an aperture about one inch wide which ringed the rocket just above the tail fins. So devious a vacuum line was expected to have a rather low pumping speed. As it happened, the minimum pressure reached in the spectrograph during flight was 0.1 mm of mercury, a value some ten times greater than that which was desired.

The installation work on the rocket fins described above was done by Naval Research Laboratory personnel working under the direction of U. S. Army Ordnance and General Electric Company personnel.

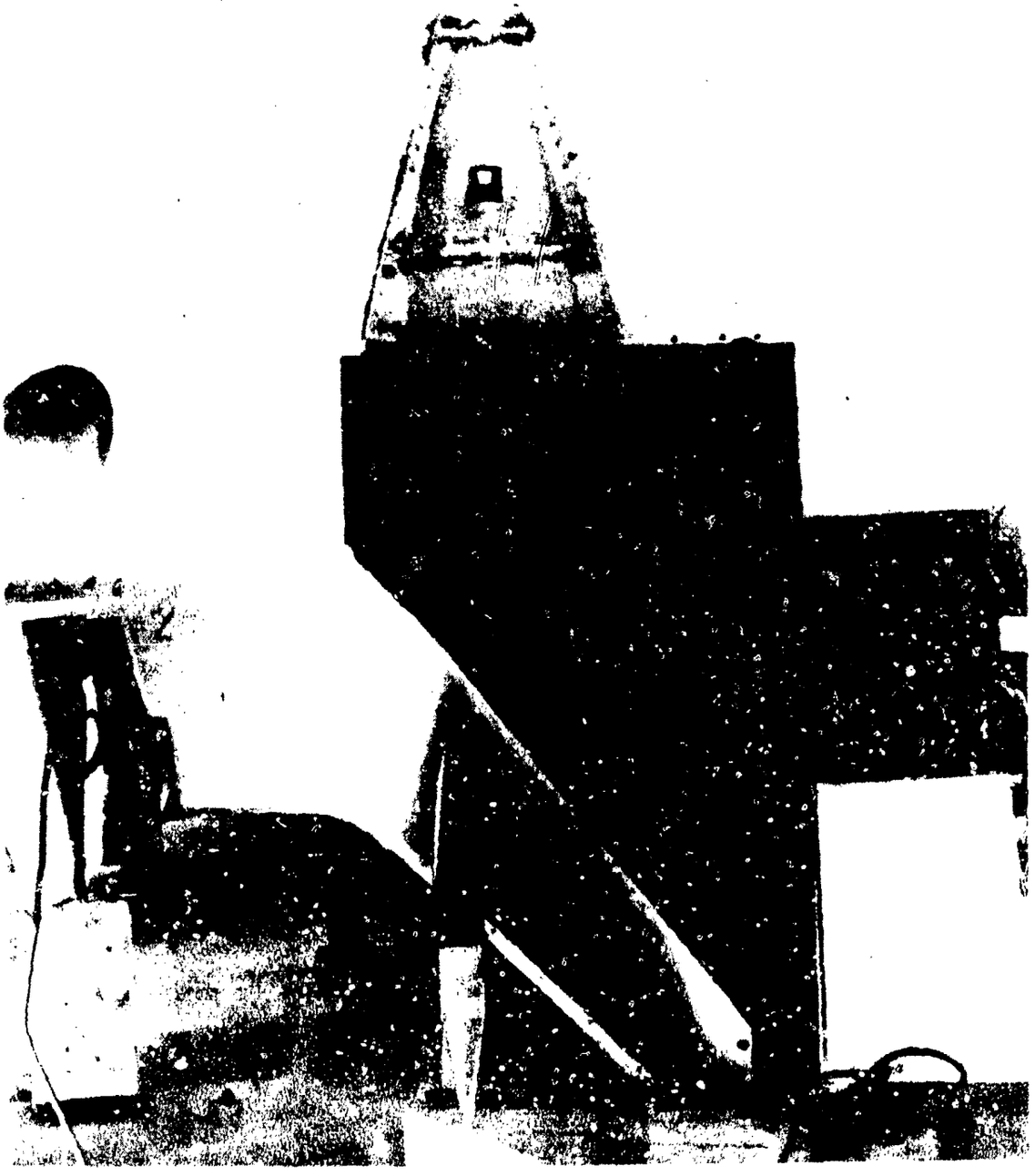

SPECTROGRAPH FAIRING SHIELD

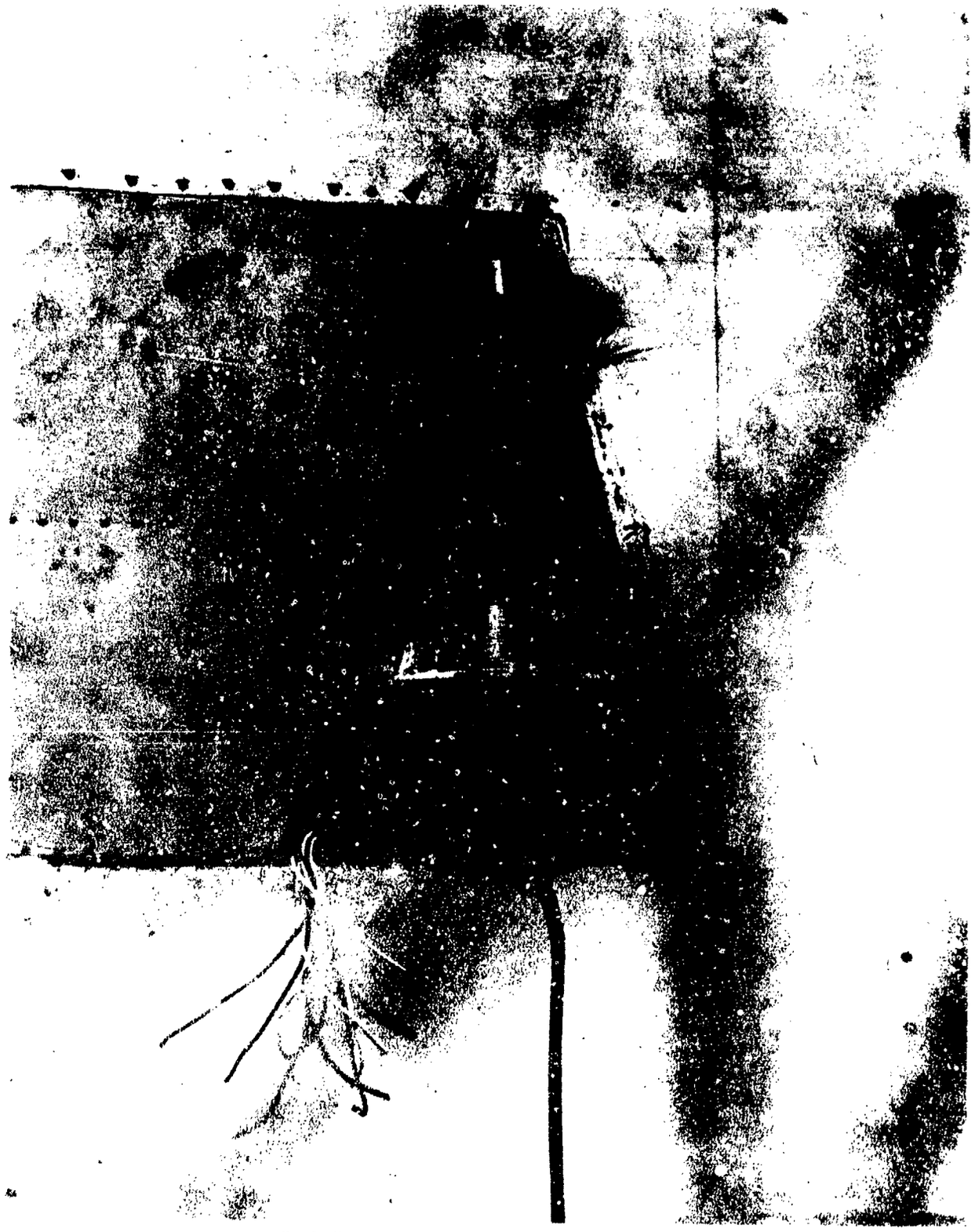

SPECTROGRAPH MOUNTED IN FIN

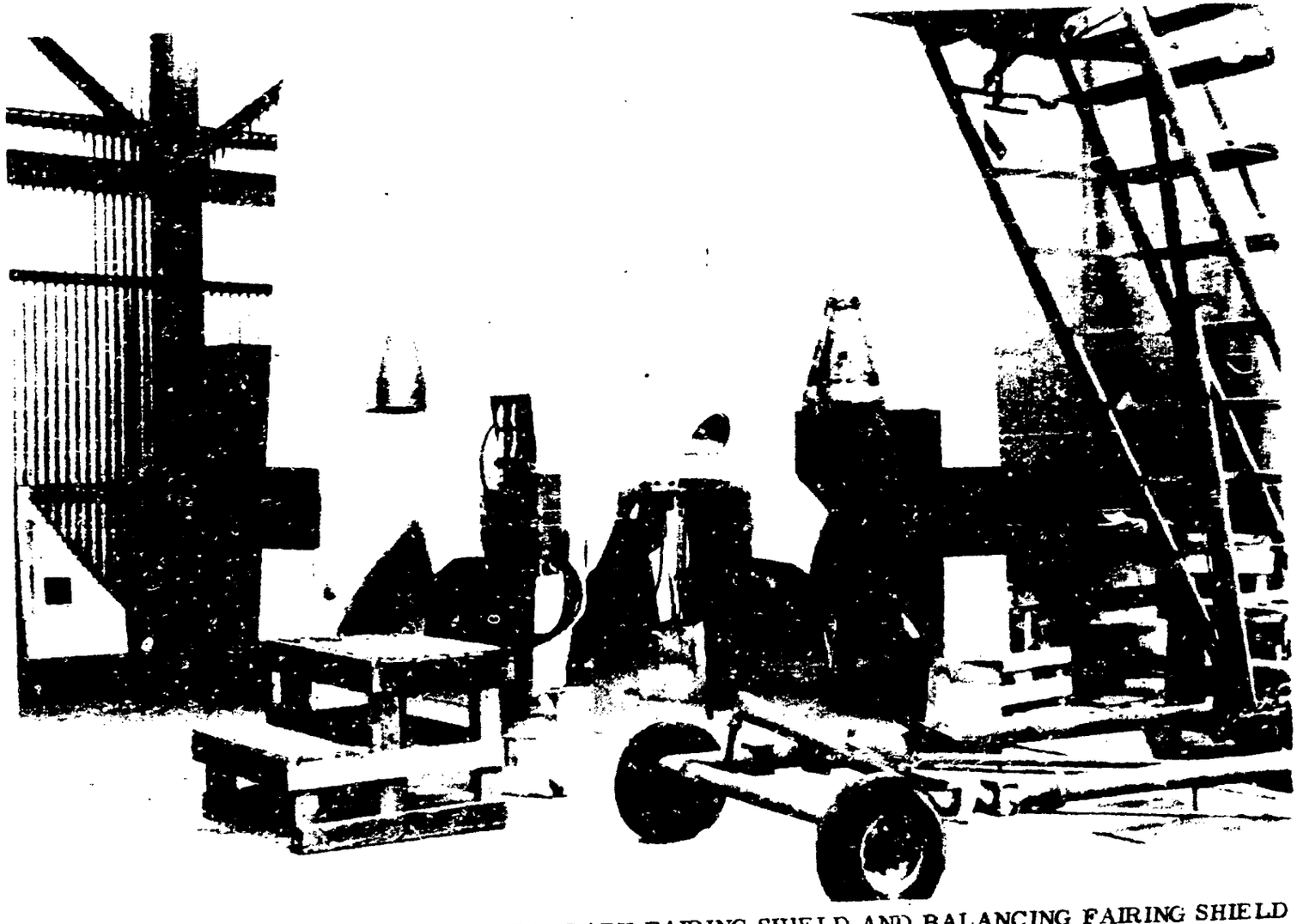

V 2 TAIL ASSEMBLY SHOWING SPECTROGRAPH FAIRING SHIELD AND BALANCING FAIRING SHIELD

3. Changes in the Spectrograph: The Exposure Sequence. The spectrograph as originally designed made three consecutive exposures, of 0.1, 0.6, and 3 seconds duration, repeating this cycle throughout the flight. The 3 second exposures were expected to be adequate to photograph the solar ultraviolet spectrum to wavelengths at least as short as 2000 A.U. Radiation intensities in the continuum below 2000 A.U. and for the 1216 A.U. line are believed to be rather low compared to intensities above 2000 A.U., and it was considered rather doubtful that a 3 second exposure would produce a satisfactory spectrogram at the shortest wavelengths sought. In order to increase the chance of obtaining spectrograms at wavelengths below 2000 A.U. it was decided to attempt a single long exposure across the top of the trajectory.

For this purpose, the spectrograph exposure mechanism was altered so that the same series of short exposure cycles was made for the first 150 seconds after take off, followed by a single exposure of 100 seconds. During the long exposure the shutters were allowed to rotate since this was considerably simpler than attempting to stop them at an open position. The effective exposure time was accordingly only 55 seconds. At the end of the long exposure, 250 seconds after take off, the film escapement was tripped allowing the remaining film to run rapidly into the armored film container. As a separate insurance that the film would be completely wound into the film container before the warhead exploded, a solenoid operated trip was installed, which was actuated by the program timer 15 seconds before detonation of the explosive charges. For a description of the timing equipment see Section B of Chapter II.

The Quartz Mirror. It appeared probable that an exposure as long as 100 seconds would result in a considerable blackening of the film due to stray light and that this might be a principal factor in preventing detection of the 1216 A.U. line of hydrogen. Most of this stray light would be from the more intense portion of the solar spectrum above 2000 A.U. The intensity of such stray light can be reduced without significantly decreasing the intensity of the 1216 A.U. line by replacing the plane evaporated aluminum mirror by a crystal quartz mirror. The effect of this change can be seen by referring to Fig. 6 which shows reflectivity curves for polished crystal quartz and evaporated aluminum. At 1216 A.U. quartz and aluminum have nearly equal reflectivities of 23 and 30 percent, respectively, whereas at wavelengths above 2000 A.U. the reflectivity of quartz is only approximately 1/15 that of aluminum. The use of a quartz mirror instead of aluminum thus diminishes stray light by a factor of at least 10, without appreciably affecting the intensity at 1216 A.U. However, it does reduce the intensity at longer wavelengths.

The use of quartz mirrors is advantageous in reducing stray light during the long exposure near the top of the trajectory. However, for the short exposures during the earlier part of the flight, the use of aluminum mirrors is preferable in order to increase the intensity of

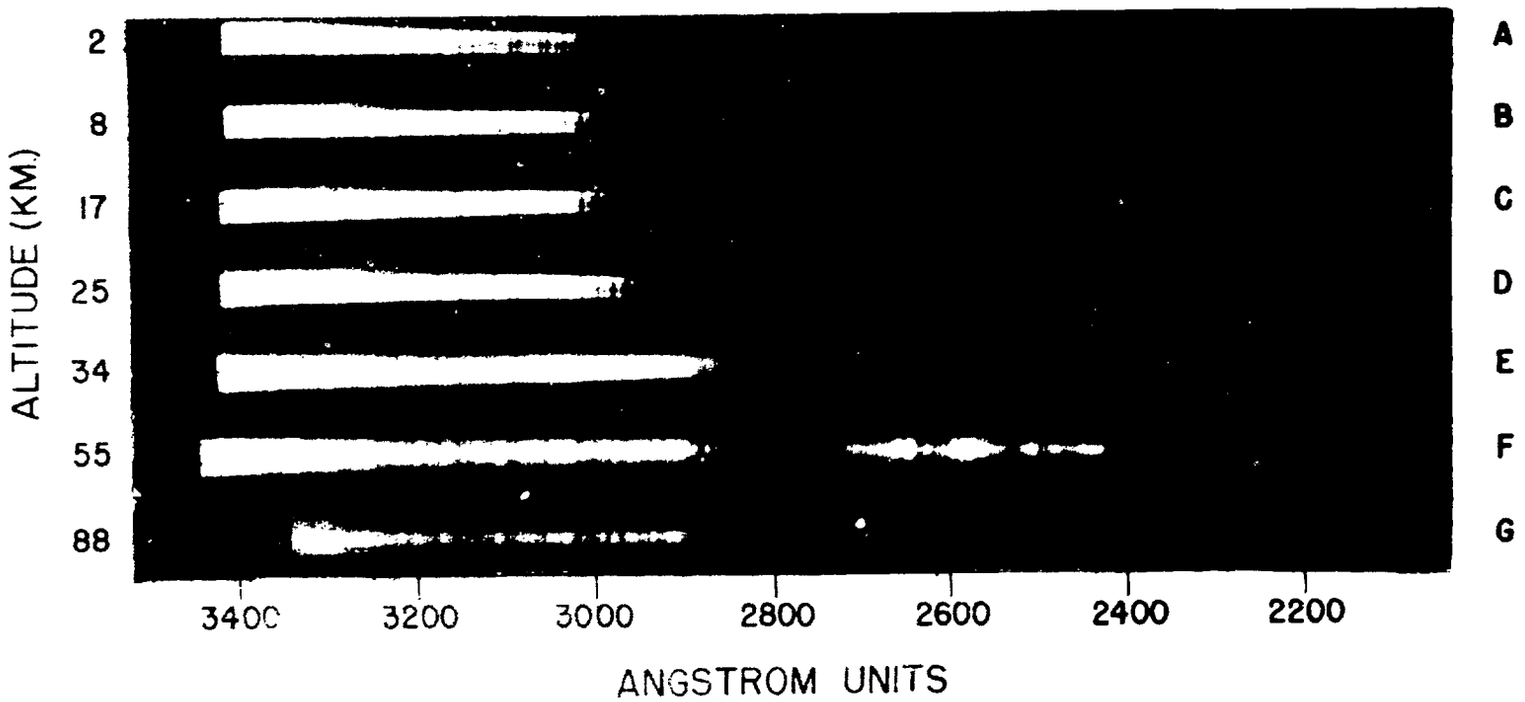

SPECTROGRAMS OBTAINED IN THE OCTOBER 10 FIRING

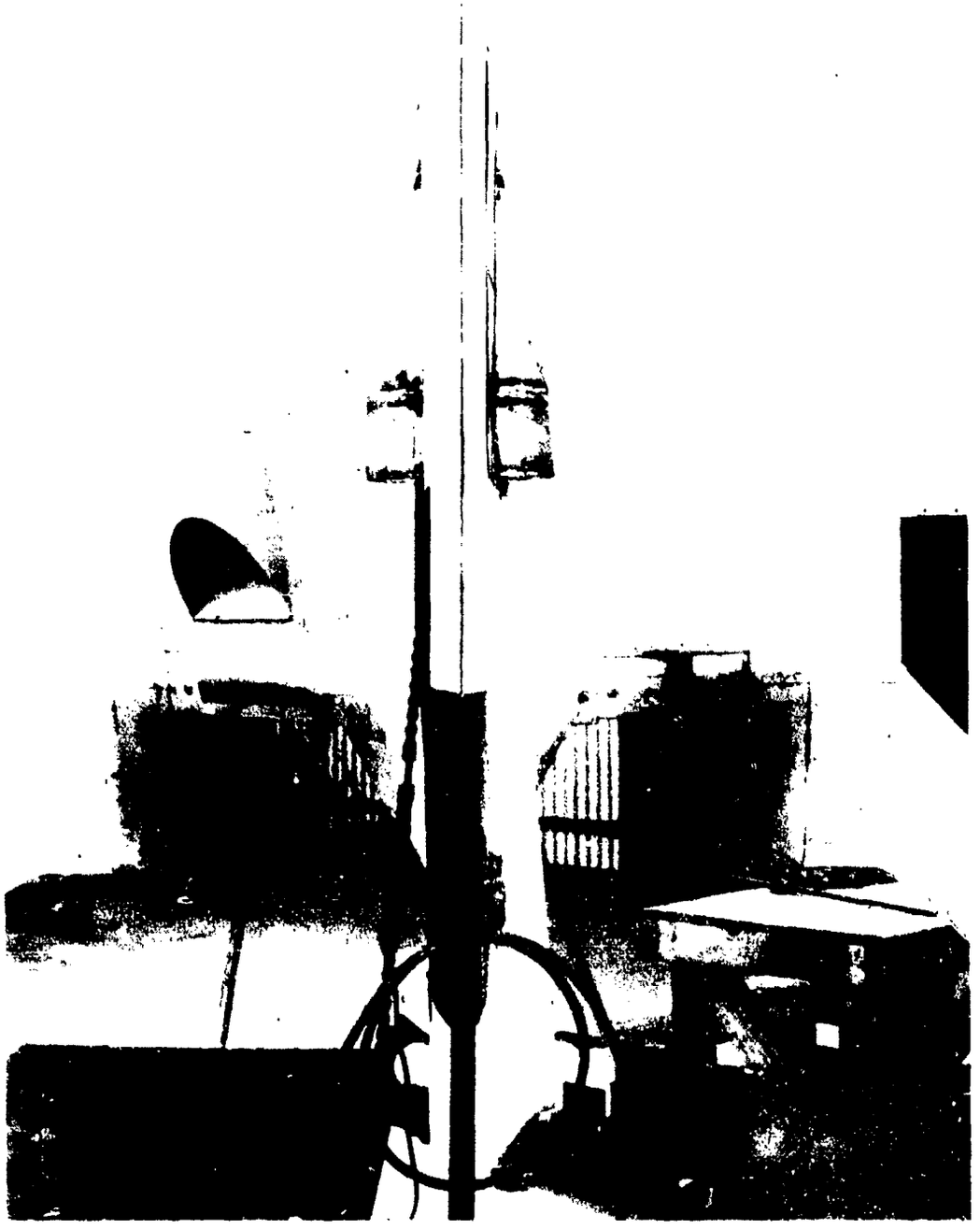

SPECTROGRAPH HOUSING AS SEEN FROM THE EXTENSION OF FIN II

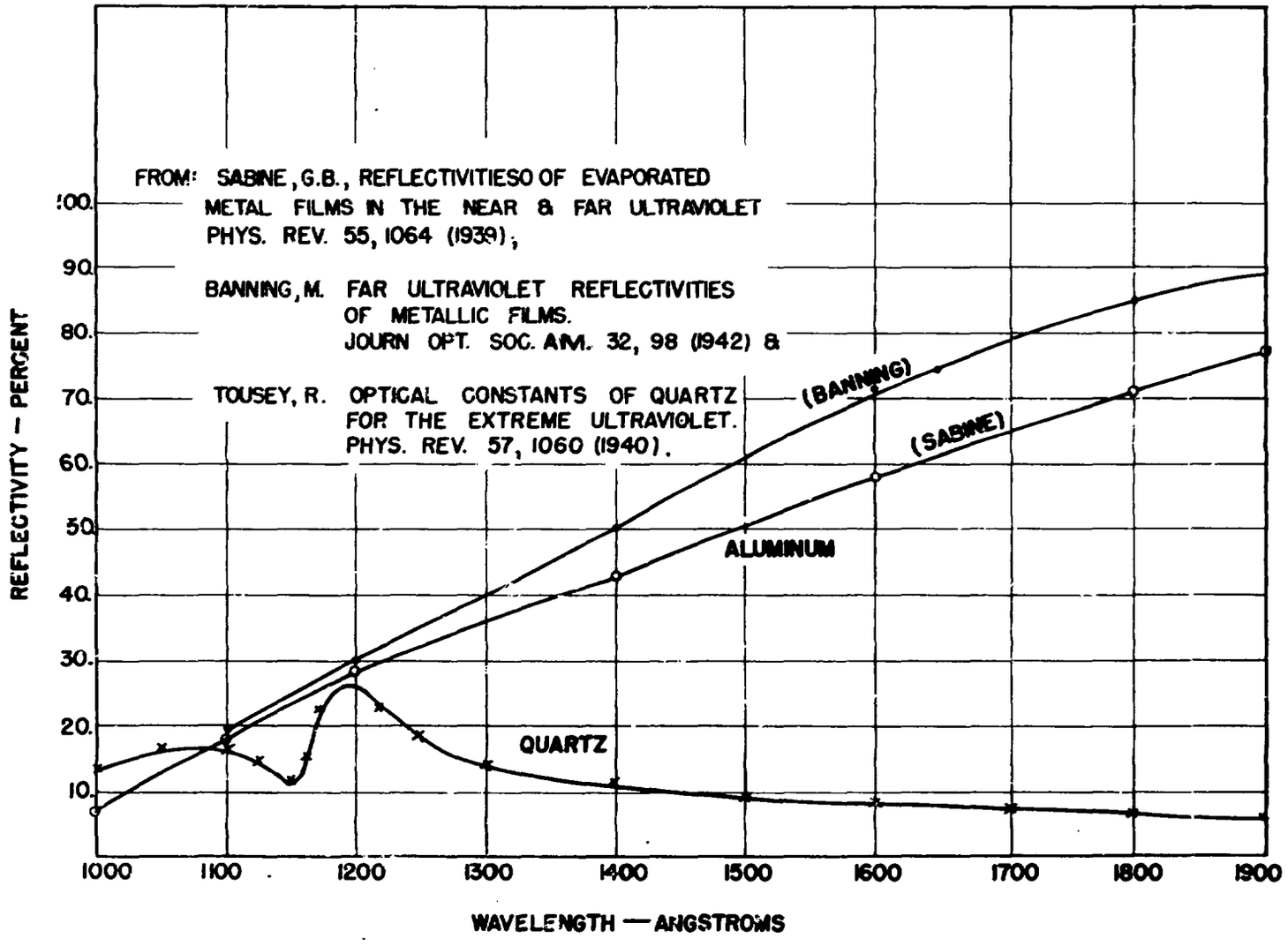

REFLECTIVITY OF POLISHED QUARTZ CRYSTAL AND EVAPORATED ALUMINUM

the spectra at longer wavelengths. As a compromise one aluminum mirror and one quartz mirror were employed, one in either side of the spectrograph.

As it happened the long exposure was not obtained, so that the effectiveness of the quartz mirrors is still to be determined.

Film Movement. The spectrograph was improved by placing a friction clutch between the film winding motor and the film take-up spool. This arrangement was found to result in a more satisfactory motion of the film than was provided by the spring coupling described in Report No. I.

4. Calibration of the Spectrograph. The spectrograph was calibrated by methods similar to those described on pages 75 and 76 of the first report. For several reasons these calibrations are only partially satisfactory. Since, however, the spectrograph was recovered after the October 10 flight, it is now possible to run complete and unhurried calibrations of the instrument to use in data reduction. Such calibrations are under way.

5. Electrical Circuits: Spectrograph Power. The power for the spectrograph motors came from the main 24 volt battery in the warhead. The spectrograph was protected from accidental operation and use of film prior to take off by two switches in series. One was a manual siwtch and was closed shortly before take off. The other was at the tail of the rocket and was automatically closed at the exact instant of take off as the rocket left the ground.

Telemetering. To determine the altitudes at which the successive spectrograms were taken it was necessary to know accurately the time after take off at which each exposure was made. From these data together with the altitude-versus-time relation determined by other agencies, the altitude for each exposure could be calculated. In order to obtain the time for each exposure a microswitch was arranged in the spectrograph so that it opened momentarily each time the film moved. This switch was connected into a telemetering network in the program timer as shown in Fig. 2 Chapter II, Section B. When the microswitch opened the voltage fed to telemetering channel No. 13 increased, as a result of which a signal was relayed to the telemetering ground station.

6. Preparation for Flight. Prior to the flight the spectrograph was taken to White Sands Proving Ground where it was used to make sure that it would fit into the fin installation which had been prepared. Before the firing the operating and telemetering circuits, along with the mechanical operation and the optical focus of the spectrograph, were checked. The film was loaded into the spectrograph on October 8 and the spectrograph installed in the fin on October 9. The lithium fluoride spheres were left covered with tape until 30 minutes before take off.

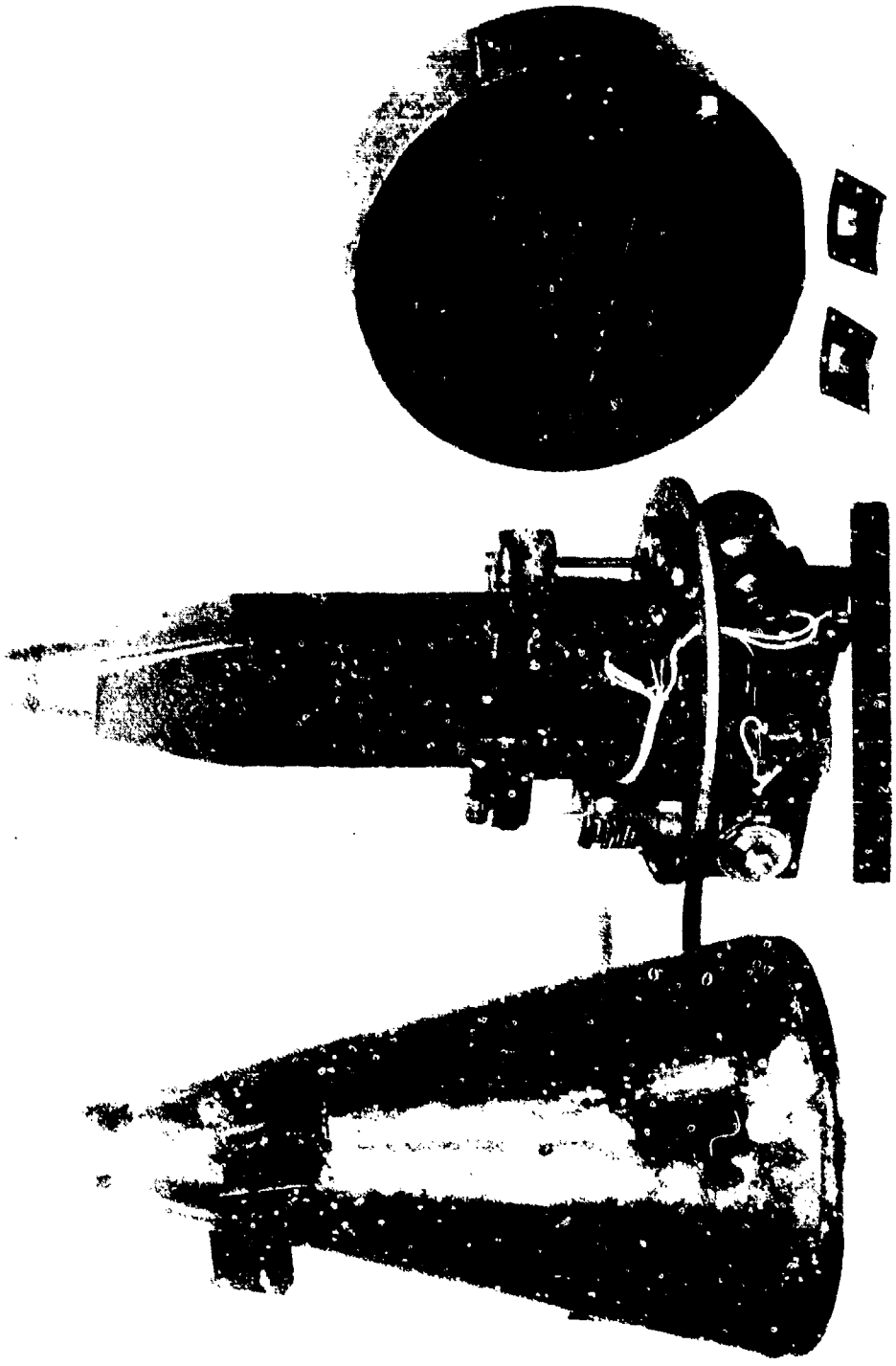

SPECTROGRAPH AFTER RECOVERY

7. Flight and Recovery. The rocket flight of October 10 was described above in Chapter I. The spectrograph was found on October 16 and returned to Washington two days later. The instrument was in excellent shape, as can be seen from the photograph shown in Fig. 7, which was taken at the Naval Research Laboratory following the recovery. There were only two small dents in the housing. The exposed surfaces of the lithium fluoride beads were somewhat pitted and quite dirty, but it is believed that this damage was due largely to exposure in the desert.

8. Time and Altitude Data. The telemetering record giving the times of film motion in the spectrograph showed signals of unexpectedly small amplitude and these could be followed for only 40 seconds after take off. The cause appeared to be the presence of an unanticipated voltage drop along the long lead from the battery in the warhead to the spectrograph in the tail. During the first 40 seconds the record indicated that the film was moving quite regularly with an 8 second exposure cycle. Times for the exposures made after 40 seconds were obtained by assuming that the spectrograph continued to operate with an eight second cycle and there is no particular reason to suspect that it did not.

The master time signal was not recorded due to failure of the radio link carrying the Aberdeen time signal from the block house to the telemetering ground stations. There are, however, two secondary time scales available, namely that given by a multivibrator in the cosmic ray equipment in the V-2, and that provided by the length of the telemetering record which presumably was run at constant speed. These two scales agree quite closely and were used to obtain the time at which exposures were made. The data shown in Fig. 1 of Chapter I were used to obtain the altitudes at which the exposures were made.

9. Film Development: The film recovered from the spectrograph was developed at the Naval Photographic Center in Washington. A large 35 mm developing machine was used in order to provide the most uniform development possible. Personnel of the Naval Photographic Center took great pains in determining the proper processing conditions and in handling the film. The development rate was adjusted so that the same characteristic curve was obtained as with 5 minutes of tray development at 20 degrees centigrade in D-19 as recommended by the Eastman Kodak Company.

10. Preliminary Results. The preliminary results obtained from visual examination of the spectrograph film are described in a letter to the Editor of the Physical Review, reproduced below.

* * * *

SOLAR ULTRAVIOLET SPECTRUM TO 88 KILOMETERS

by

W. A. Baum, F. S. Johnson, J. J. Oberly,
C. C. Rockwood, C. V. Strain and R. Tousey

Naval Research Laboratory
Washington, D. C.

The ultraviolet spectrum of the sun below 3400 A. U. was photographed to altitudes up to 88 km by means of a spectrograph mounted in the tail fin of a V-2 rocket. The rocket was fired on October 10, 1946 by Army Ordnance at the White Sands Proving Grounds, New Mexico, and reached an altitude in excess of 160 km. A series of 35 spectra was obtained during the ascent. Solar spectra above 88 km were not photographed because the rocket turned the spectrograph away from the sun, and excessively rapid use of film produced by severe vibration earlier in the ascent prevented operation above 107 km.

The spectrograph was designed for the nose of the rocket and utilized an f/10, 40 cm. radius, 15,000 line/inch grating in a Rowland mount. The grating was ruled on aluminum at the Johns Hopkins University. The film was Eastman 35 mm. 103-0 ultraviolet sensitized, and was 20 feet long. As many as 100 exposures could be taken. An eight second exposure cycle with separate exposures of 0.12, 0.66 and 3.6 seconds was provided. In place of a slit a 2 mm. diameter sphere of lithium fluoride was used. This formed a small real image of the sun which acted as source and because of the astigmatism introduced by the grating produced a line spectrum. This system accepted sunlight over a wide field of view and was many times faster than a conventional slit of equivalent width covered with a diffusing plate. A second bead was placed diametrically opposite the first to provide a second channel, thereby doubling the chance of receiving sunlight as the rocket turned. A plane mirror on each side folded the two light paths to fit the conical nose. The dispersion was 44 A.U./mm. and the resolution about 2 A.U. The spectrograph was evacuated by a port open to the atmosphere. The short wavelength limit of the spectrograph was set by the transmission limit of the lithium fluoride bead, and spectra to wavelengths as short as 1100 A.U. were produced in the laboratory.

Sample spectra are reproduced in Fig. 1*. All exposures shown were 3.6 seconds and altitudes given are above sea level. Up to about 44 km the rocket was stabilized. Above this point it rolled and yawed and spectra F and G were taken with the sun well off axis. Consequently G, the highest solar spectrum taken to date, was so lightly

* Fig. 1 of the letter is the same as Fig. 4 of this section.

exposed that it showed less ultraviolet than F. The spectra were shaded in printing to emphasize as much as possible the region of interest. Definition in E and F was reduced by vibration and by rotation of the rocket. It was a characteristic of the bead slit system that the spectra moved slightly, mainly along the lines, as the rocket rolled. The effect appears in spectra F and G which show the spectrum displaced somewhat along the lines during exposure.

Preliminary examination of the spectra showed a progressive extension of the spectrum into the ultraviolet. At 25 km the spectrum was photographed to 2925 A.U. Spectrum E taken at 34 km extended to 2650 A.U. and showed measurable blackening from approximately 2100 to 2260 A.U. which may be lost in reproduction. At 24 km therefore there was still enough ozone above to prevent recording the spectrum in the central region of the Hartley band of ozone, but transmission in the window between the Hartley band and the oxygen absorption at shorter wavelengths was observed. At 55 km sufficient ozone was passed through to permit photographing the spectrum throughout the Hartley Band.

An analysis of the absorption features of the spectrum and a determination of the solar spectral intensity curve of the sun and of the details of the ozone distribution in the atmosphere are in progress.

****

In addition to the information contained in the letter above, examination of the film revealed that the spectrograph was in operation for 120 seconds after take off. At this time the film supply became exhausted, due to the fact that after 16 exposures had been made two lengths of film were released at a time instead of one. The reason for this is not altogether clear, but whatever the explanation, the rapid windup of film exhausted the supply sooner than was intended and prevented the making of exposures above 107 kilometers.

11. Acknowledgment. The acknowledgments given in Report No. 1 in connection with the previous firing are still appropriate. In addition thanks are due to U. S. Army Ordnance and General Electric Company personnel for making the fin installation possible and for aid in recovering the spectrograph, and to Commander Greene and Mr. Trahan of the Naval Photographic Center for their generous help in developing the spectrographic film.

CHAPTER IV

UPPER ATMOSPHERE EXPERIMENTS CONDUCTED IN THE V-2

B. Pressure and Temperature Measurements at High Altitudes[1]

by

N. R. Best, E. Durand
and R. J. Havens

1. Introduction. On 10 October 1946 pressure and temperature measurements were made in the upper atmosphere by means of gages carried aloft in a V-2 rocket fired at White Sands. The experimentation described below is a continuation and extension of that of the June 28 firing, the results of which were incomplete and not entirely conclusive. The discussion also includes a critical evaluation of data recovery methods and gage performance. The details of the telemetering system employed for data transmission and a basic description of the gages is given in the report of the previous flight[2].

All gages used consisted of resistance elements, the resistances of which varied with the quantities to be measured. These gages were connected in series with fixed resistors across a battery. The voltage developed across either the variable or the fixed resistance was applied to the telemetering input terminals. All gages developed voltages in the range from 0 to 5 volts, eliminating the need for amplifiers.

Two channels were used for telemetering pressure and temperature measurements, and each of these was divided into 14 sub-channels by a motor driven commutator. Each sub-channel was sampled about once a second.

2. General Procedures: Calibration. Five sub-channels of each main channel were used for calibration. Separate precision dividers for each main channel were placed across the 24 volt supply battery and delivered 0, 1.5, 2.5, 3.5, and 4.5 volts to appropriate commutator contacts. Also, since the thermistor gage operated from a 6 volt battery, a third divider across this source delivered 3.5 volts to one of the contacts on the first channel in order to furnish a check on this source of potential.

---

(1) Cf. also Best, N.R., Durand, E., Gale, D.I., and Havens, R.J.: Pressure and temperature measurements in the upper atmosphere, The Physical Review, Vol. 70 (Dec., 1946)

(2) Naval Research Laboratory Report R-2955.

Although measurements showed that the supply battery delivered only 23.5 volts prior to takeoff, no correction was made to the readings since the gage voltages and the true calibration voltages were reduced in proportion. Comparison between readings from the 24 volt and the 6 volt sources during the flight showed that there was no further voltage change.

Reading the Record. Data was recorded at two telemetering ground stations. At the first station, the 23 channels were divided equally between two recording oscillographs with deflections of 1.5 inches for each of the pressure and temperature channels. At the second station, all 23 channels were applied to a single oscillograph, with only 0.75 inches per channel. The first station failed at about 60 seconds after the takeoff. With the exception of several short intervals during which the signal was lost, the second station operated until the rocket came apart at 410 seconds.

Since most of the data were taken from the record with the smaller deflection, great care was required in measuring deflections. The following procedure was adopted: A single fine pencil line was drawn parallel to the direction of paper travel, usually between adjacent calibration marks. A draftsman's rule with 60 divisions per inch was laid with its index at the estimated center of the telemetering mark, and the distance to the nearest reference (or calibration) line measured to the nearest 0.1 division. This distance could usually be checked by independent observers to within $\pm$ 0.1 division, which is $\pm$ 0.22 percent of full scale in the case of the record with the smaller deflection. The marks of known voltages appearing each cycle furnished a calibration of the telemetering system's linearity and sensitivity.

The first station, during its 60 seconds of operation, gave a remarkably clean record, so that the error in reading deflection was always negligible in comparison with other errors. The installation at the second station was slightly out of order, with the result that a small, variable "ripple" was superimposed on the record. When the ripple character was the same for datum and calibration marks, consistent results were obtained; but in other cases it was possible to introduce an error up to 1 percent of full scale by incorrectly locating the line.

As a result of a defect in the telemetering decoder at station No. 2, low data voltages on sub-channels which followed directly after high voltage indications were subject to an additional error of unknown amount. This defect introduced a high time constant in the response of the recorder, capable of masking the value of the voltage on succeeding commutator segments. This actually happened in the case of the platinum Pirani gages at low altitudes, the sampling of which followed the 3.5 and 4.5 volt calibrations.

For most of the record, and for any gage, the probable error in voltage read at the ground station is less than ± 1 percent, or ± 0.05 volts at most.

The general self-consistency of the data indicates that random errors are normally well below this. The question of systematic errors will be discussed later.

3. Gage Locations. Fig. 1 shows the longitudinal distribution of the 17 gages installed for the October 10 flight. Table I identifies the gages and gives the angle between the surface and the rocket axis, the wall thicknesses at various locations, and the range in which the gage could operate. In the case of the temperature gages, the approximate maximum temperatures reached during the flight are indicated in the last column.

4. Pressure Measurements: The Bellows gage. Pressure in the lower atmosphere was measured by a sylphon bellows gage, L, mounted behind the surface in the tail section. Pressures were communicated to the gage chamber through a 1/2 inch hole. Bellows displacement under the influence of changing pressure was transformed into rotation of the shaft of a Microtorque potentiometer through a lever attached to a waxed linen thread wrapped around the potentiometer shaft, as is shown in Fig. 2. Longitudinal acceleration effects were avoided by mounting the gage with the lever parallel to the thrust axis. The gage was found to be insensitive to vibrations up to 12g at 60 cps.

To provide equal strain about the free bellows configuration, about 1/2 atmosphere of air was sealed into the bellows. Hence, a temperature correction to the pressure reading was required, which for constant temperatures, was the same over the full pressure range. To allow for this correction, the calibration curve was shifted linearly in pressure to make the pre-takeoff readings agree with the local barometer reading. A similar adjustment was made for each Pirani gage, since these are also temperature sensitive.

The bellows gage broke on the ascent at an altitude of 11.5 km, presumably because of excessive vibration. At the end of this period, temperature gages on the skin in the tail location showed a rise of 30° C. Since the heat capacity of the gage was many times that of an equal area of wall, the air inside the bellows could not have changed temperature appreciably during the time available. As further evidence, one may note that a tail pressure gage, in a similar location, showed essentially a vacuum at the top of the flight when a temperature correction valid at the start of the flight was used. This shows that its temperature likewise did not change. Other systematic errors in the bellows gage should be small in comparison with the ± 1 percent (7.6 mm of Hg) telemetering error.

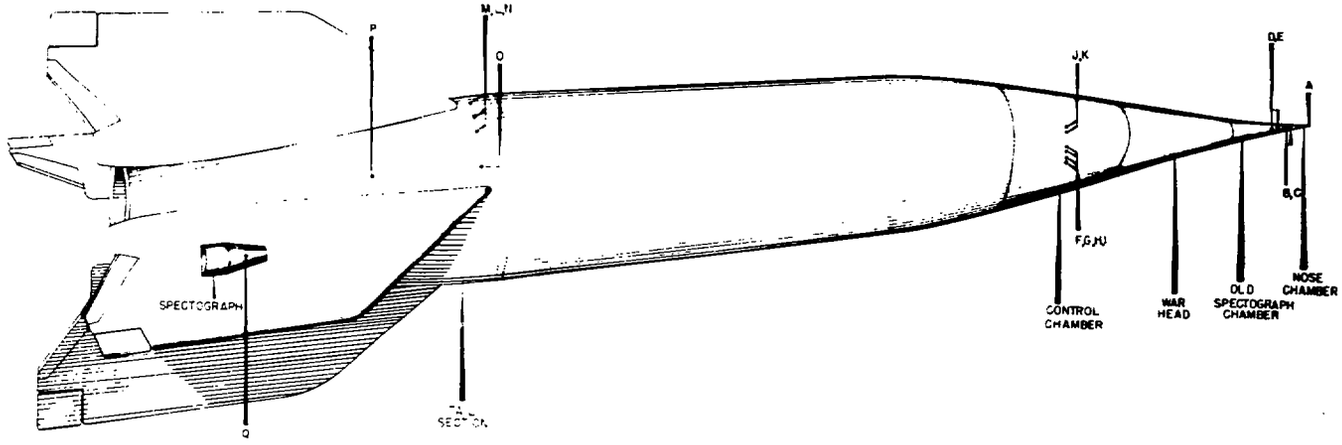

PRESSURE AND TEMPERATURE GAUGE LOCATIONS

CH. IV SEC. B FIG. 1

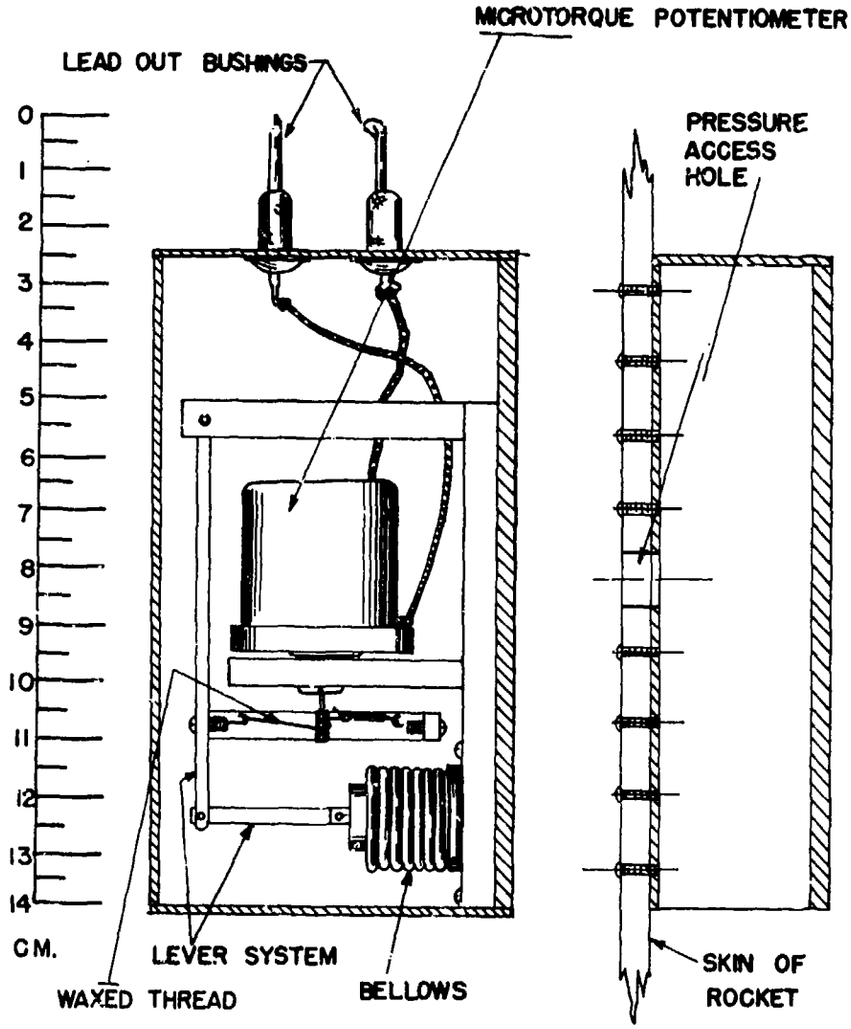

BELLOWS GAUGE

CH. IV SEC. B FIG. 2

The reduced bellows gage data are shown in Fig. 3. The solid curve was computed from data taken by balloon radio-sonde over El Paso, Texas, (altitude 1150 meters, 70 km from White Sands) at 8 AM on the morning of the flight. Similar balloon soundings made within a few kilometers of the launching site just after the flight show that atmospheric conditions at El Paso also existed over White Sands at the time of the flight. These latter data, however, were not used in the preparation of Fig. 3, since they were received too late. The heavy points are the experimental observations made by the bellows gage in the rocket. The agreement is good, except in the region where the rocket was passing from sub-sonic to super-sonic velocity. This indicates that in the location used, the gage read very nearly ambient pressure, i.e., static pressure, which would have been measured by a stationary gage in the atmosphere at that point. Furthermore, ambient pressures were recorded while the missile velocity varied over a wide range. This is in effect a calibration of the gage for (1) use in the specific position on the rocket at which the gage was installed, and (2) for use in the range of Mach numbers from 0 to 2. In the absence of more complete and accurate wind tunnel measurements of the pressure distribution over the rocket, it has been assumed that such a gage installation serves to measure ambient pressures over the much wider range of Mach numbers reached during the flight.

The Platinum Pirani Gages. The nose chamber gage assembly is shown in Fig. 4. The fine platinum filament, 0.7 mil x 2 cm, shown at C, is drawn heavily for clarity. Fig. 5 is a photograph of the tail gages. Here the filaments do not show. In the gage of Fig. 5C, the platinum wire is suspended between the wire arch and the center contact of the pilot lamp socket used as a base. The heavy radiation shields in which the gages were enclosed had a large enough heat capacity that their temperature did not change appreciably during the flight. Since the gas inside the shield would follow the shield temperature within a fraction of a degree the gages did not have to be corrected for temperature changes.

The gages were used in series with 330 ohm fixed resistors across a 24 volt battery. They developed about 1.1 volts at atmospheric pressure and 3.5 volts in a vacuum, where the operating temperature was approximately 1000° C. Most of the change occurred in the region between 1 and 5 mm of Hg., but usable sensitivities remained at 0.5 mm and at 20 mm of Hg.

Since the October 10 firing, a variation with time has been discovered in the calibration of the platinum gages. This time dependency is as yet unexplained. Readings taken at various times up to several hours after the admission of an air sample show a progressively reduced gage resistance, although the McLeod gage standards show no change. Different results are also obtained depending on whether the calibration run is taken by pumping out or by admitting the air. Be-

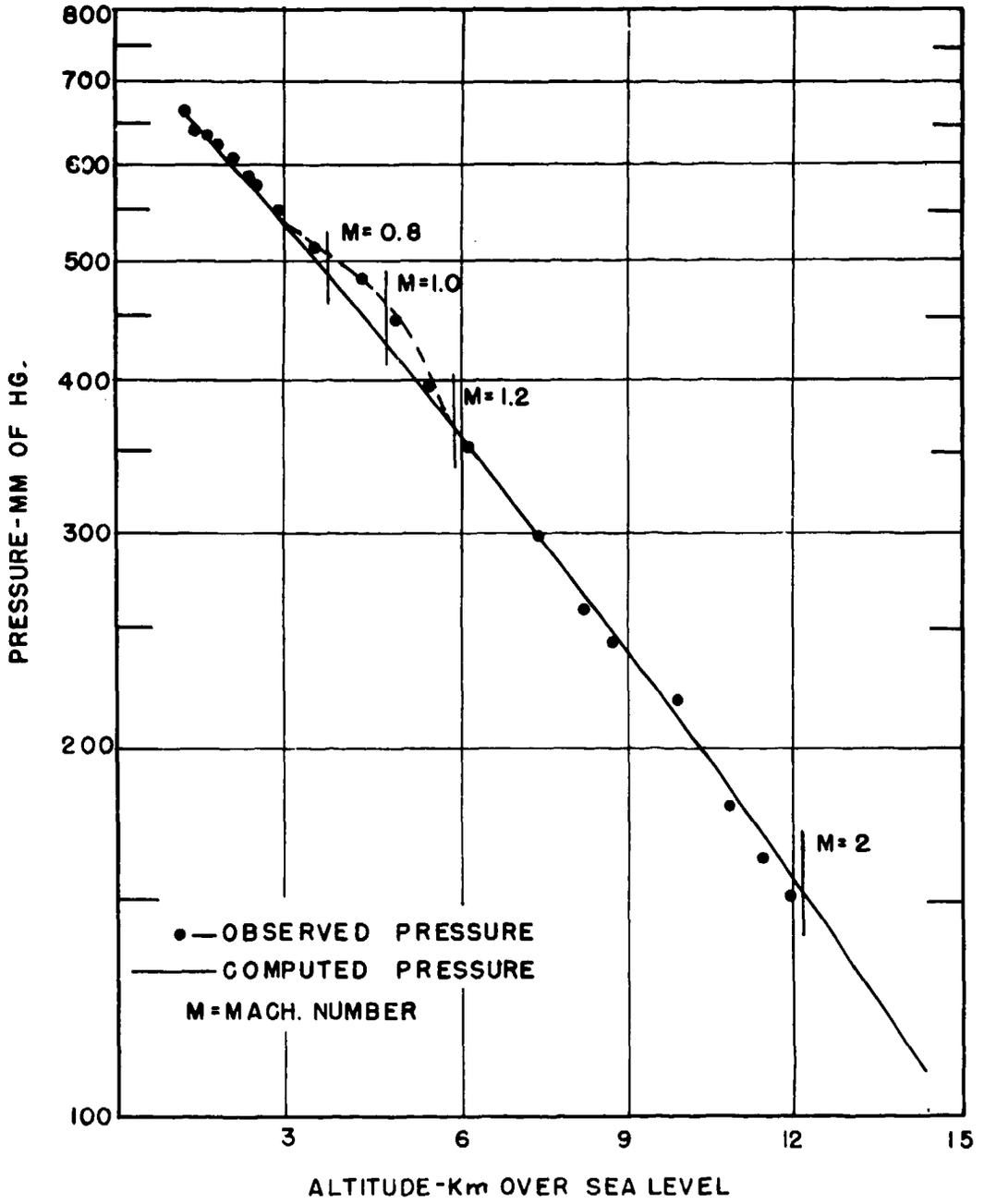

PRESSURES VS. ALTITUDE—BELLOWS GAUGE

CH. IV SEC. B FIG. 3

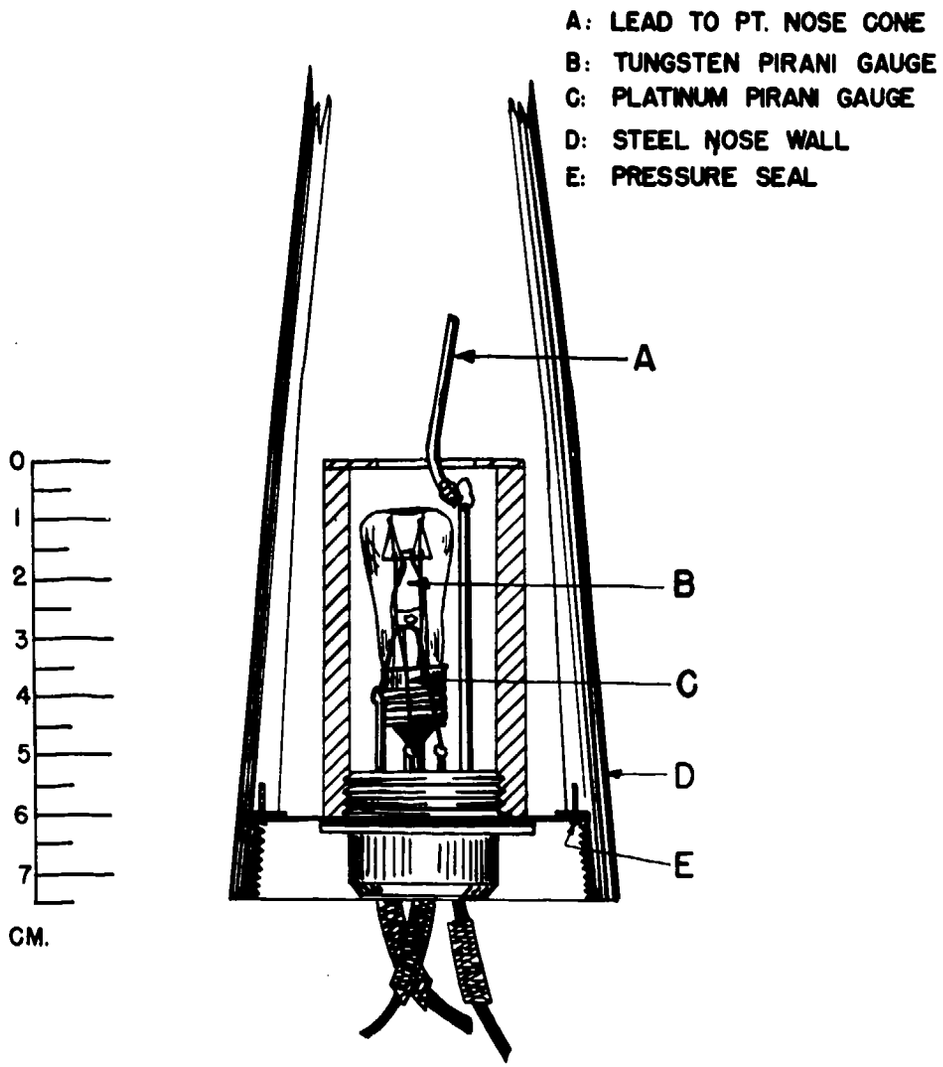

NOSE CHAMBER GAUGES

CH. IV SEC. B FIG. 4

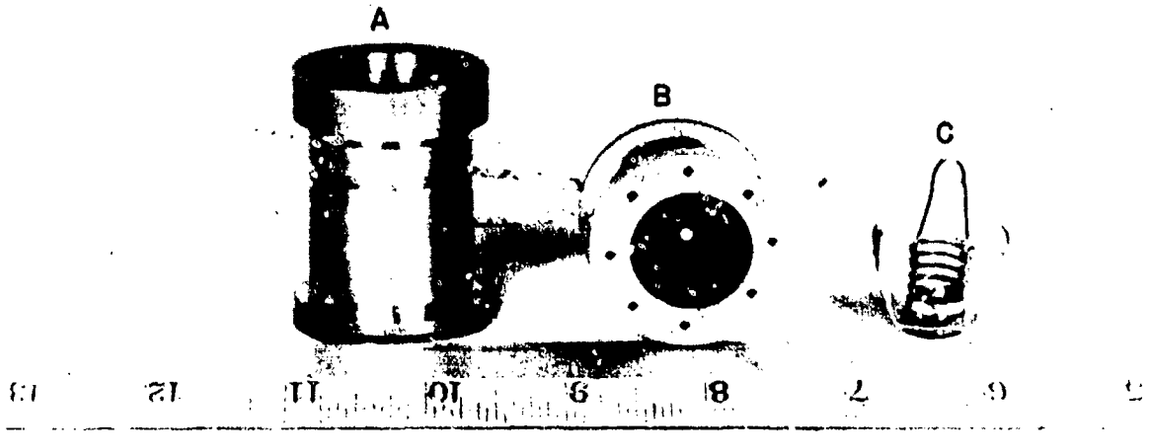

TAIL SECTION GAUGES

A. MOUNT (EITHER GAUGE).

B. TUNGSTEN PIRANI GAUGE IN MOUNT.

C. PLATINUM PIRANI GAUGE ELEMENT.

cause of this, and because of the special telemetering error previously mentioned, curves of the observation taken with the platinum gages are not published at this time.

The Tungsten Pirani Gages. Three tungsten Pirani gages were installed in the nose, tail, and spectrograph chambers as shown in Fig. 1, points B, N, and Q, respectively. The nose gage may be seen at B in Fig. 4; the tail gage is shown in Figs. 5B and 6. The third gage was installed as a service to the spectroscopy program.

The gage elements were simply 6 watt, 110 volt Mazda pilot lamps with the top portion of the glass bulb removed and supporting wires firmly cemented to the filament. They were used with 2700 ohm series resistors across the 24 volt battery, developing about 1.7 volts at atmospheric pressure, and 3.6 volts in a vacuum. In the range from 1 to 50 microns of Hg., the voltage varied linearly with pressure, with a slope of about 65 microns per volt. The assumed telemetering error of $\pm$ 0.05 volts therefore corresponded to $\pm$ 3.3 microns in this region. Above 100 microns, the voltage was almost linear in the reciprocal of the pressure, the slope being about 160 in (micron volts)$^{-1}$. The percentage error, therefore increased with pressure. At 200 microns, the uncertainty was from 100 to -50 microns. The results, which are plotted in Figs. 7 and 8, do not exhibit this much variability, especially at the high pressure end, so that the random telemetering error must have been much less than the estimated $\pm$ 1% for these points.

Laboratory experiments have shown that the tungsten gages are not afflicted with the calibration difficulties of the platinum gages. Furthermore, one does not expect any large systematic errors in their operation. Consequently, it is difficult to understand why the nose and tail tungsten gages have almost identical readings at the various altitudes covered, since both theoretical and experimental work by Taylor and Maccoll (2) has shown that the pressure on the side of a cone of the type used, moving at the speed of the V-2, should be about twice ambient pressure.

Zdenek Kopal, of the Electrical Engineering Department, M.I.T., has made calculations, as yet unpublished, of the pressure on the side of a moving cone for a variety of cone angles and Mach numbers, taking into account higher order terms in the Taylor-Maccoll theory. An accuracy of better than 1% is claimed. The calculations indicate that at 80 seconds after takeoff the pressure at the nose should have been 2.35 times ambient. German wind tunnel data likewise show about the same pressure build up, and also show that gages at the tail locations used should read ambient pressure to within $\pm$10%. These facts are clearly at variance with the tungsten gage data.

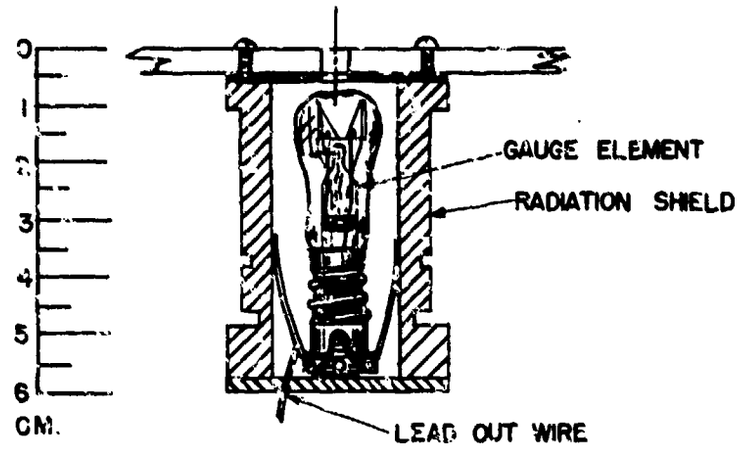

TUNGSTEN PIRANI GAUGE-TAIL MOUNT

CH. IV SEC. B FIG. 6

5. General Discussion of the Pressure Data from the October 10 Experiments. The good agreement between the bellows gage data, Fig. 3, and the curve computed from Weather Bureau soundings shows that ambient pressure can be determined by measurements made at a suitable location in the tail of the V-2 rocket.

The upper atmosphere measurements made at the tail location, shown in Fig. 7, are in good agreement with the "Standard Atmosphere" published by the National Advisory Committee for Aeronautics[3] with which the measurements are compared. The temperature of the troposphere on the day of the flight was higher than the NACA standard temperature from which the standard atmosphere pressures were derived. At 12 km, therefore, the true pressure was greater than standard pressure. Between 12 km and the upper limit of the radio-sonde flight which was at 17 km, the temperature was below the standard temperature, with the result that the pressure was equal to the NACA value at the highest altitude reached by the balloon. This stratospheric temperature, if maintained below standard for a few more kilometers above the 17 to which the balloon observations were made, would account for the slight difference between observed and NACA pressures in the 50-80 km region.

Temperature Measurements. Seven platinum wire skin temperature gages and three thermistor temperature gages were installed at points D to K, O and P as shown in Fig. 1 and in Table I. Fig. 10 shows details of their construction.

Two platinum wire gages were on the warhead nose piece where the walls were 8.5 and 9.0 mm in thickness and the angles between the surface and the axis of the rocket were 10.5° and 16.7° respectively. Because of the thickness of the skin there was a considerable time lag between outside and inside temperature.

Three platinum and three thermistor gages were on three plates of thicknesses approximately 0.25, 0.5 and 1.0 mm located at D to K. The angle between the surface and axis at these points is 9°. It was intended that the three points with different heat capacities should furnish an indication of the rate of heating of the surface of the rocket from which boundary layer temperatures could be deduced. Actually, however, the surface is too irregular to give consistent data. A platinum cone at the nose of a rocket the translational velocity of which is not greater than thermal velocities could be used to calculate ambient temperatures up to about 50 km. Since the October 10 rocket was not slow, in this sense, the adiabatic heating was much larger than the absolute ambient temperature. However, the results demonstrated that this method should work on slow rockets.

The platinum cone was installed on the tip of the nose as shown in Fig. 1, location A. The gage is shown in detail in Fig. 9. It

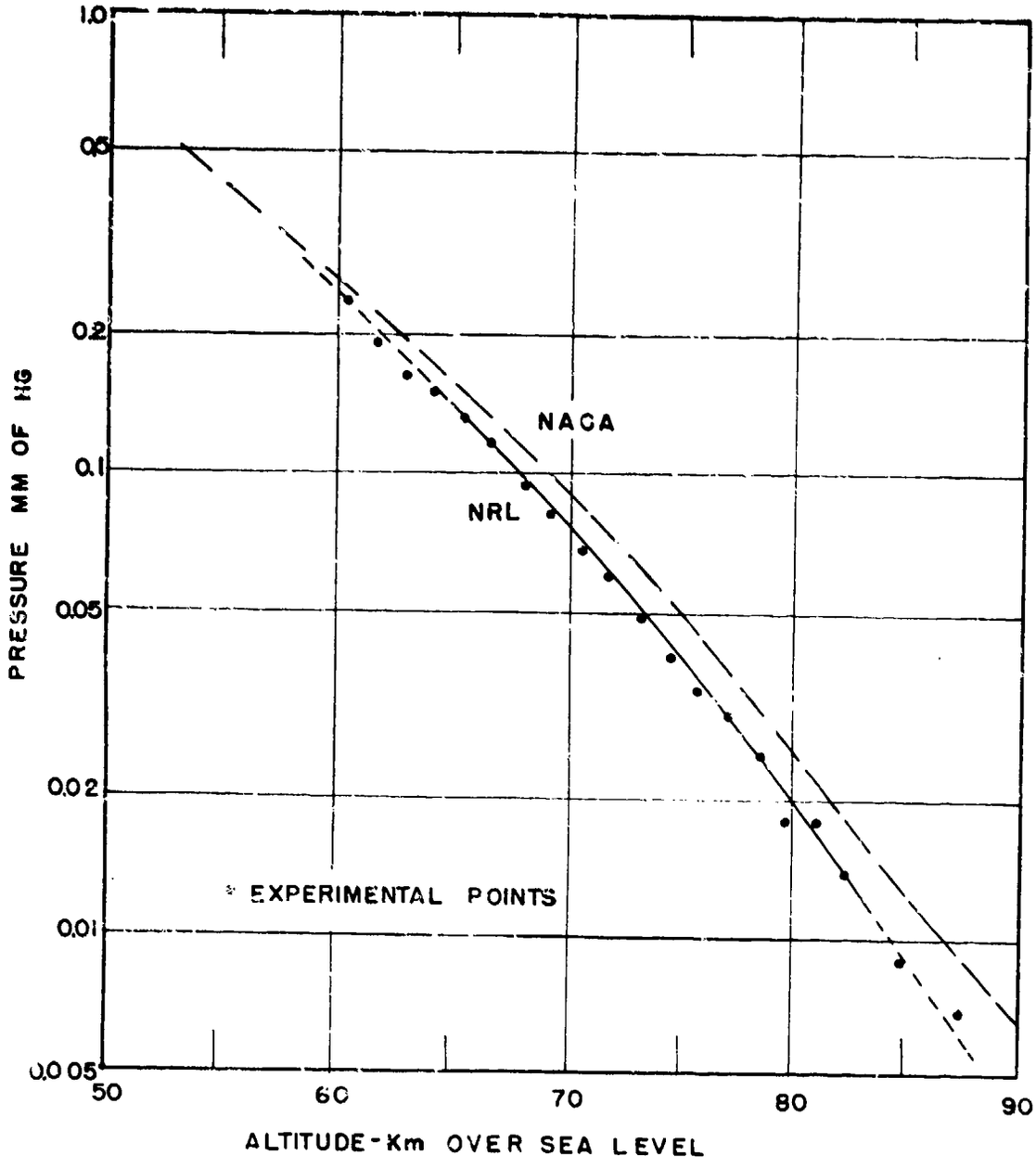

TAIL TUNGSTEN PIRANI GAUGE.

CH. IV SEC. B FIG. 7

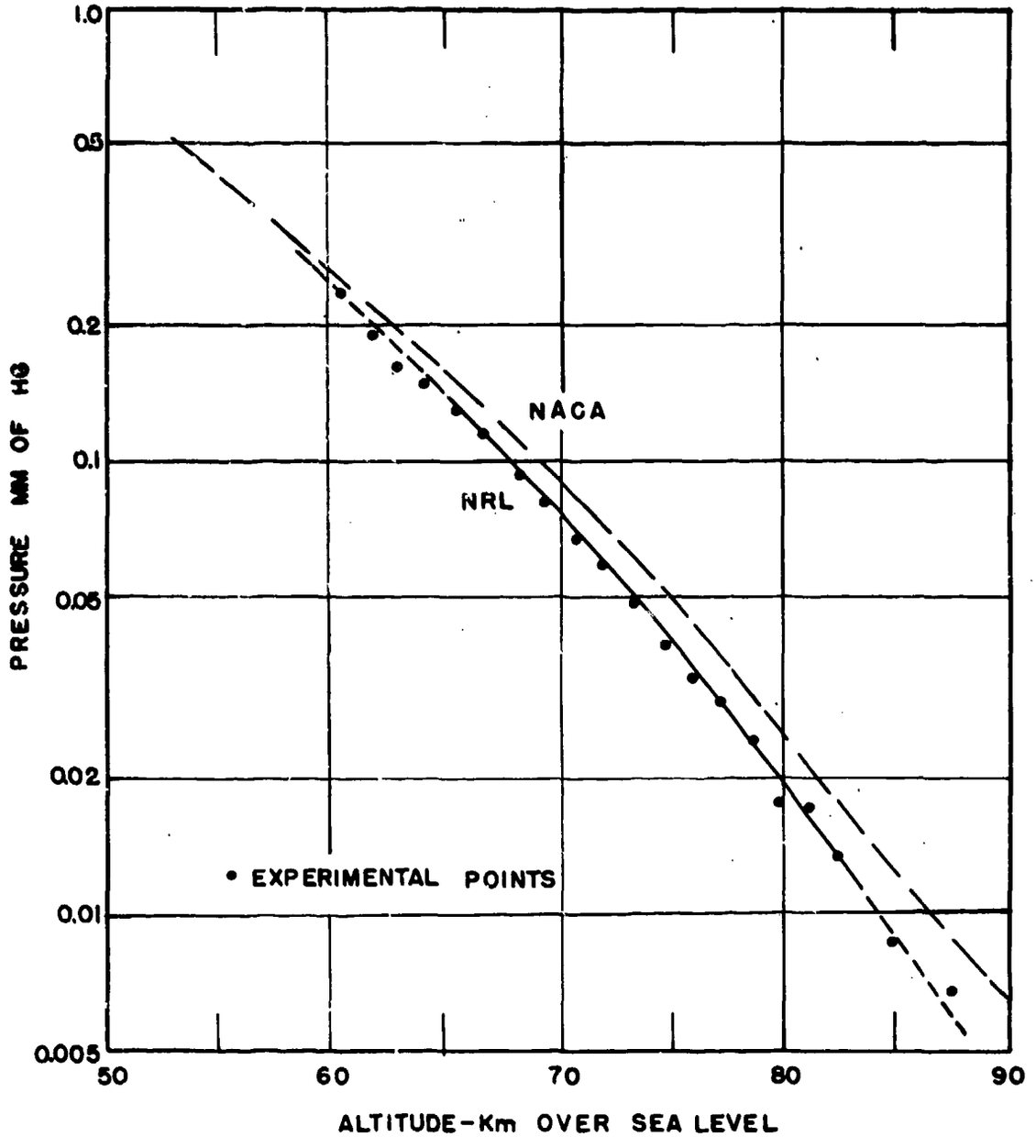

NOSE TUNGSTEN PIRANI GAUGE.

CH. IV SEC. B FIG. 8

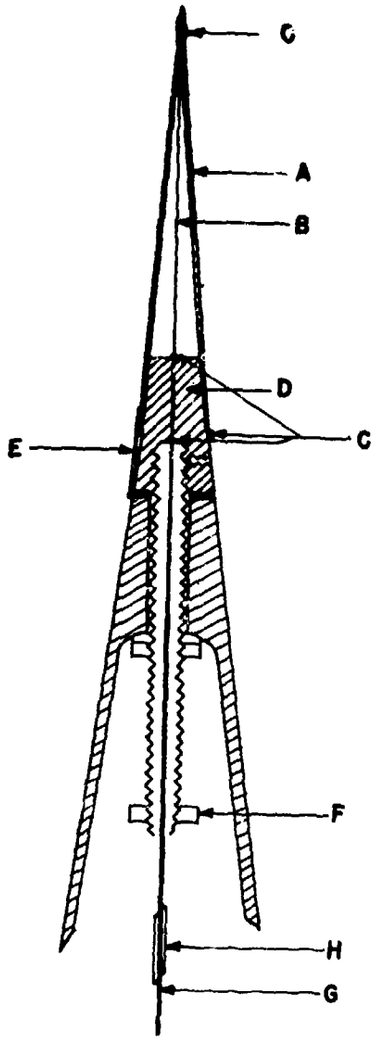

A. PLATINUM FOIL CONE
B. PLATINUM WIRE
C. INSALUTE CEMENT
D. LAVA CONE
E. PLAT. WASHER & STRAP
F. LOCKING NUT
G. LEAD OUT WIRE
H. INSULATOR

NOSE CONE TEMPERATURE GAUGE

CH. IV SEC. B FIG. 9

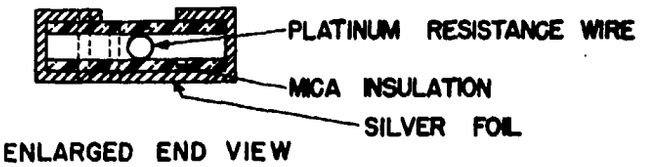

ENLARGED END VIEW

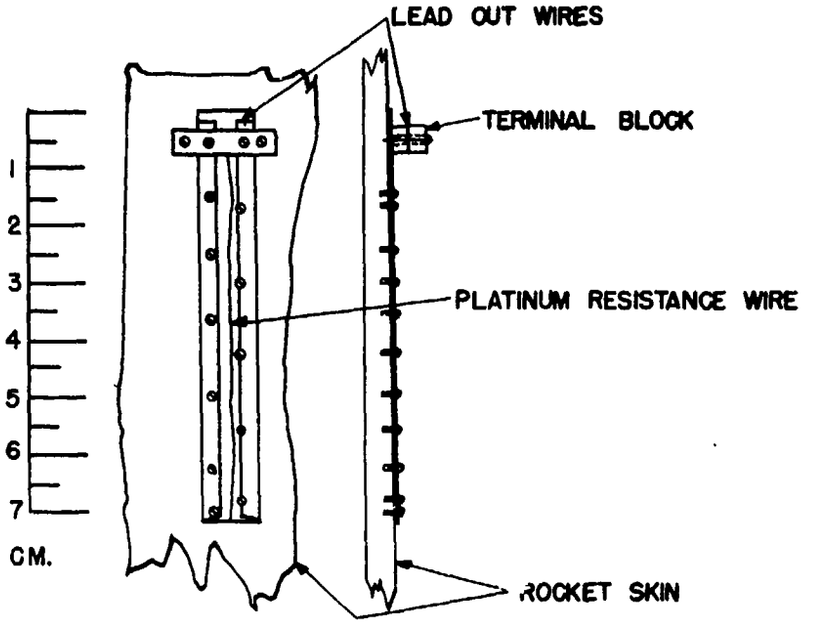

PLATINUM RESISTANCE TEMPERATURE GAUGE

CH. IV SEC. B FIG. 10

consisted of a polished platinum cone of 2 mil wall thickness. Heat capacity and emissivity were purposely kept low in its construction. The cone and its supporting wire acted as a resistance thermometer.

Other gages were located just past the start of the inward curve near the tail of the rocket as shown in Fig. 1, location O. Another gage was installed at P in Fig. 1, where the inward curvature of the skin was considerable.

The maximum observed temperatures, which were all reached at about 70 seconds after takeoff, are listed in Table I. The values of some of the platinum gages after 50 seconds were too high, because each tends to act as a Pirani gage in the lower pressure regions when perfect contact is not made with the surface to be measured. The gages that showed this effect could be determined from the readings after the rocket re-entered the atmosphere. The erroneous readings were eliminated.

The use of rate-of-change-of-temperature data is an approach to the problem of measuring ambient temperature. For constant composition, which is assumed to 80 km, the temperature may be determined by measuring the slope of the curve of logarithmic pressure vs. height. Use of this method, however, requires great accuracy in the determination of individual points. In Fig. 7, for example, the slope of the experimental curve was measured at altitudes of 65 and 78 km, and was found to correspond to temperatures of 300° K and 220° K respectively. These are to be compared with 330° K and 240° K taken from the NACA tables. These experimental temperatures are only approximate. For instance, a straight line is not incompatible with the observed points, considering probable errors. This would correspond to a constant temperature of 265° K over the range covered. On the other hand, the curvature of experimental points as plotted is seen to conform to the curvature of the NACA curve, which corresponds to a negative temperature gradient.

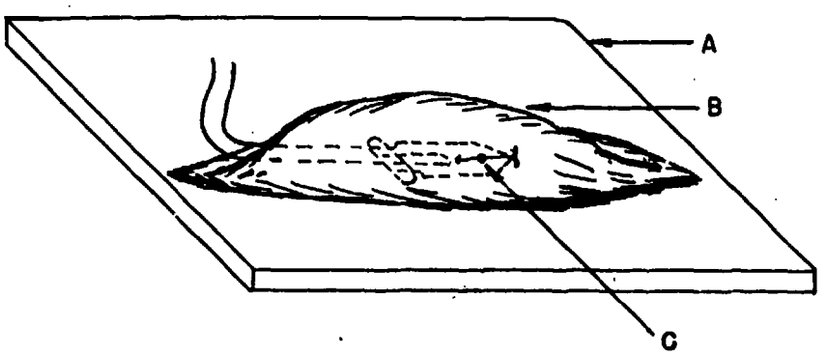

A - SKIN

B - CEMENT

C - THERMISTOR BEAD

THERMISTOR MOUNT

CH. IV SEC. B FIG. 11

TABLE I

TABLE OF GAGES USED ON THE OCTOBER 10 FLIGHT

SYMBOL	DISTANCE FROM NOSE (Meters)	ANGLE BETWEEN SKIN AND AXIS	GAGE	SKIN THICKNESS (Millimmeters)	APPROXIMATE RANGE COVERED BY GAGE	MAXIMUM TEMPERATURE CHANGE MEASURED (°C)
A	0	5°	Platinum Cone	0.05	0 - 1200°	600 ± 20
B	0.24	6.3°	Tungsten Pirani	--	0.01 - 0.5 mm	--
C	0.24	6.3°	Platinum Pirani	--	0.5 - 20 mm	--
D	0.52	10.5°	Platinum Resistance	8.5	0 - 700°C	50 ± 5
E	0.64	16.7°	Platinum Resistance	9.0	0 - 700°C	60 ± 10
F	3.11	9°	Thermistor	0.3	0 - 140°C	140
G	3.11	9°	Thermistor	1.0	0 - 140°C	--
I	3.11	9°	Platinum Resistance	0.3	0 - 700°C	170 ± 15
J	3.11	9°	Platinum Resistance	0.5	0 - 700°C	160 ± 10
K	3.11	9°	Platinum Resistance	1.0	0 - 700°C	--

TABLE I (Cont'd)

SYMBOL	DISTANCE FROM NOSE (Meters)	ANGLE BETWEEN SKIN AND AXIS	GAGE	SKIN THICKNESS (Millimeters)	APPROXIMATE RANGE COVERED BY GAGE	MAXIMUM TEMPERATURE CHANGE MEASURED (°C)
L	10.15	0°	Bellows	—	20 - 760 mm	--
M	10.15	0°	Platinum Pirani	—	0.5 - 20 mm	--
N	10.15	0°	Tungsten Pirani	--	0.5 - 20 mm	—
O	10.15	0°	Platinum Resistance	0.5	0 - 700°C	145 ± 10
P	11.37	--	Platinum Resistance	0.5	0 - 700°C	45 (at 40 sec.) -80 (after 100 sec.)
Q	—	--	Tungsten Pirani	—	0.01- 0.5 mm	—

REFERENCES

(1) Upper Atmosphere Research Report No. 1. NRL Report R-2955, October 1, 1946.

(2) TAYLOR, G. I. and MACCOLL, J.W.: Proc. Roy. Soc. 139, 278 (1933)

(3) National Advisory Committee on Aeronautics, Tentative Tables for the Properties of the Upper Atmosphere, Table III (Prepared by Calvin N. Warfield) Sept. 1946.

(4) KRAUS and HERRMANN: The magnitudes of boundary layer temperatures, heat transfer coefficients and skin temperatures of vertically and obliquely launched A4 missiles and A4b glider. Hydraulic Research Institute, Munich, February 25, 1945.

CHAPTER IV

UPPER ATMOSPHERE EXPERIMENTS CONDUCTED IN THE V-2

C. The Cosmic Ray Experiment

by

S. E. Golian, E. H. Krause, and G. J. Perlow

The essential details of the cosmic ray experiment performed in the V-2 on October 10, and of the results obtained, are given in a letter to the Editor of The Physical Review. The letter is reproduced below.

* * * *

ADDITIONAL COSMIC RAY MEASUREMENTS WITH THE V-2 ROCKET

The Naval Research Laboratory, Washington, D. C.

Another Cosmic Ray experiment has been done in a V-2 rocket fired on October 10 at White Sands, New Mexico (Geom. $\lambda = 41°N$). Measurements were made with the counter arrangement shown in Figure 1, of the ratio of total intensity as measured in the three-fold telescope 1,2,3, to the intensity below 15.2 cm. of lead as measured by the four-fold coincidences 1,2,3, (6+7+8). The quantities included in the parentheses were electronically paralleled for this data. Because of space limitations, it was not possible to make the solid angle of the four-fold set completely include that of the three-fold. The ratio of these solid angles was determined to be 0.37 by a ground calibration. A third channel measured six-fold coincidences 1,2,3, 6,7,8. Each of these three channels was protected against the shower rays found in a previous experiment[1] by anti-counters 4 and 5 all operating in parallel. In a fourth channel, unprotected coincidences 1,2,3, were transmitted. The difference between this data and the similar, protected data give a measure of the showers.

---

1. S.E.Golian, E.H.Krause, and G.J.Perlow, Phys. Rev. 70 223 (1946)

The counters used had 0.8 mm. brass walls. Resolving times for each channel were 5×10^{-6} sec. Data were transmitted to ground by the same radio system used in the previous flight. The altitude attained was in excess of 160 km.

The telescope axis pointed south at a zenith angle of 45° through a 3 mm. steel "window". Both zenith angle and azimuth were preserved through the atmosphere, but the telescope axis precessed about the zenith in free space. "Free space" is taken as the region of less than 2 mm. Hg. pressure.

Curve A in Figure 1 shows the altitude dependence of the protected total intensity. It is seen that the counting rate in free space (based on 252 counts) was about 1/3 that at the maximum (based on 22 counts.) For the hard component, however, the counting rate within the atmosphere was too low to permit drawing a curve. Only two points are shown; the ground point determined by several hours of calibration, and the point in free space for which 150.6 seconds of data (63 counts) was used. It is seen that the penetrating component amounts to about 70% of the total radiation. The shower rate in free space (480 counts) was again high as may be noted by curve B which is the difference between the unprotected and protected coincidences 1,2,3. The validity of the dip in this curve at 12 mm. Hg. is questionable. Of the 63 hard counts in free space 13 were associated with showers below the lead.

In the experiment of Schein, Jesse, and Wollan[2], it was reported that very few of the particles penetrating 4 cm. of lead produced showers under 2 cm. The present results would appear to be consistent with that data if the non-penetrating radiation were fairly soft. Further experimental work is in progress.

The writers wish to acknowledge the aid of their colleagues in the Rocket Sonde Research Section of the Naval Research Laboratory, and are especially indebted to Professor J. A. Wheeler, Princeton University, for helpful discussion.

---

2. M. Schein, W.P.Jesse, and E.O.Wollan, Phys. Rev. 59 615 (1941)

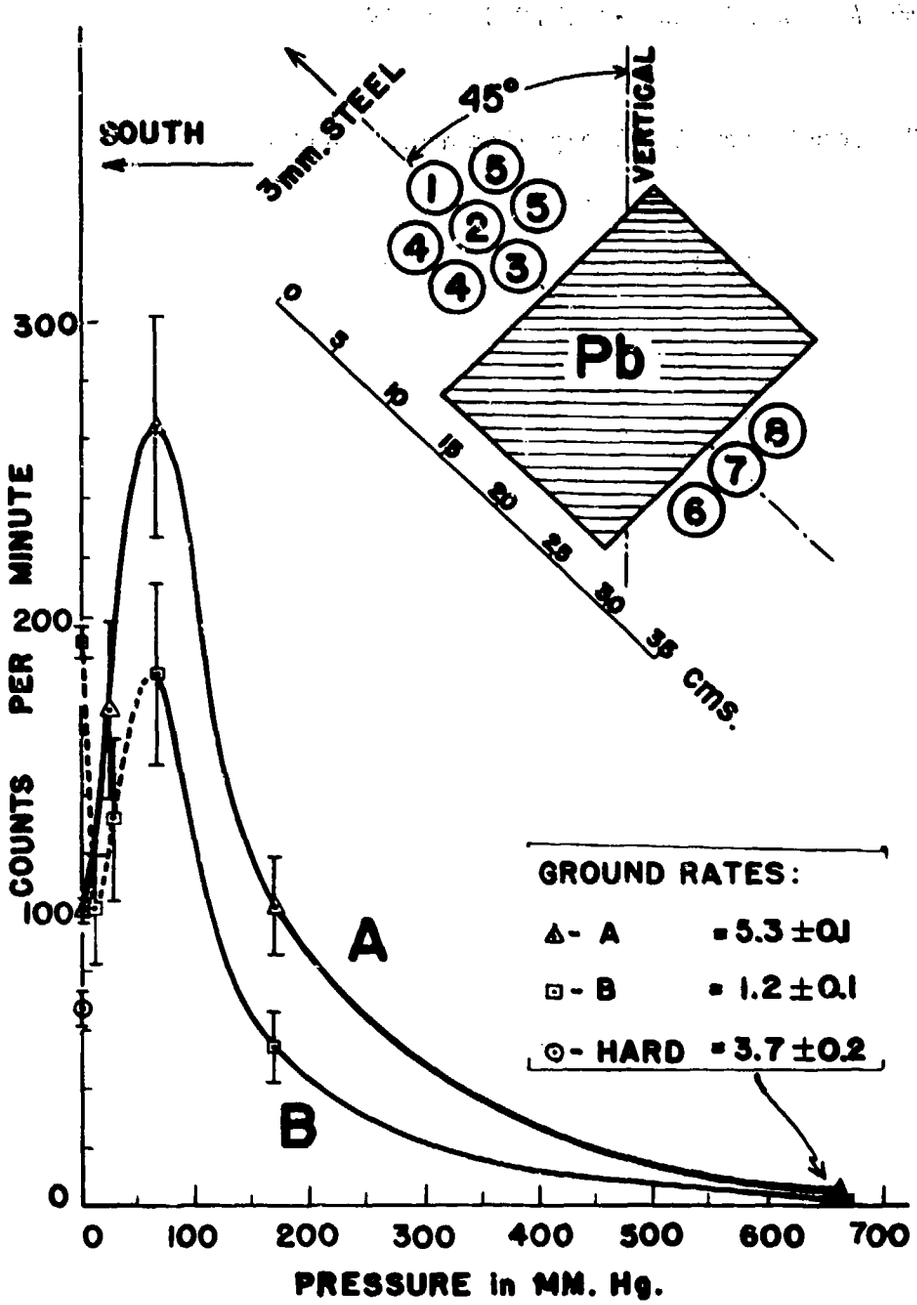

COSMIC RAY INTENSITY VS. ALTITUDE

CH. IV SEC. C FIG. 1

CHAPTER IV

UPPER ATMOSPHERE EXPERIMENTS CONDUCTED IN THE V-2

D. The Cosmic Ray Auxiliary Electronics and Recorder

by

B. Howland and M. L. Kuder

In the October 10 firing, provision was made to return cosmic ray data to the earth in two ways. The primary method was similar to the one which was used in the June 28 firing and was described in the first Upper Atmosphere Research Report*. It employed the Naval Research Laboratory's telemetering system, which is discussed both in that report and in Chapter III of this report. The second method is described here as part of the cosmic ray experimentation, but it will be plain that the method is more generally applicable than just to cosmic rays.

The method employs a compact ten channel recorder capable of recording both periodic and transient phenomena. The recorder comprises two elements: (1) a modified 16 mm motion picture camera which photographs a bank of neon lamps; and (2) associated electronic circuitry. The instrument affords a means of recording a relatively large amount of data in return for a small expenditure of space.

The camera used is a Bell and Howell type N-6A 16 mm movie camera, shown in Fig. 1. It is driven by a self contained electric motor which operates on 24 volts DC. Normally the camera produces intermittent motion of the film at the standard speeds of 16, 32, or 64 frames per second. By removing the dog which normally pulls the film along one frame at a time, the camera was modified to allow the film to run continuously. The film was then driven continuously at the usual magazine sprocket, and two extra pulleys were added to guide the film. The revolving shutter was removed. Also, the gearing between the motor drive and the film sprockets was changed, reducing the film speed to 4/11 of its normal value. The 15.24 meters (50 feet) of film contained in the standard magazine was enough for approximately 6.9 minutes of recording.

The recording elements in the system were 1/25 watt neon lamps. Ten such lamps were mounted in two staggered rows of five behind a plate containing ten correspondingly placed apertures, 0.8 mm (1/32 in.)

---

* Naval Research Laboratory Report No. 2955 (1 October 1946)

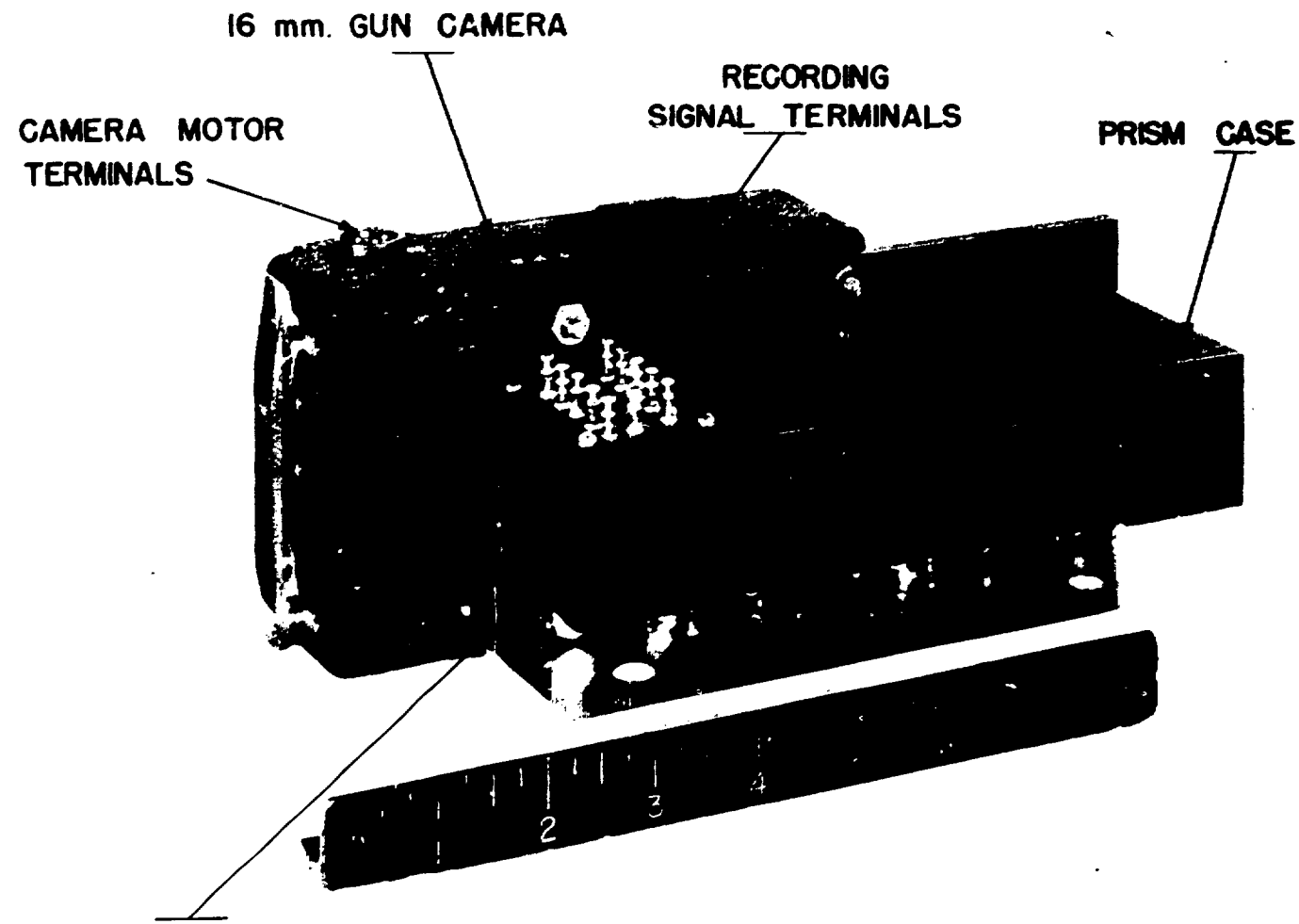

THE 10 CHANNEL RECORDER ASSEMBLED

in diameter. The general arrangement is illustrated in Figs. 2 and 3, and a diagram of the optical system appears in Fig. 4. Since the diameter of an image spot on the film was 0.165 mm (0.0065 in.) the maximum frequency which could be resolved was, theoretically, 223 cycles per second. Actually, current pulses through a lamp occurring at a rate of 250 per second could be distinguished on the film even though the spots overlapped slightly. The lamp circuit current was 3 milliamperes and the lens stop was set at f 3.5. Under these conditions, super XX Kodak film is completely exposed, producing a high contrast record such as that shown in Fig. 5. It was estimated that this combination of exposure factors would easily provide a safety factor of 4.

The electronics used with the recording camera is shown in Fig. 6. Three types of channel were provided: type A, which accepts an input pulse from the cosmic ray electronics; type B, which accepts a direct current data voltage; and a time reference channel.

The electronics for the cosmic ray channels consisted of a cathode follower converting a very high impedance input to a low impedance output for the neon lamps. Four of these channels were provided for recording different cosmic ray data concurrently.

The direct current metering channel, type B, was more complex. It converted a DC voltage level to a frequency. This was accomplished by applying the amplified DC data voltage to the common bias grid return of the two tubes of a symmetrical multivibrator. The data voltage was applied to the multivibrator through an amplification stage which had a high impedance input. The frequency of the multivibrator decreased from 50 to 24 cycles per second as the data voltage level increased from 0 to 5 volts. The output of the multivibrator was coupled to the neon lamp through a cathode follower of the type employed in the cosmic ray channels. The response of the system was approximately linear, and was improved by providing some degeneration in the cathode circuit of the amplification stage. The use of a regulated power supply provided some degree of stability. The record appeared as a series of short bright lines, as shown in Fig. 5. It is interpreted in conjunction with the time channel record.

Time reference was provided by a freely running multivibrator whose period was fixed at one second by an adjustable potentiometer. Its output was recorded on the film by the method employed for the other multivibrators. A sample record is reproduced in Fig. 5.

The number of cycles occurring per second in a direct current metering channel may thus be read directly from the film record. This frequency may be interpreted as a voltage by making reference to the calibration curves of input voltage vs. multivibrator frequency which

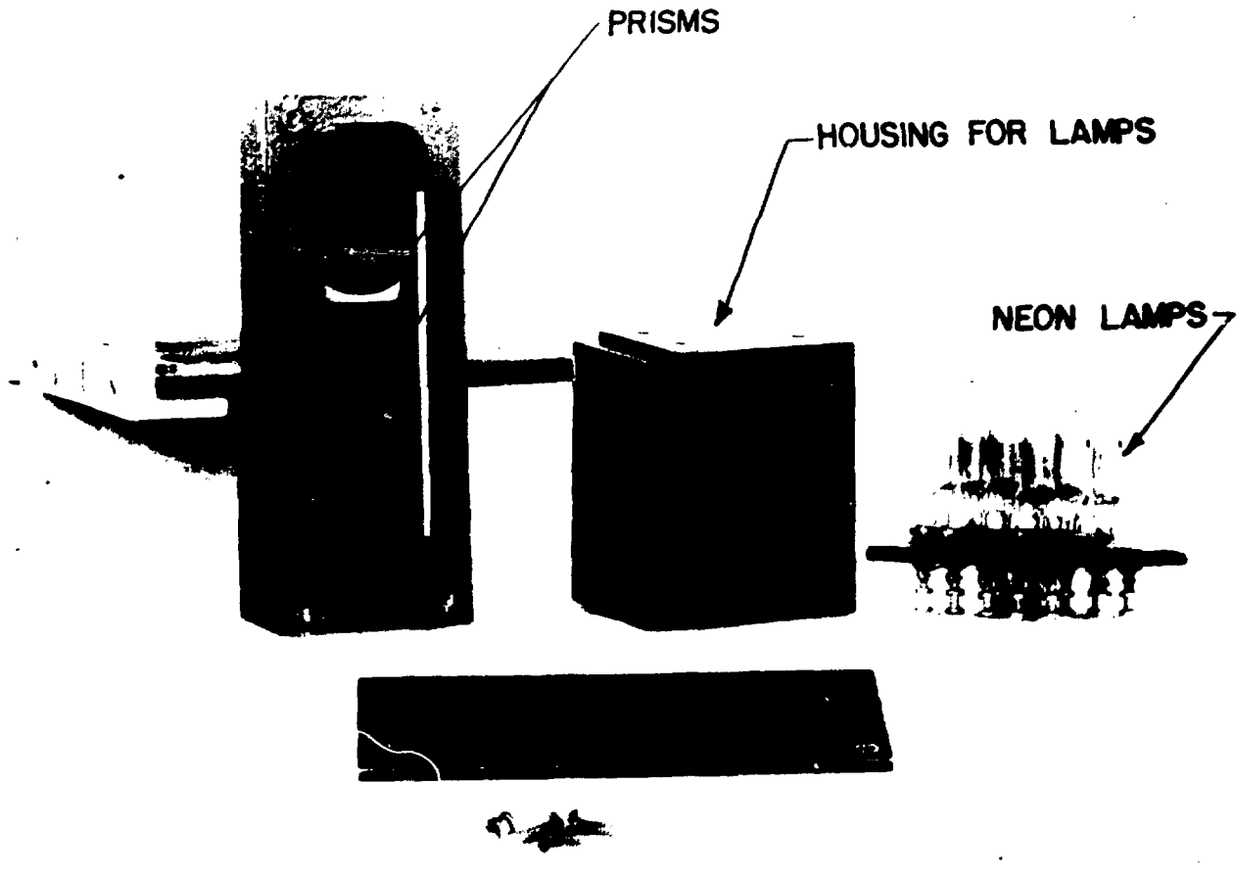

THE 10 CHANNEL RECORDER SHOWING
THE NEON LAMPS & HOUSING

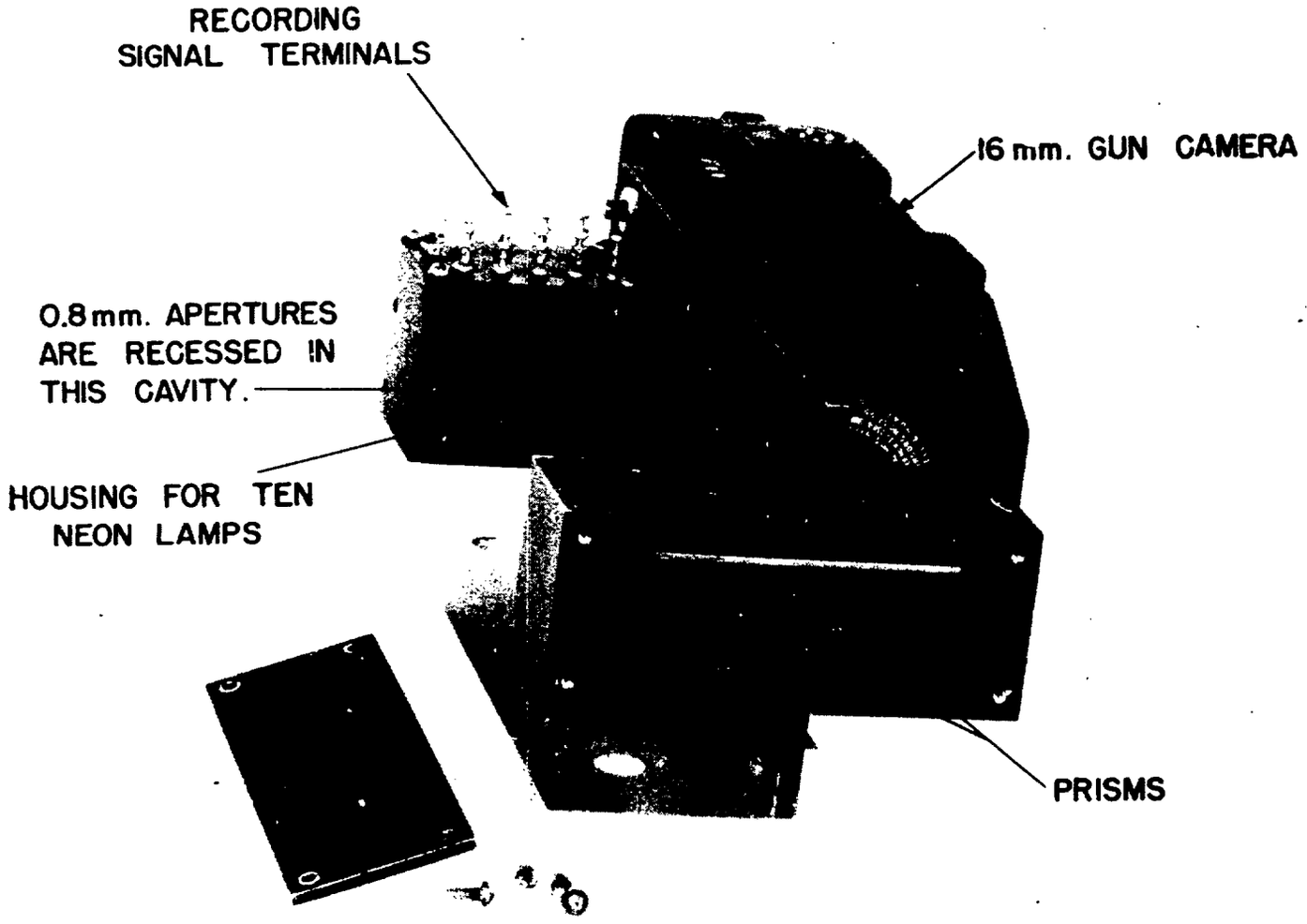

THE 10 CHANNEL RECORDER
WITH LIGHT COVERS REMOVED

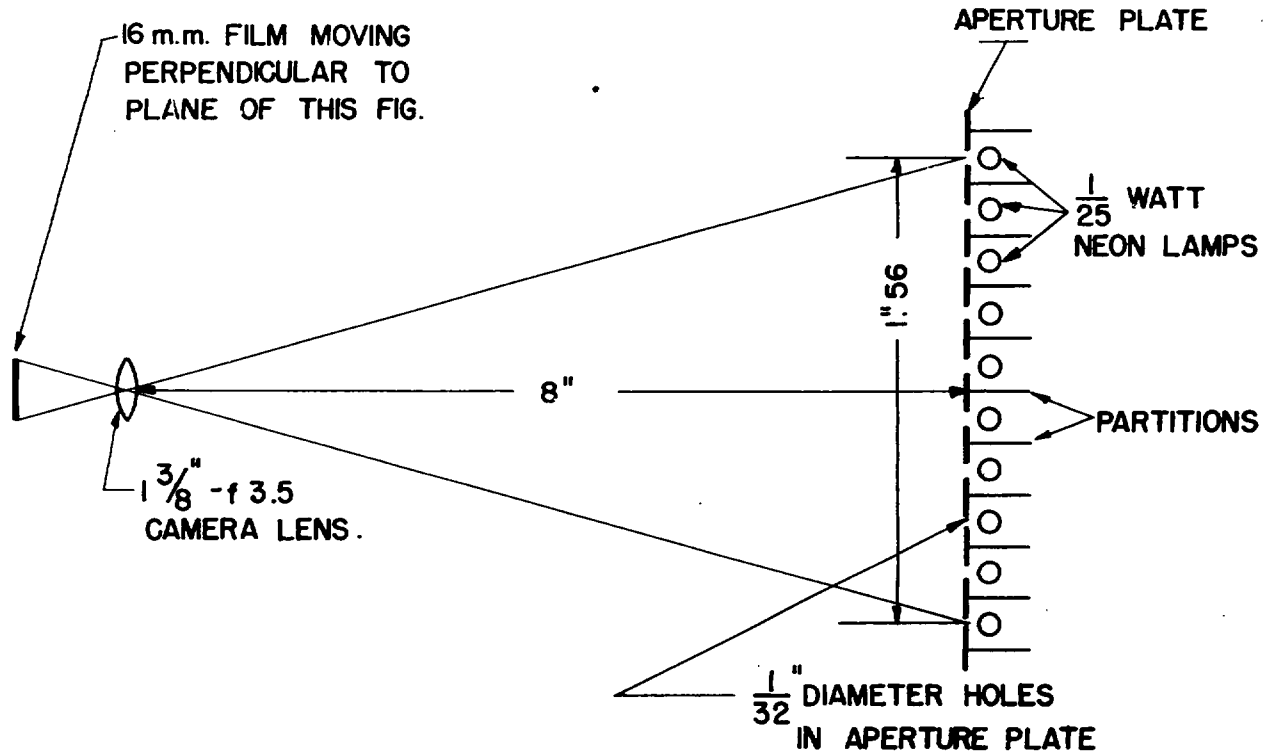

OPTICAL SYSTEM
OF 16 m m. RECORDER
(10 CHANNEL)

CH. IV SEC. D FIG. 4

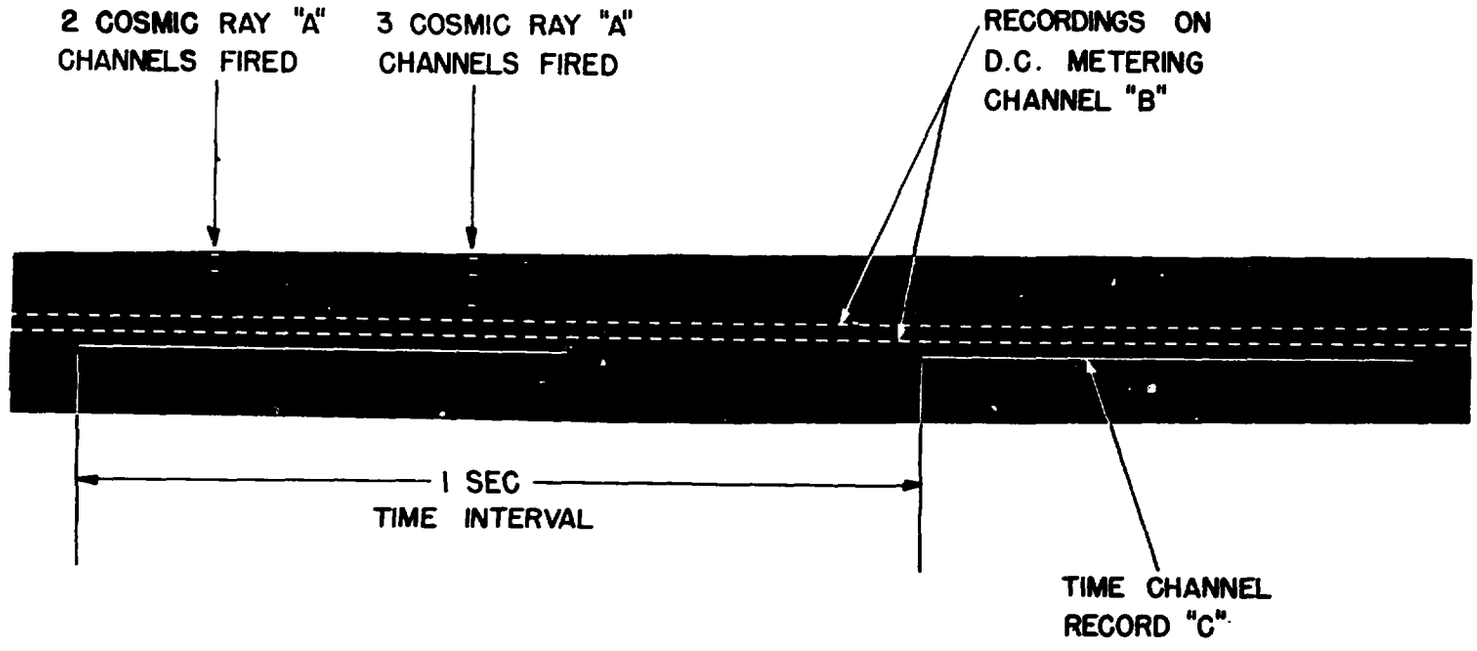

SAMPLE
16 mm. FILM RECORD
TAKEN WITH
10 CHANNEL RECORDER

CH. IV SEC. D FIG. 5

were drawn for each channel.

The error introduced by the timing channel was probably not greater than 2 percent, while the overall system error was approximately 5 percent.

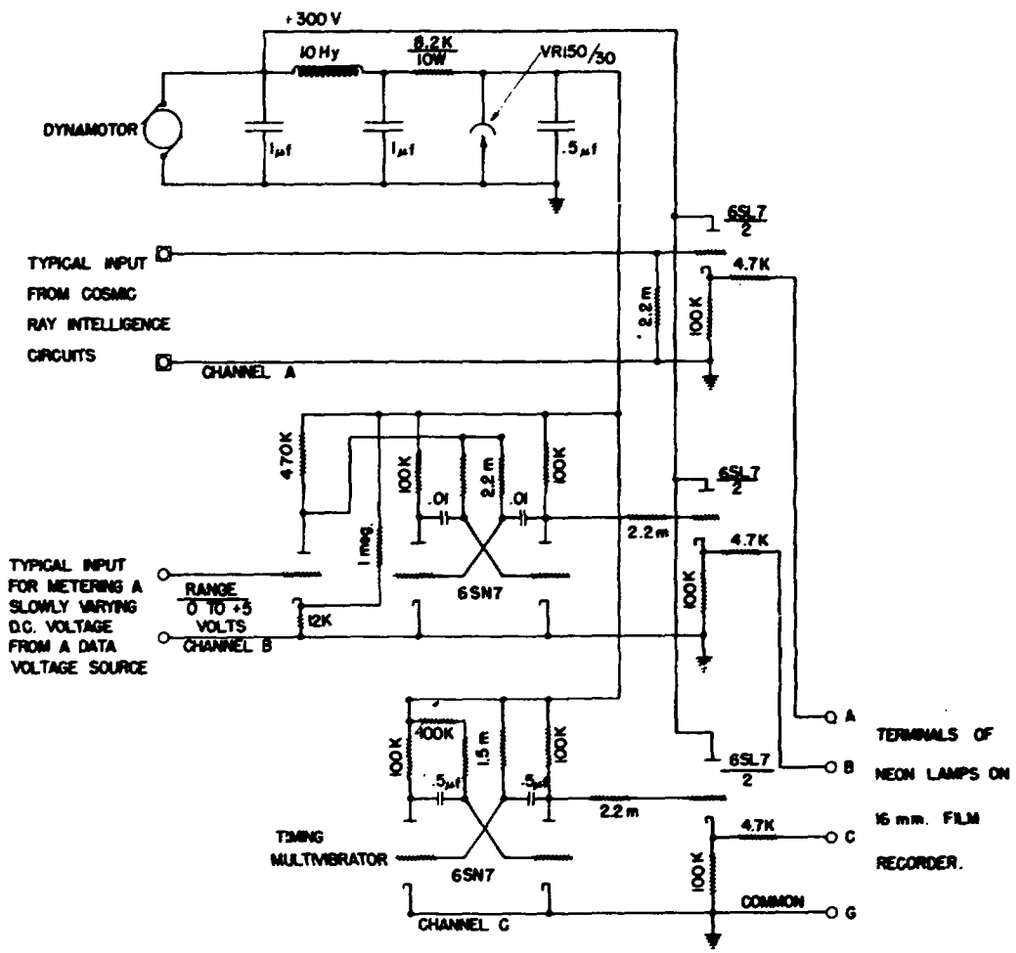

ELECTRONIC INTELLIGENCE TRANSLATING CIRCUIT

CH. IV SEC. D FIG. 6

CHAPTER IV

UPPER ATMOSPHERE EXPERIMENTS CONDUCTED IN THE V-2

E. The Ionosphere Experiment

by

J. F. Clark, T. M. Moore
and J. C. Seddon

The program of ionosphere investigation which was begun by the Naval Research Laboratory in the first cycle of V-2 firings was continued in the flight of October 10. The basic experiment planned for that date was similar to the one attempted on July 30 and described in Upper Atmosphere Research Report No. I*. No data leading to information on ion density in the ionosphere was obtained in the October 10 experiment due to the loss of one antenna during launching. However, signals were received on one frequency throughout the flight and information regarding antenna pattern, missile roll, trajectory, and time of Brennschluss has been obtained from a study of the record. In addition, in order to determine the types of motion executed in flight by the trailing wire antennas, cameras were installed in the tail-ring and mid-section of the missile.

The experiment of October 10 differed from the July 30 effort in several ways. Only the two highest frequencies used in the July 30 experiment were radiated on this flight. This permitted an increase in radiated power on the two remaining frequencies. In addition, a more powerful transmitter was used. As a result, the power output was about 50 watts per frequency on the October 10 flight, as against only 15 watts on previous flights. The length of each trailing wire antenna was made equal to three quarters of one wavelength. On previous flights, a multiple of a half wavelength had been used. The change was made in order to reduce the effect of the capacity of the cable which carried radio frequency power from the transmitter to the antenna. The transmitter was matched to the antenna with a π section transformer. At the ground station half wave antennas were employed.

The frequencies used on the October 10 flight were 25.632 mc and 4.272 mc. The corresponding antenna lengths were 7.92 meters (26 feet) and 51.82 meters (170 feet). In order to increase the strength and the heat capacity of the longer antenna, and thus to decrease the probability of its being annealed or snapped off or perhaps both, a 4.8 mm

---

* Naval Research Laboratory Report No. 2955

(3/16 in.) diameter cable was used instead of the 3.2 mm. (1/8 in.) cable which had been used previously. Unfortunately, as this antenna left the release box at takeoff, the last few feet either became entangled or caught on the launching platform, with the result that the wire broke at the point at which it was attached to the rocket. The 4.272 mc transmission was nevertheless received for the first 3.5 seconds of flight.

During the remainder of the flight, only the 25.632 mc signal was received. It was recorded throughout the flight for a period of 412.6 seconds, and much useful information has been obtained from a study of its record.

As the rocket rose above 3 km. the power input, as measured at the rocket and telemetered to earth, decreased steadily until Brennschluss, which occurred about 68 seconds after takeoff. It is thought that this decrease with altitude may be due to increasing flame size, glow discharge in the region of the antenna or both. At Ground Station No. 1 the received signal had dropped to zero at 67.2 seconds. It remained there for one second and then increased abruptly to a large value. Ground Station No. 2 also recorded the zero at 67.2 seconds, but the signal level began to rise gradually after only a half second, reaching the normal value in 25 seconds. This may be interpreted as evidence of the gradual disappearance of glow discharge at the antenna.

The reception was then characterized by a periodicity which was symmetric, in time, about the instant 72 seconds after takeoff. This may be taken as an indication that the direction of rotation of the rocket reversed at that time, being counter-clockwise as seen from below during the interval from Brennschluss until 72 seconds after launching and clockwise after that time. The period of the latter rotation is apparently 59 seconds. This is deduced from the rate at which the major lobes of the 25.632 mc trailing wire antenna pass the receiving station. The rocket antenna pattern is evidently characterized by four narrow high gain lobes and several smaller lobes.

The power input was also subject to a periodic variation, four cycles of slightly different length occurring in approximately 60 seconds. This is thought to be caused by a variation in the distance between the antenna and particular fins, the variation being caused by rotation and yaw.

The rapid fluctuations in received signal strength ended abruptly 85 seconds after takeoff and reappeared 391 seconds after takeoff. These fluctuations may be interpreted as resulting from those motions of the antenna which were caused by high winds in regions where the atmospheric density was sufficiently great to cause drag. This data locates the peak of the trajectory at 238 seconds after takeoff. The strength of the received signal reached values as large as 250 microvolts, even when the rocket was at an altitude greater than 160 km.

Strong signals were received until the end of the flight and it is therefore concluded that the 25.632 mc antenna remained intact throughout the flight.

In order to acquire a better knowledge of the forces which are experienced by wire antennas in flight, eight gun type cameras were installed at various points in the V-2. Thus, it was hoped to obtain accurate information as to the position and modes of oscillation of the trailing wires. Six of the cameras were mounted around the opening of the venturi as shown in Figs. 1 and 2. The other two were placed in the midsection between the fuel tanks as shown in Fig. 3. All of the cameras pointed earthward while the rocket rose. The camera motors near the venturi were encased in plastic covers to prevent sparks from igniting the gases. This is shown in Fig. 4. A sequence program was arranged so that continuous photographs were taken from takeoff until shortly after the rocket began its descent.

As noted elsewhere in the report the warhead was separated in flight from the remainder of the rocket, with the result that recovery was unusually good. Five of the tail ring cameras were recovered, as shown in Figs. 5 and 6, but when the films were developed they showed only a vague, shifting grayish mass which apparently was vapor trailing the vehicle. The side cameras, whose field of view may not have been obscured by vapor, were not recovered.

The experience gained in the October 10 flight may be summarized as follows:

1. The ionized layers caused no noticeable effect on the 25.632 mc transmission, but the rolling of the rocket may have obscured any phenomena which were present.

2. The moment of Brennschlus is indicated in the record of received signal strength.

3. It was discovered that the pattern of the 25.632 mc trailing wire antenna was so sharply lobed as to be impractical for use in the ionosphere experiment.

4. Eight meter trailing wire antennas can remain on the rocket throughout a flight under normal conditions. However, the launching of 50 meter trailing wire antennas introduces serious difficulties.

5. Excessive difficulty is experienced in the tuning of π section transformers with condensers which will withstand the severe rocket vibrations. Matching sections employing smaller condensers are recommended as being more practical.

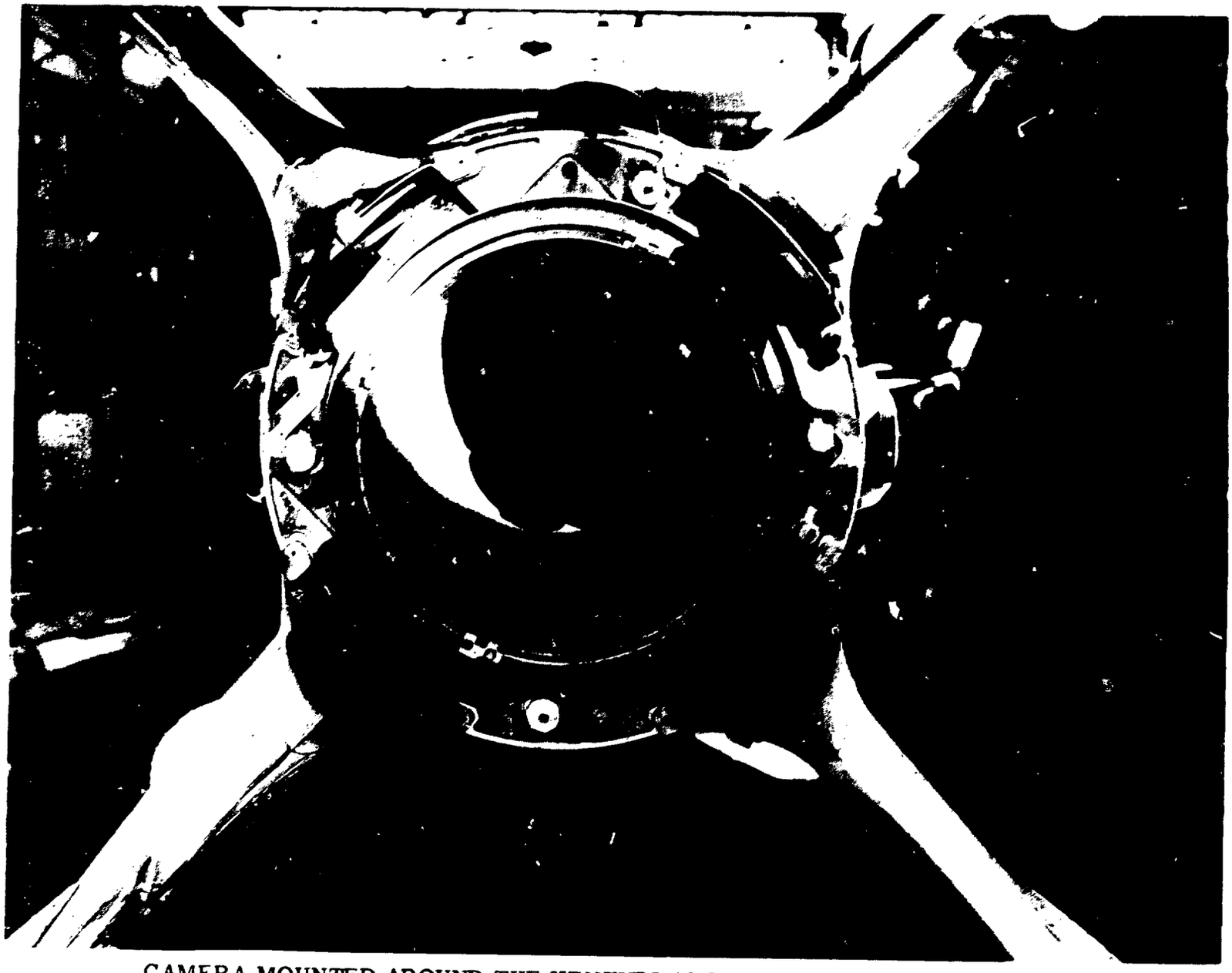

CAMERA MOUNTED AROUND THE VENTURI AS SEEN FROM OUTSIDE THE V-2

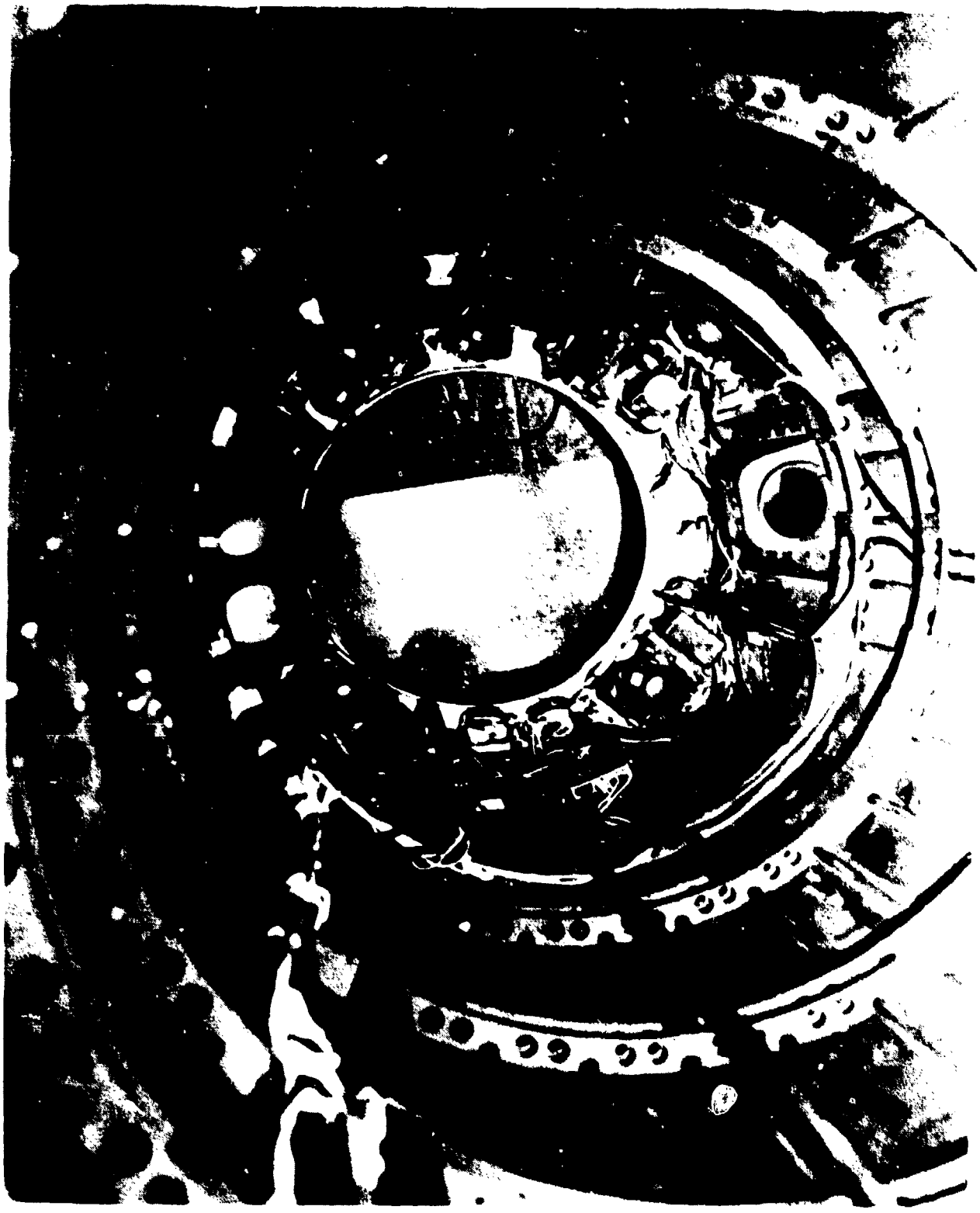

CAMERAS MOUNTED AROUND THE VENTURI OPENING
AS SEEN FROM INSIDE THE V-2 BEFORE ASSEMBLY

MIDSECTION CAMERA

CH. IV SEC. E FIG. 3

VENTURI CAMERA INSTALLATION SHOWING PLASTIC CAMERA MOTOR COVERS

TAIL RING AS FOUND AFTER IMPACT

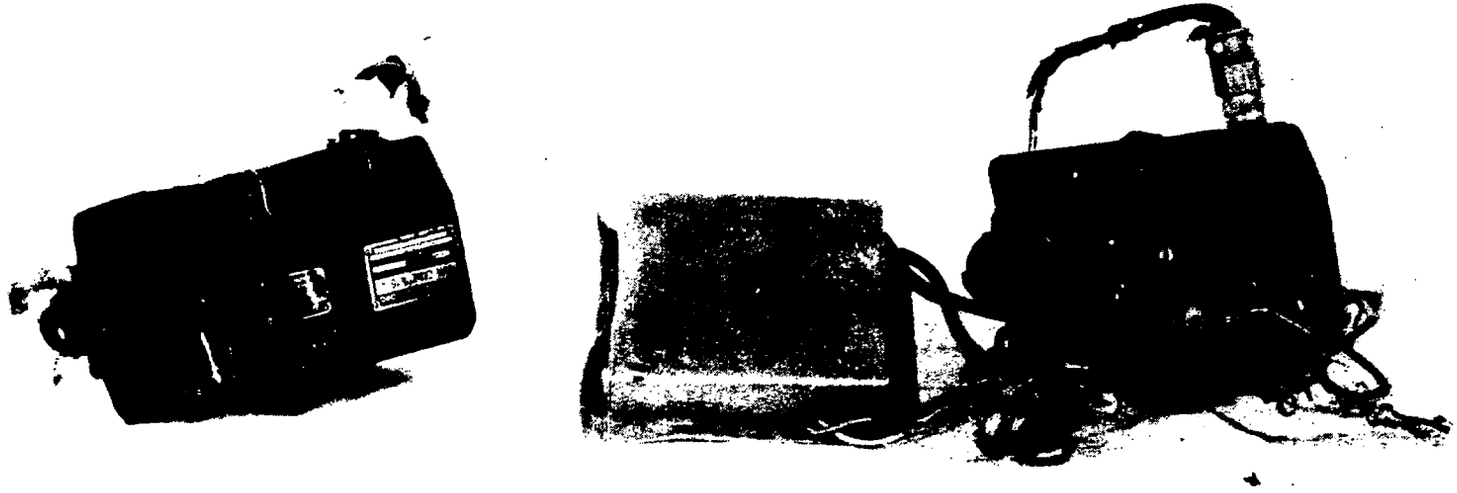

TWO TAIL RING CAMERAS AFTER IMPACT

CHAPTER IV

UPPER ATMOSPHERE EXPERIMENTS CONDUCTED IN THE V-2

F. The Ejection and Recovery of Instruments

by

T. A. Bergstralh, M. W. Rosen, and C. H. Smith

The problem of physical recovery of equipment from the V-2, which was discussed in connection with the first cycle of V-2 firings*, continued to received considerable attention in the October 10 flight. The method of causing an air burst of the rocket appeared to be only partially satisfactory for recovering instruments and specimens. Therefore, specific ejection experiments for separating data or equipment from the rocket during flight were carried out.

Successful recovery of equipment ejected from the rocket is possible only if the ejected equipment in falling is decelerated to a safe landing speed, and can be located after it has landed. The ejection device used in the October 10 firing was essentially the same as that used in the 19 July 1946 flight and described in the earlier report. To provide for a rapid deceleration, the equipment container was made in the form of a rectangular metal box, as shown in Fig. 1. The rectangular shape of the container insured a high drag coefficient so the principal deceleration during the early stages of fall was caused by air forces on the container itself. A small metal parachute was used to orient the container in such a way as to obtain maximum advantage from this effect since it prevented slow tumbling and the accompanying reduction in drag. To reduce the landing speed still further a larger parachute canopy of nylon was included within the metal container. Its release was initiated by a timer after the container had been decelerated sufficiently to insure that the canopy would not be destroyed in opening. To facilitate location of the device after it had landed, three smoke flares were included in the assembly. These flares were to be electrically ignited at specific intervals by a second time device.

In Fig. 2 the recovery device has been partially disassembled to show the two parachutes and the breakaway cover which protects the cloth parachute prior to its release. The protective cover plate has

---

*See Naval Research Laboratory Report R-2955, Chapter III, Section I.

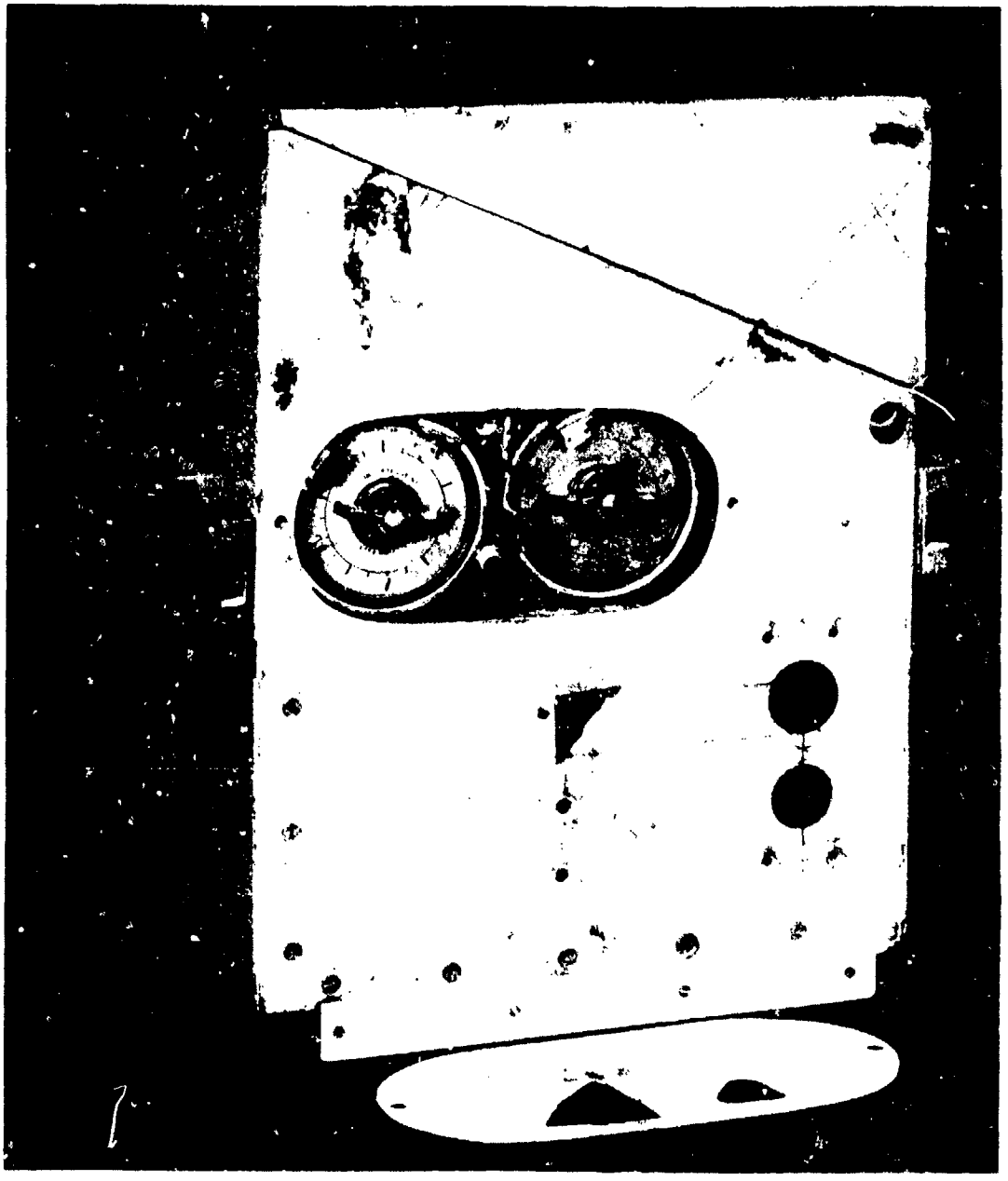

RECOVERY CONTAINER

RECOVERY CONTAINER PARTIALLY DISASSEMBLED SHOWING THE TWO PARACHUTES AND THE BREAKAWAY COVER

been removed to reveal the timers mounted within the container. Fig. 3 shows the chasis carrying the two timers, the smoke flares, and the batteries. In Fig. 4 the ejection well and solenoid can be seen attached to the door of sector IV of the control chamber. The details of the trigger solenoid and trigger mechanism may be seen. Fig. 5 shows the device installed in the October 10 rocket.

A normal sequence of operation is as follows. After 240 seconds of flight the container is ejected from the missile. At this time the rocket should be just beyond the peak of the mean expected trajectory. Upon ejection static lines release the 77 mm (5 inch) metal parachute and initiate the operation of the two timers. The recovery device is permitted to fall freely for a period of 265 seconds. After this interval the first timer operates the main parachute release causing the metal housing over it to break away. This chute then opens, and one minute later the first smoke flare is ignited by a second signal from the parachute timer. This flare is designed to provide a smoke trail during the latter stage of the fall. The remaining two smoke flares, ignited after landing by the second timer, are actuated two and one quarter hours and four and one quarter hours, respectively, after ejection from the rocket in order to permit searchers to reach the impact area.

The main parachute was designed to withstand the forces associated with opening at speeds in excess of 150 meters (about 500 feet) per second at sea level. This figure was chosen as the velocity to which the recovery container should be decelerated before the parachute is released. Since reliable pressure actuated devices were not available, mechanical timers were used to perform the parachute release and flare ignition functions, as described above. To determine a timer interval between ejection and parachute release which would allow the container to be decelerated to a safe velocity, the velocity of the container as a function of time was calculated from the two extreme predicted rocket trajectories. This information is plotted in Fig. 6. The dropping velocities of the container were obtained by numerical integration. For this computation the drag coefficient in the supersonic range was assumed to have a constant value of 2, and in the subsonic range to have a value of 1.2, the latter value being verified by a series of drop tests from an airplane. Atmospheric density as a function of altitude was taken from the date of Whipple*. Actually, the drag coefficient is not constant in either the subsonic, or supersonic range; but, only a relatively small increase in accuracy would have resulted from the assumption of the true drag coefficient. For example, although the curves of Fig. 7 were calculated assuming supersonic and subsonic drag coefficients of 4.0 and 2.4 respectively, they do not vary greatly from the curves shown in Fig. 6.

---

*Whipple, F.L.: Meteors and the earth's upper atmosphere, Rev. Mod. Phys., vol. 15, pp. 246-264, Oct. 1943.

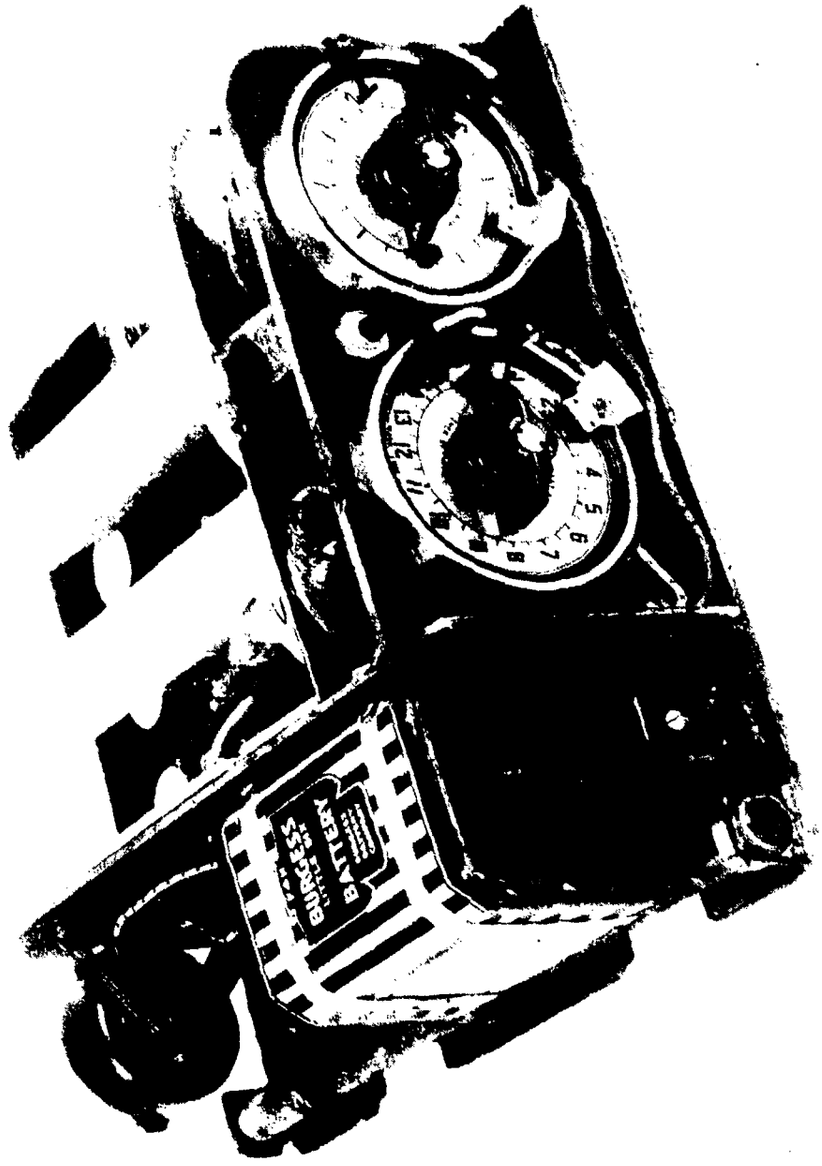

TIMER CHASSIS

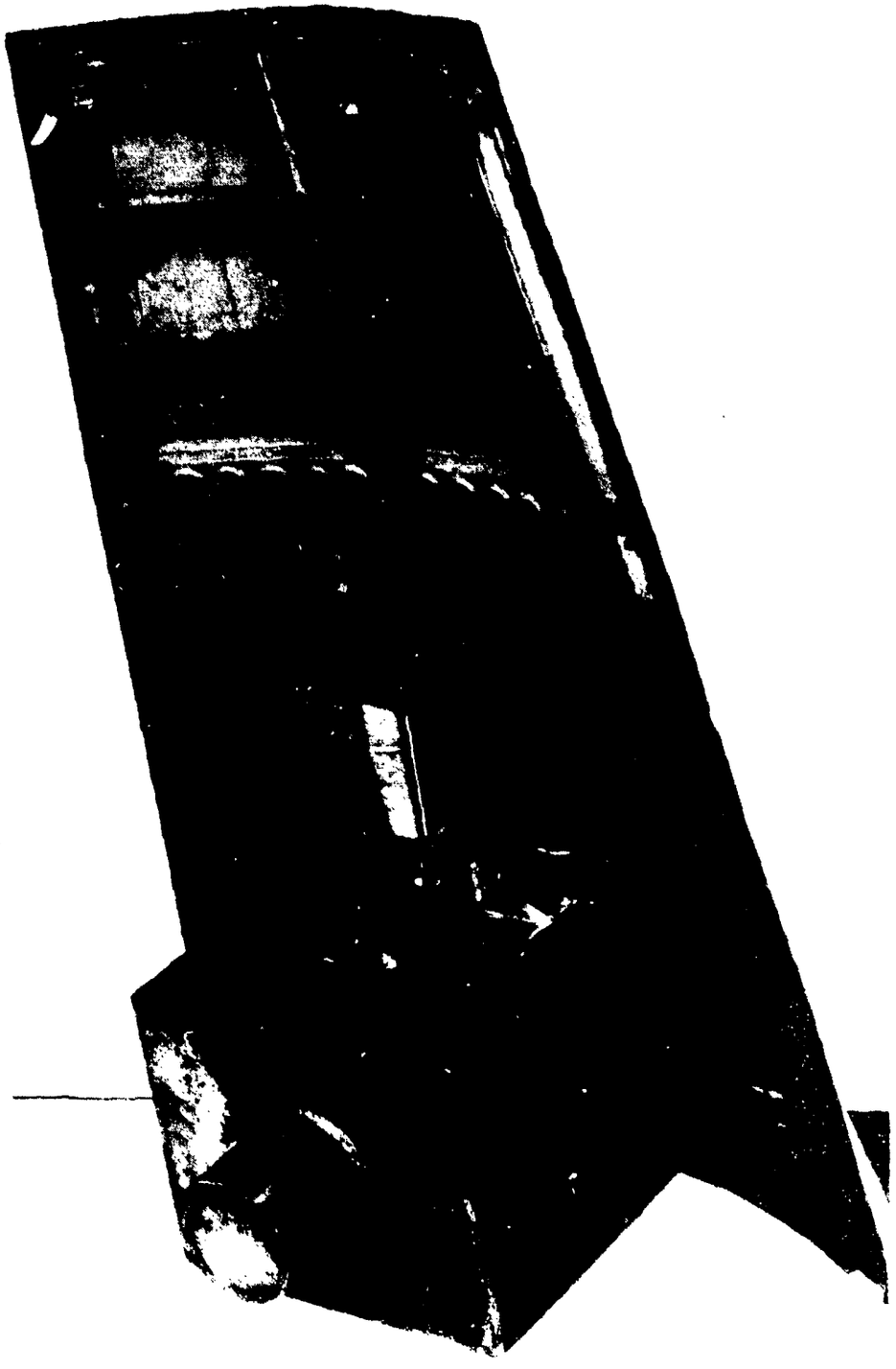

EJECTION WELL AND SOLENOID ATTACHED
TO DOOR OF CONTROL CHAMBER

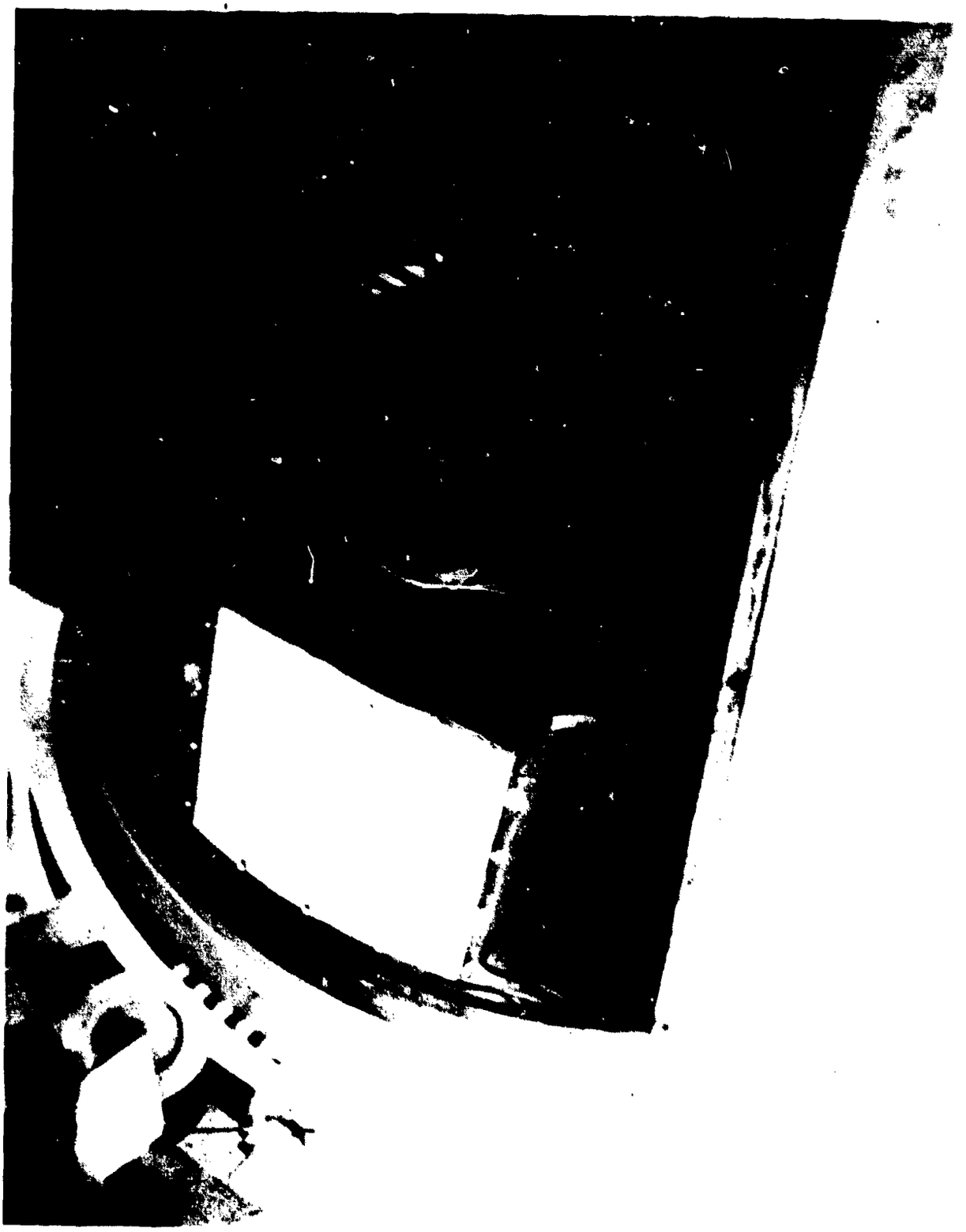

RECOVERY APPARATUS INSTALLED IN THE OCTOBER 10 ROCKET

CH. IV SEC. F FIG. 5

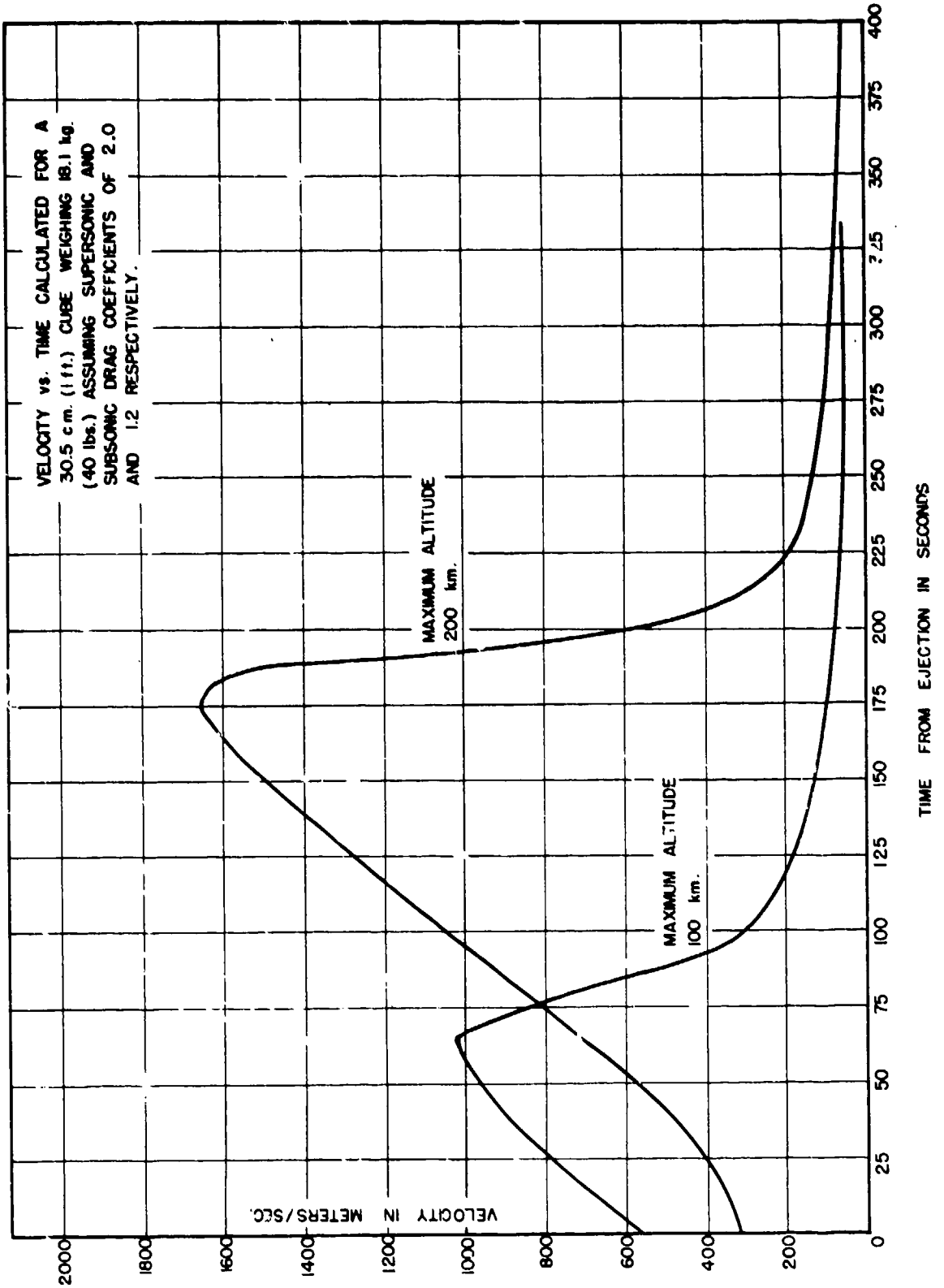

CH. IV SEC. F FIG. 6

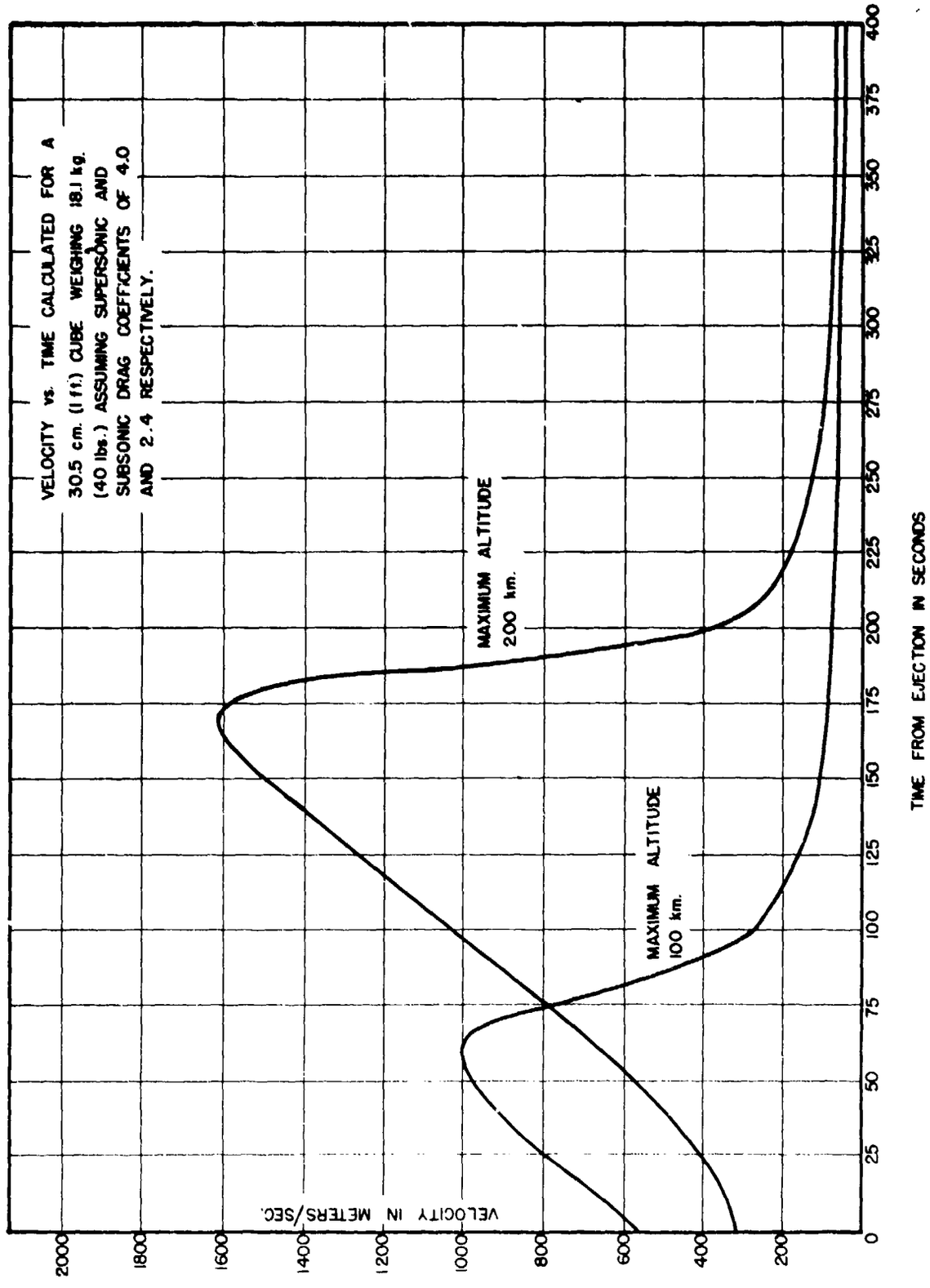

CH. IV SEC. F FIG. 7

It was known that the smoke flares would not operate successfully at high altitudes, and this also influenced the selection of the time at which the parachute was released. The altitude of the container was plotted as a function of time for the highest and lowest trajectories expected. This is shown in Fig. 8. A time interval of 265 seconds was selected since at this time the velocity of the container would be less than 150 meters (500 feet) per second and the altitude would be 7,500 $\pm$4,500 meters.

In the October 10 experiment a 10 channel camera recorder was mounted in the instrument chamber of the recovery container. Information was fed to the recorder from the cosmic ray equipment through a pressurized cable and a pull-away plug. In addition to the recorder two packets of seeds and two packs of photographic emulsions were carried in the instrument chamber. The seeds were especially prepared by Harvard University to study the effect of exposure to cosmic rays. The film packs each contained 24 heavy emulsions which were packed closely to detect cosmic rays.

No extra precautions were taken to protect the seeds and film from high temperatures since previous calculations had shown that the 3 mm (1/8 inch) steel container wall provided sufficient thermal insulation.

At the time of flight several observers reported that they had seen the large parachute in the air. One observer in an airplane reported that he had seen the recovery container on the ground. No observations of the smoke flares were reported and although an extensive search was conducted, the recovery container was never found. On the other hand, the ejection mechanism was recovered and appeared to have operated properly.

The rocket evidently suffered an air burst which scattered its parts over a large area. There is, therefore, reason to doubt that the parachute actually was observed in flight. Other parts of the rocket, such as the oxygen tank which landed intact, could easily have been mistaken for the parachute.

As noted above, the smoke signals were not observed, and were accordingly of no assistance in the search for the container. The search which was conducted to find other equipment, such as the spectrograph, in addition to the recovery container, was carried out principally in the impact area. It is entirely possible that the recovery device does not lie in this area since the parachute may have caused the container to drift more with the wind than did other parts of the rocket. In the absence of any indication as to the general area in which the device is located, further search is considered to have small chance of success.

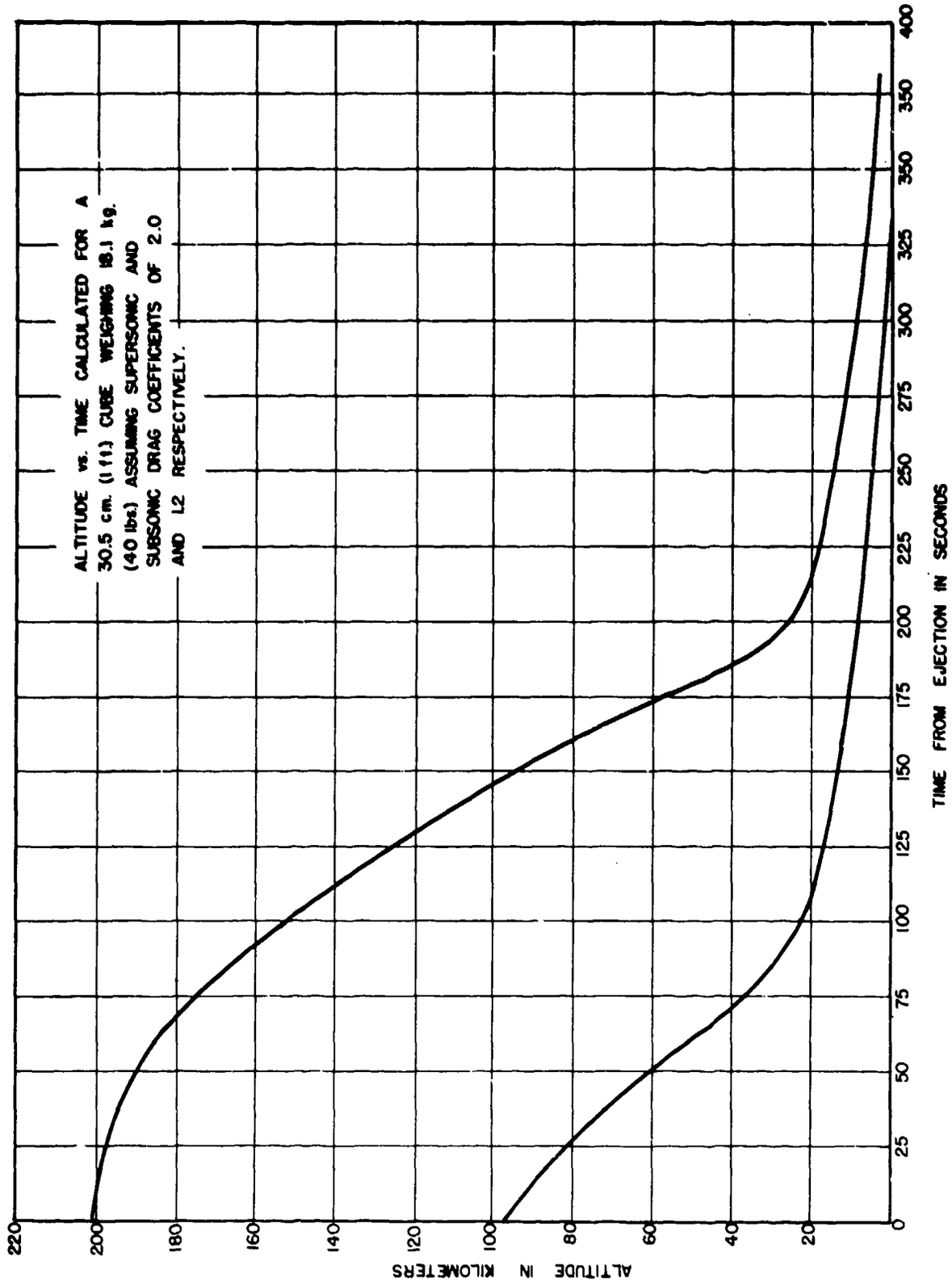

CH. IV SEC. F FIG. 8

It is believed that the general principles employed in this experiment are adequate to accomplish the return of data or equipment to the ground in satisfactory condition. The delayed action parachute should have as high a landing speed as the nature of the equipment will permit in order to reduce wind drift. In the October 10 experiment the landing speed of the parachute should have been approximately 15 meters per second.

Apparently the problem of locating ejected equipment is at present the more difficult part of the overall problem of recovery. Adequate means of location must be found. Various possibilities which suggest themselves are now under consideration.

The members of the Rocket Sonde Research Section wish to express their appreciation to the General Textile Mills for constructing the recovery container and parchute mechanism. Thanks are also due Mr. L. D. Jackson of the Naval Ordnance Laboratory for his part in providing the smoke flares used in this experiment.

CHAPTER IV

UPPER ATMOSPHERE EXPERIMENTS CONDUCTED IN THE V-2

G. The Biological Experiments

by

T. M. Moore

The collaborative program of biological research begun by Harvard University and the Naval Research Laboratory in the first cycle of V-2 firings was continued on October 10. Rye seeds having known characteristics were provided by Harvard. Containers of various types were furnished by the Naval Research Laboratory and by Harvard. The Naval Research Laboratory installed these in the V-2, and undertook to recover them after the firing.

Several methods and types of container were used in an effort to insure that as many of the specimens as possible would be recovered. To this end, a study was made of the impact area after each previous firing in order to determine which portions of the rocket offered the most likelihood of recovery. In general, the tail assembly appeared to suffer the least damage.

In several of the later flights, an effort was made to separate the warhead from the after part of the missile on the downward portion of the flight while the rocket was still above the resisting portion of the atmosphere. Each time that this was accomplished successfully, at least some fragments of the tail were recovered.

Fig. 1 shows the tail section and venturi of the rocket which was fired on October 10. In that firing, the warhead, which was separated in flight, was also recovered in unusually good condition. It is shown in Fig. 2 of Chapter I.

For the various V-2 flights, several types of containers have been used by the Naval Research Laboratory for the biological experiments. The seeds have been tied in a nylon ribbon at intervals of about one foot, as shown at the top of Fig. 2. The ribbon, if tied to the structural rims of the rocket, is easily recovered, unless the rocket is completely destroyed.

A second method, similar to the first, consists of tying the seeds in spaghetti tubing, a length of which is also shown in Fig. 2.

AFTER PORTION OF THE V-2 AS FOUND IN THE IMPACT AREA

CH. IV SEC. G FIG. 1

VARIOUS TYPES OF SEED CONTAINERS

The tubing may then be mounted in any suitably protected place. In the October 10 firing it was placed in the rails which guide the tail assembly when it is slid over the venturi before being attached to the main frame of the rocket. This location is shown in Fig. 3.

A third method is to place the seeds in a suitably rugged metal container. Containers have been constructed of high pressure tubing having a wall thickness of 9.5 mm (3/8 inch). The tubing is welded at one end and provided with a pressed fitted cap at the other end. One of these containers is shown in Fig. 2. The container is then placed at some relatively protected point. In the July 30 and October 10 firings, it was placed in the main frame of the rocket at the junction point of the control compartment and the alcohol tank. Recovery was effected from this point only after the July 30 firing. In the October 10 firing containers were also located in the warhead and in the main frame of the rocket between the alcohol tank and the oxygen tank as shown in Fig. 3.

The ejection apparatus developed, constructed, and installed by the Naval Research Laboratory in the October 10 firing and described in the preceding section, also contained seeds. There was a recess provided especially for such things as seeds, but for the October 10 firing they were enclosed in a paper envelope and placed in the interior of the block. Calculations indicated that the temperatures within the block would not become excessive. The block used in the October 10 firing has not yet been recovered. Permission was also obtained to install seeds in "Daughter", a recovery device developed under the supervision of the Army Ordnance Department at White Sands. This apparatus has not been found either.

Although seeds were not recovered on October 10, nevertheless the overall record on recovery of equipment from the V-2 was excellent. It is anticipated that in the near future seeds will be recovered after a flight.

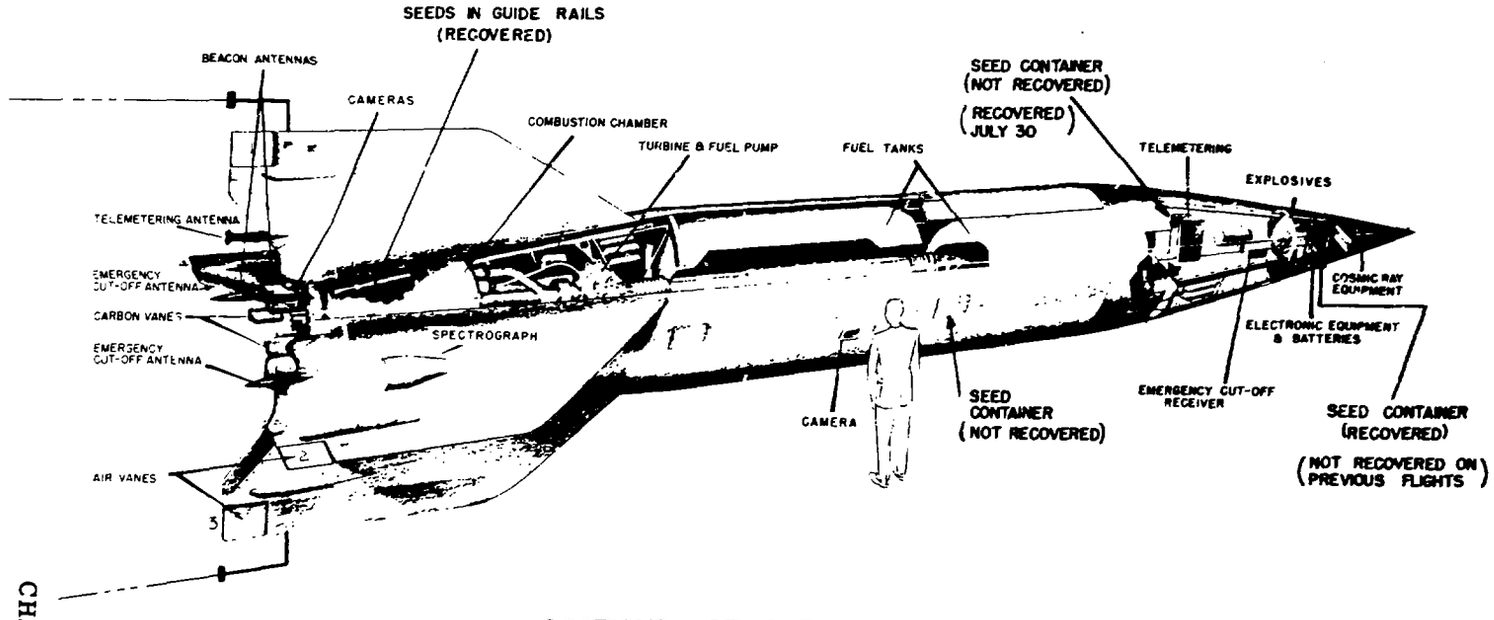

LOCATIONS OF SEED CONTAINERS

CH. IV SEC. G FIG. 3

CHAPTER V

THEORETICAL DISCUSSIONS

A. Determination of Ambient Temperatures and Pressures in the Atmosphere from Pressure Measurements Made at Various Points on the Surface of a Rocket

by

M. A. Garstens

It is well know that the pressure and temperature on or near a rapidly moving missile is not the same as the ambient pressure and temperature. In order, therefore, to obtain ambient pressure and temperature from a V-2 sounding, it is necessary to interpret correctly the readings observed. It is proposed to discuss how this can be done in that region of the atmosphere in which the mean free path of the air molecules is much smaller than the dimensions of the aperture leading to the pressure measuring devices. This includes the region up to about 70 kilometers above the earth's surface. In this region aerodynamic methods of analysis can be applied. In a subsequent report, the methods of kinetic theory, applicable to the more rarefied regions of the atmosphere, will be applied to the problem.

As the rocket approaches and transcends the speed of sound, a conical shock wave forms about the nose of the V-2. The theory of such conical shock waves has been developed by Taylor and Maccoll[1]. They obtained expressions for the surface pressure on a cone moving at high speeds as a function of the Mach number and the angle of the cone. Fig. 1, reproduced from their paper, indicates values of the expression $\frac{P_s - P_1}{\rho_1 U^2}$ as a function of $\frac{U}{a}$, the Mach number, for various indicated cone angles. Both computed curves and observed points are shown. The letters A, B, C in Fig. 1b indicate successive points along the cone. U is the velocity of the cone; a, the velocity of sound; P_s, the surface pressure along the cone; and P_1 and ρ_1, the ambient pressure and density.

It is clear that if the surface pressure P_s, the Mach number $M = \frac{U}{a}$ and the speed U of the cone are known, the ambient pressure P_1

1. The Air Pressure on a Cone Moving at High Speeds, Proc. Roy. Soc. 139 (1933)

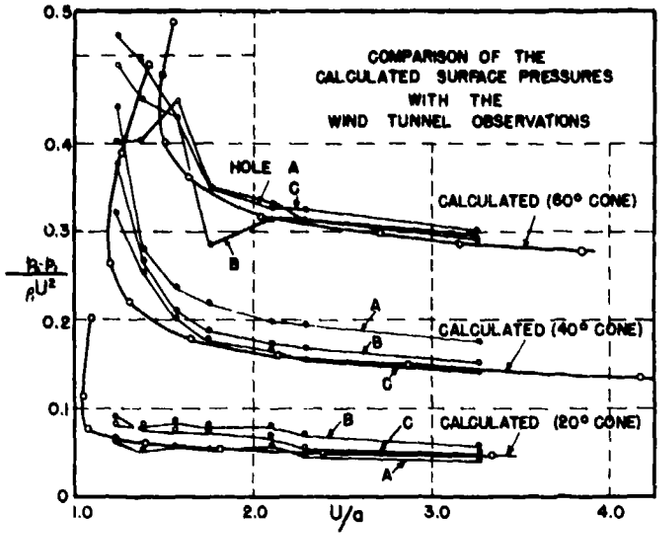

REPRODUCED FROM: TAYLOR, G.I. AND MACCOLL, J.W.: "THE AIR PRESSURE ON A CONE MOVING AT HIGH SPEEDS", PROC. ROY. SOC., SERIES A, VOL. 139, NO. A838, FEB. 1, 1933.

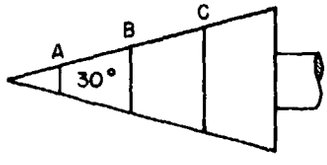

LOCATION OF POINTS A,B,C ON CONE

CH. V SEC. A FIG. 1

can be deduced for a given cone angle. Thus, if the values of $\frac{P_s - P_1}{\rho_1 U^2}$ in Fig. 1a are set equal to K, then since

$$\rho_1 = \frac{P_1}{RT_1}$$

ambient pressure may be expressed in the form:

$$P_1 = \frac{P_s}{1 + \frac{KU^2}{RT_1}} \tag{1}$$

where T_1 is fixed by the given values of M and U. In an actual flight, however, the ambient temperature T_1 is not known. An additional relation between P_1 and T_1 is therefore needed. If another sounding were taken at the same height but with a different velocity U' (and therefore with different values for P_s and K), P_1 and T_1 would be determined simultaneously from two equations of the same form as equation (1). This method is obviously not practical. An additional relationship between P_1 and T_1 can be obtained, however, by measuring the nose pressure P' on the same rocket.

In a previous report[2], it was shown how Rayleigh's theory of planar shock waves may be applied to determine ambient pressure from the pressure P' at the nose, and the Mach number. Since the velocity is known, the ambient pressure is therefore determined as a function of the ambient temperature.

Combining equation (1) with the values obtained from Rayleigh's theory, the ratio $\frac{P'}{P_s}$ can be obtained as a function of the rocket velocity U and the ambient temperature T_1. Fig. 2 shows a plot of $\frac{P'}{P_s}$ as a function of velocity for various ambient temperatures. In addition a plot of $\frac{P'}{P_s}$ against Mach number is shown. For a given velocity and value of $\frac{P'}{P_s}$, T_1 can therefore be determined. Substituting this value into equation (1) the ambient pressure P_1 is obtained.

If the pressure ratio $\frac{P'}{P_s}$ is increased, greater accuracy can

2. Naval Research Laboratory Report R-2955

PLOT OF $\frac{P'}{P_s}$ VERSUS TEMPERATURE IN °K
FOR 30° CONE

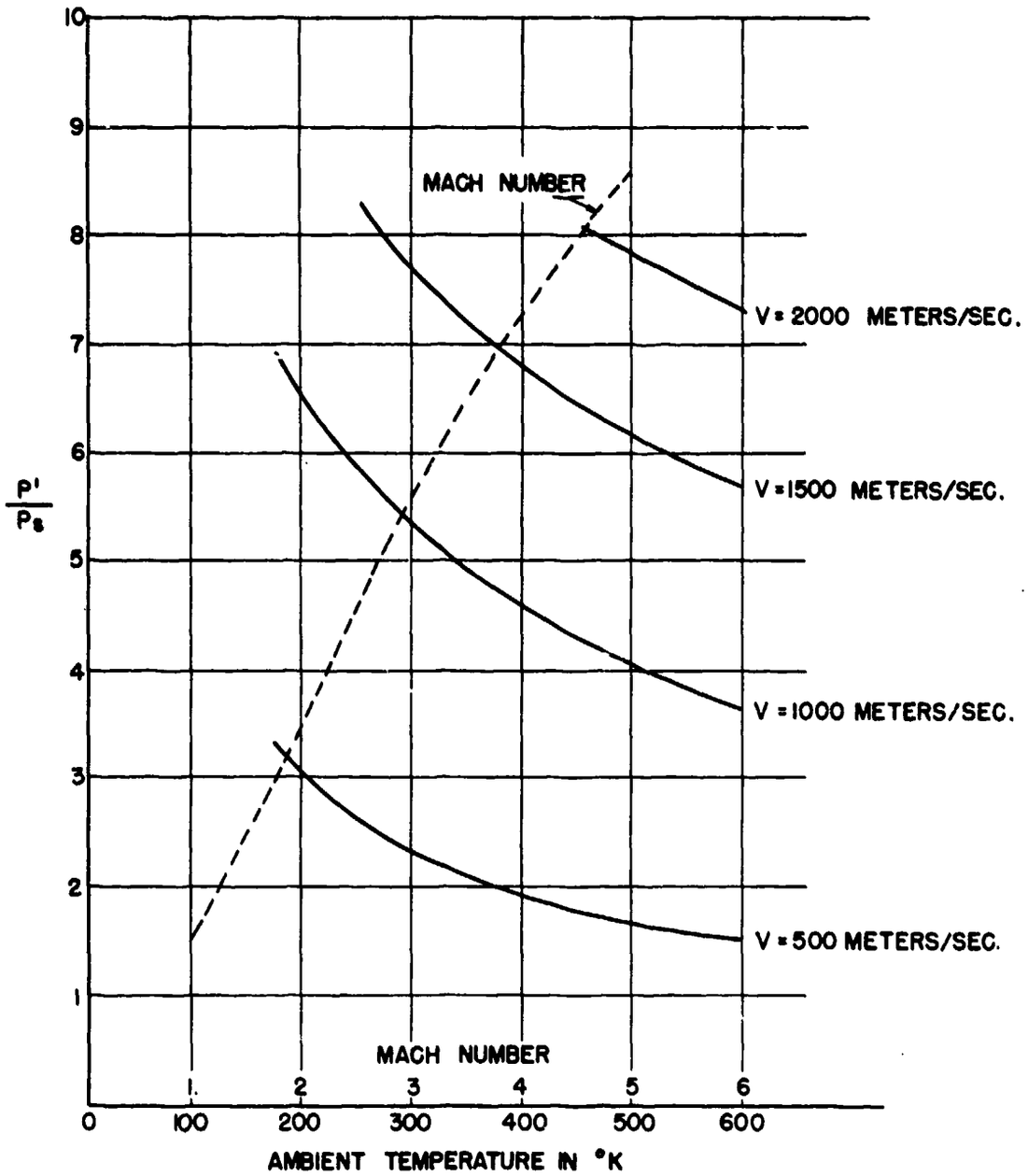

CH. V SEC. A FIG. 2

be attained. This can be done by taking the surface reading P_s at a point where the pressure is much lower than along the surface of the cone. To determine this point use is made of German wind tunnel data which were obtained from tests made on a model of the V-2. Figs. 3 and 4, which reproduce the data, show the pressure distribution along the V-2 as measured in the wind tunnel. The abscissa is given in calibres. The calibre of the V-2 is equal to 1.65 meters. α is the angle of yaw. The ordinates are given in terms of $\frac{P_s - P_1}{\frac{1}{2}\rho U^2}$, which is designated as $K(M)$ to indicate its dependence upon Mach number. If a and b, expressed in calibres, represent two arbitrary points on the rocket, and P_{sa}, P_{sb}, represent the surface pressures at those points, then from Fig. 2 or Fig. 3 it is clear that:

$$P_{sa} = P_1 + K_a(M_1)\,\tfrac{1}{2}\rho_1 U^2, \tag{2a}$$

$$P_{sb} = P_1 + K_b(M_1)\,\tfrac{1}{2}\rho_1 U^2, \tag{2b}$$

where $K_a(M_1)$ is the value of K at the point a when the Mach number is equal to M_1, and similarly for $K_b(M_1)$. Dividing equation (2a) by (2b) and making use of the equation of state,

$$P_1 = \rho_1 R T_1$$

one obtains:

$$\frac{P_{sa}}{} = \frac{RT_1 + \frac{1}{2}K_1(M_1)U^2}{RT_1 + \frac{1}{2}K_2(M_1)U^2}\ . \tag{3}$$

Thus, as in the case of the cone, the ratio $\frac{P_{sa}}{P_{sb}}$ is completely determined by the ambient temperature T_1, and the velocity U. Plots of this ratio for two sets of values of a and b are given in Fig. 5. For a given measured pressure ratio and velocity the ambient temperature can therefore be determined. The ambient pressure is then obtained from equation (2).

A more useful pressure ratio is that of the pressure at the nose to the pressure at a point 6 calibres from the nose. Fig. 6 shows the ratio of the pressure at the nose to ambient pressure, or, within narrow limits of error, the ratio of the pressure at the nose to that at a point 6 calibres from the nose, as a function of temperature, and also of Mach number.

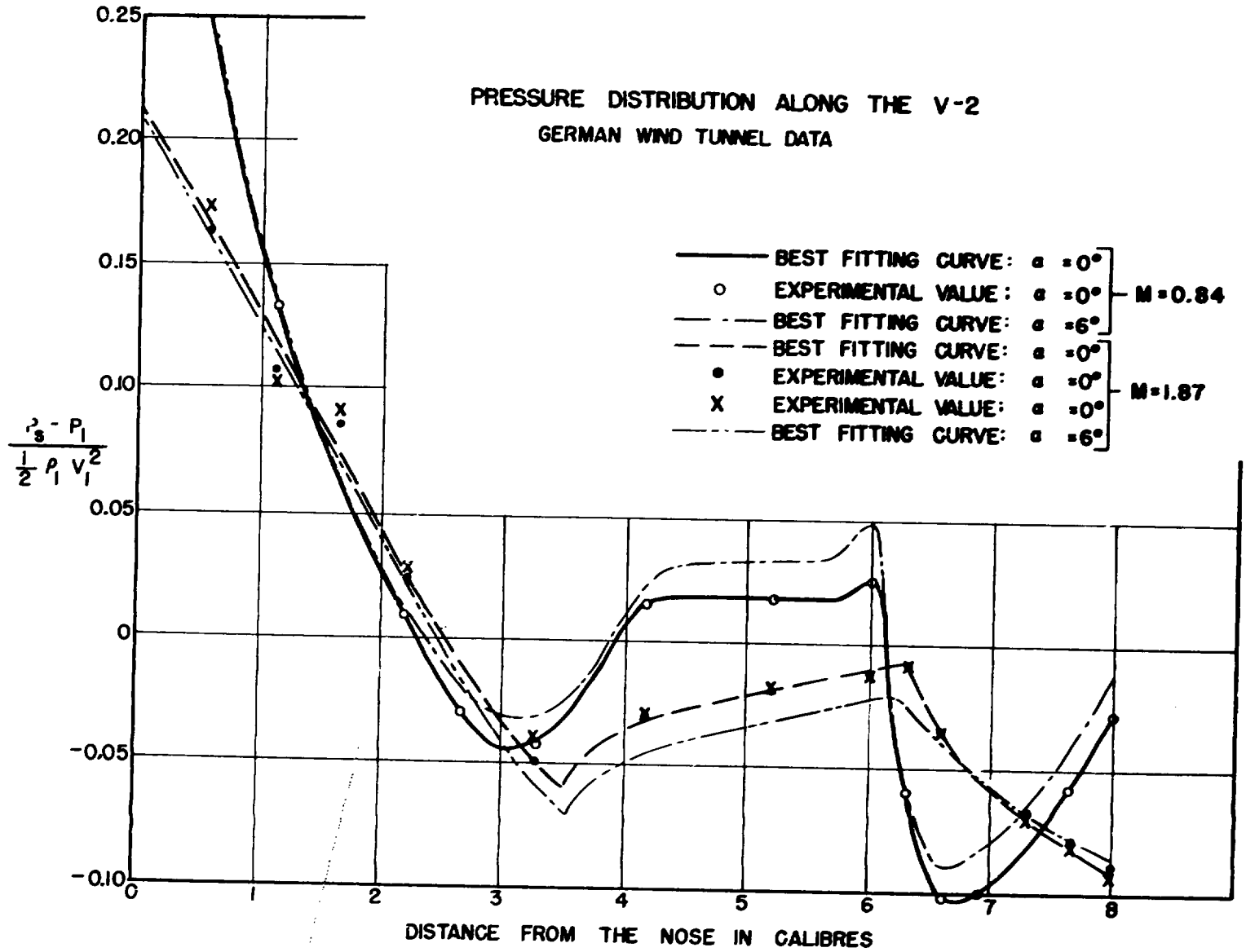

CH. V SEC. A FIG. 3

PRESSURE DISTRIBUTION ALONG THE V-2
GERMAN WIND TUNNEL DATA

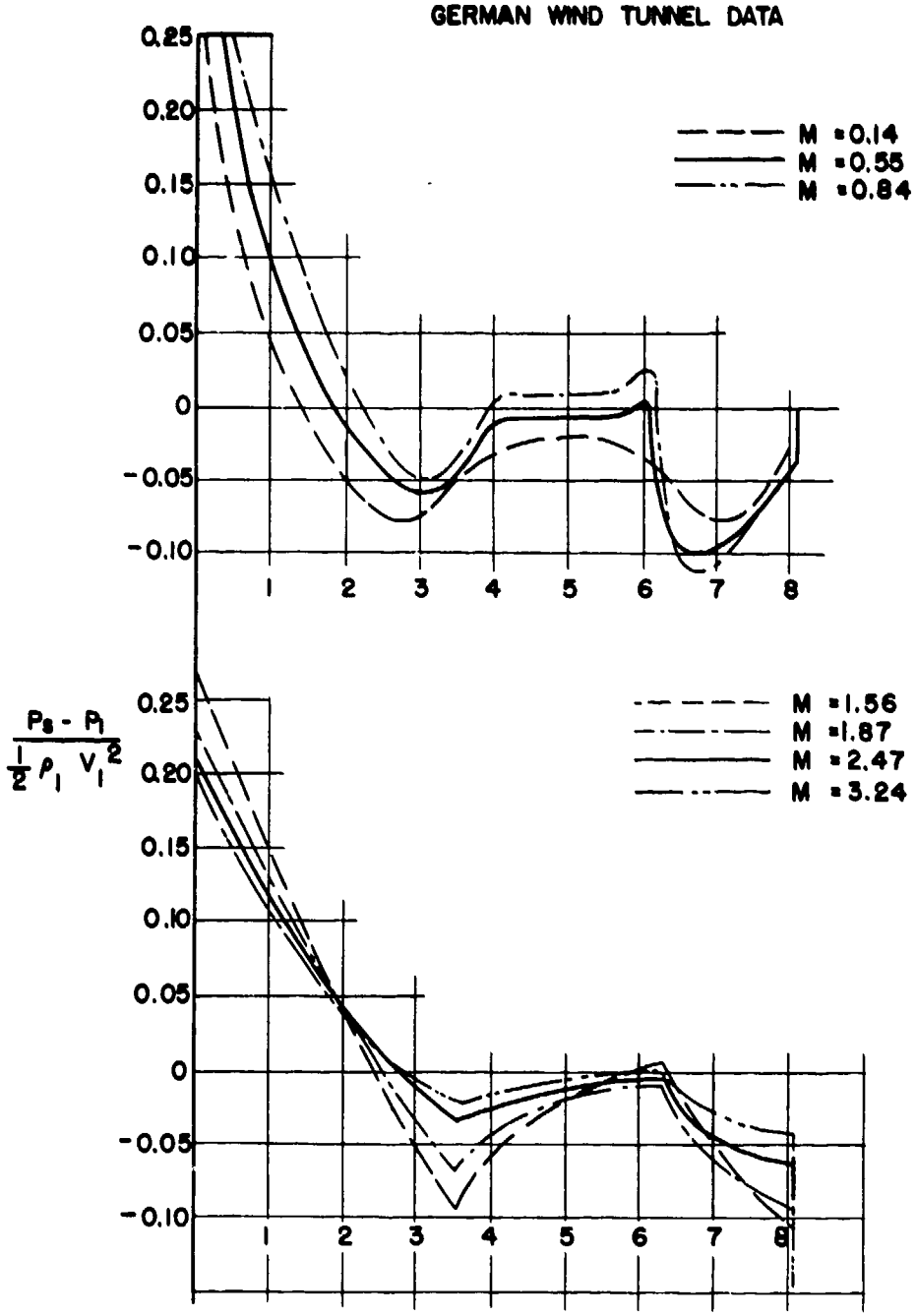

DISTANCE FROM THE NOSE IN CALIBRES

CH. V SEC. A FIG. 4

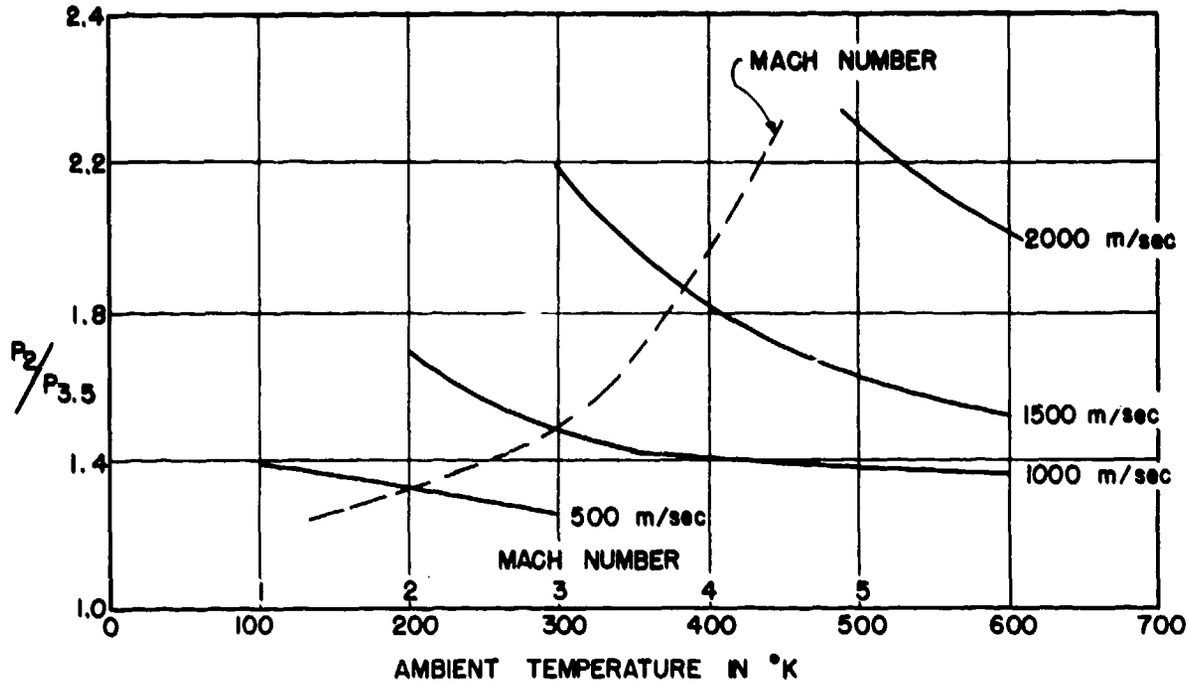

RATIO OF PRESSURE AT 2 AND 3.5 CALIBRES FROM THE NOSE OF THE V-2 VERSUS AMBIENT TEMPERATURE

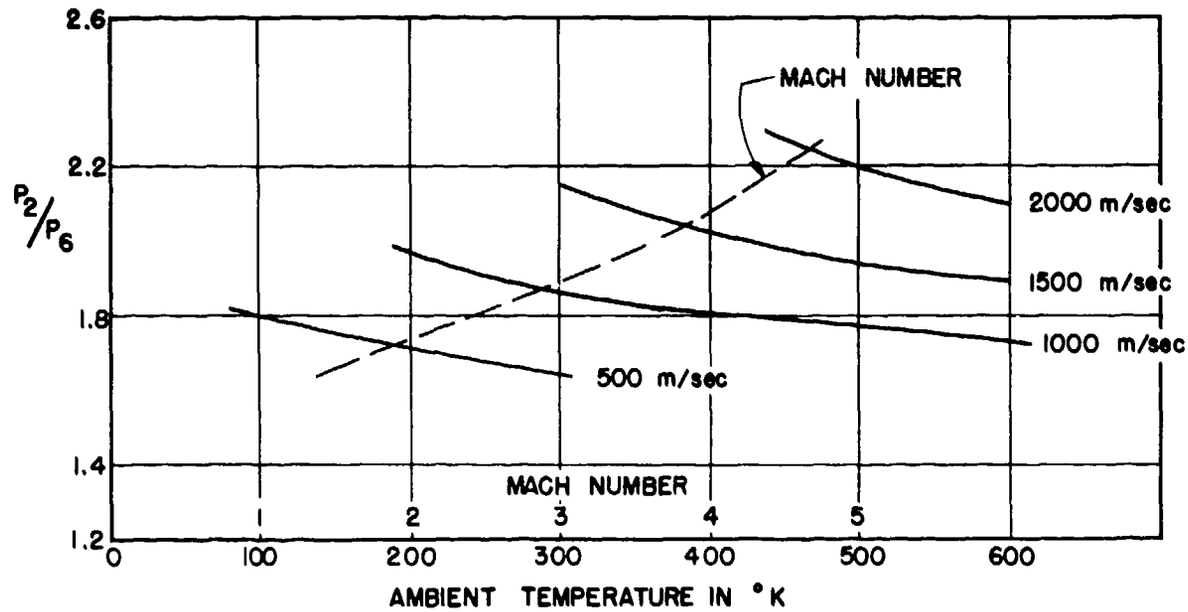

RATIO OF PRESSURE AT 2 AND 6 CALIBRES FROM THE NOSE OF THE V-2 VERSUS AMBIENT TEMPERATURE

CH. V SEC. A FIG. 5

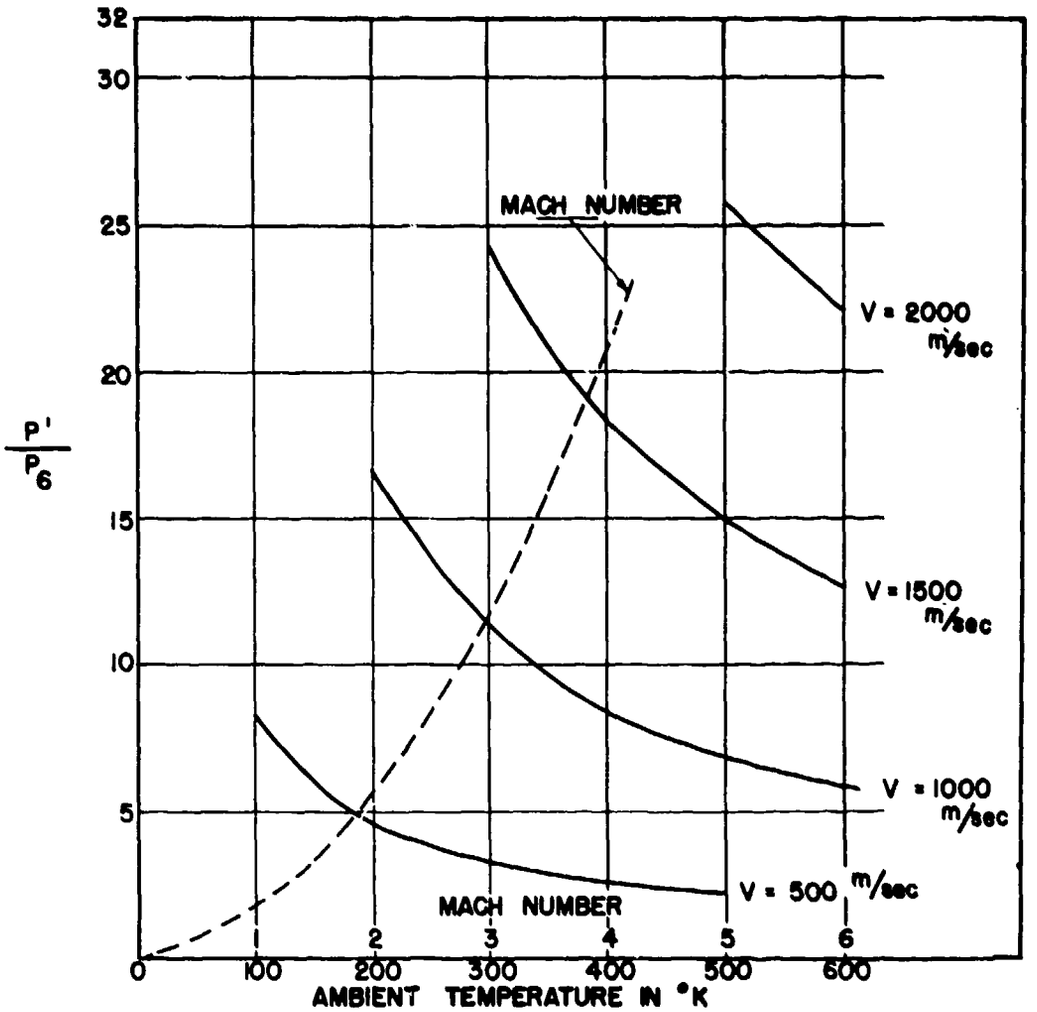

RATIO OF PRESSURE AT THE NOSE AND AT 6 CALIBRES FROM THE NOSE OF THE V-2 VERSUS AMBIENT TEMPERATURE

CH. V SEC. A FIG. 6

On the basis of the Taylor-Maccoll and Rayleigh theories, an estimate can be made of the precision necessary in the measurements of pressure at the nose, and along the surface of a 30° cone, in order to maintain a relative percentage error in the ambient pressure P_1, of 10%, or of 20%. It is found that the relative error in ambient pressure P_1 in terms of the relative errors in P_s and P' is given by the expression:

$$(4) \qquad \frac{\Delta P_1}{P_1} = \frac{\Delta P_s}{P_s}\left\{1 + \frac{\gamma KM^2}{1+\gamma KM^2}\left(\frac{3M-20}{M-10}\right)\right\} - \frac{\Delta P'}{P'}\left\{\frac{\gamma KM^2}{1+\gamma KM^2}\left(\frac{3M-20}{M-10}\right)\right\}$$

Assuming that the terms on the right contribute equally to the relative error, the values in Table 1 are obtained for the percentage error admissible in P_s and P' over the range of Mach numbers from 2 to 6, if the relative error in P_1 is to be that indicated.

Fig. 7 shows an estimate of the variation of Mach number with height, and with time, for the October 10 firing.

If the pressure measured at six calibers from the nose is used to indicated ambient pressure, then Fig. 4 shows that the relative error in ambient pressure is:

$$\frac{P_{s6} - P_1}{P_1} = -\frac{0.01M^2}{2}$$

For a Mach number of 2, this error is only 2%. For a Mach number of 6, however, it rises to 18%.

To estimate the precision necessary for the ambient temperature measurements, the curves of pressure ratio versus Mach number are used. These appear in Figs. 2, 5a, 5b, and 6. The pressure ratio $\frac{P_a}{P_b}$, in each of these figures is a function of the Mach number, i.e.:

$$M = \frac{U}{\sqrt{\gamma R T_1}} = f\left(\frac{P_a}{P_b}\right).$$

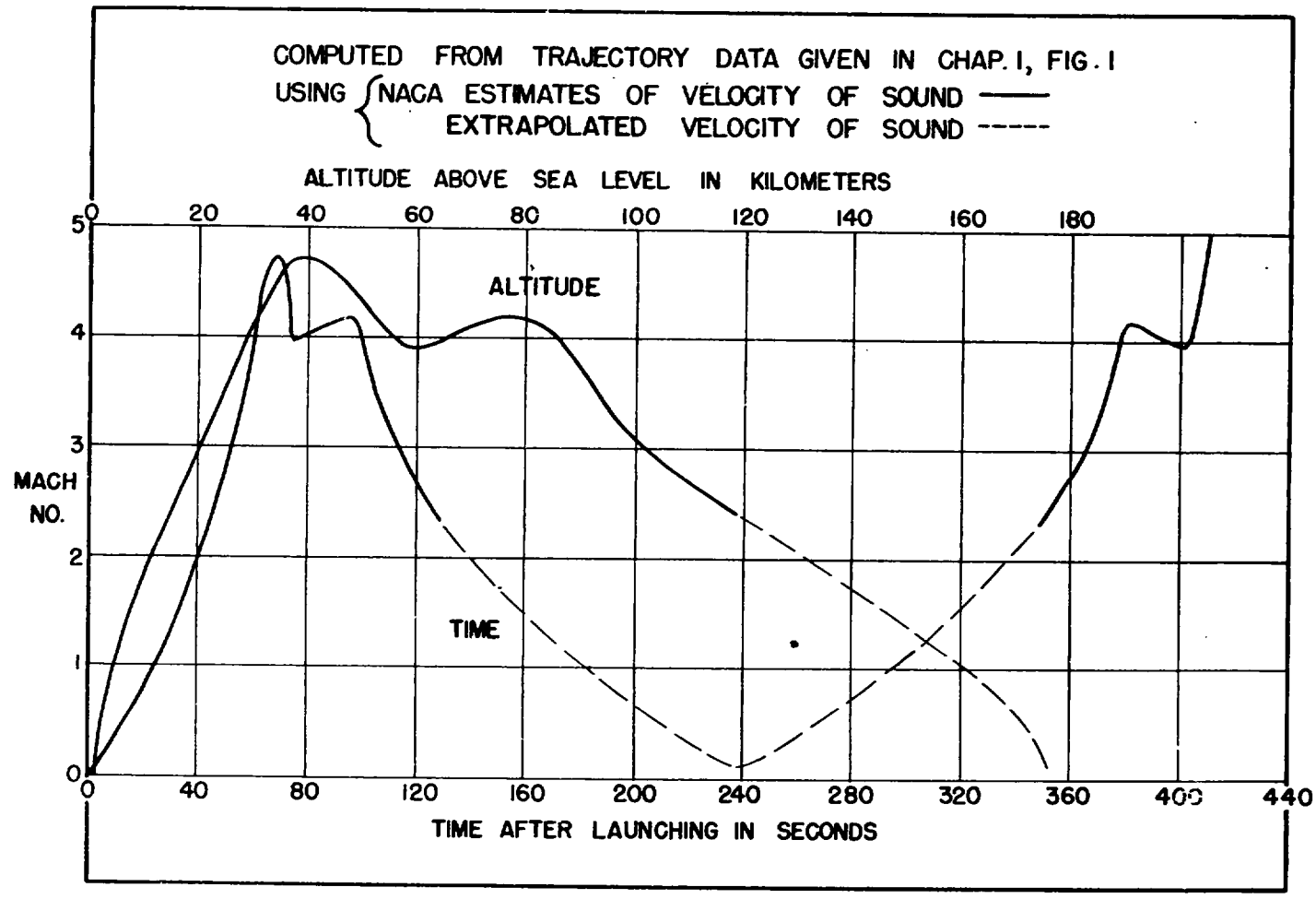

MACH NUMBER VERSUS ALTITUDE & TIME FOR 10 OCTOBER FIRING

Hence:

$$(5) \qquad \frac{\Delta T_1}{T_1} = \frac{2\Delta U}{U} - \frac{2}{f} \cdot \frac{\partial f}{\partial \left(\frac{P_a}{P_b}\right)} \left\{ \frac{\Delta P_a}{P_a} - \frac{\Delta P_b}{P_b} \right\} \frac{P_a}{P_b} .$$

Assuming that the velocity can be measured with great accuracy, the error in T_1 enters primarily through the last two terms on the right. Table II shows the errors tolerable in P_a and P_b for the different cases represented by Figs. 2, 5a, 5b, and 6. It is clear from this table that the use of the nose pressure P' is desirable in measuring the ambient temperature.

TABLE I

RELATIVE ERROR TOLERABLE IN MEASURED NOSE PRESSURE AND MEASURED SURFACE PRESSURE TO ATTAIN INDICATED ACCURACY IN COMPUTED AMBIENT PRESSURE

	Relative Error in Ambient Pressure			
	10%		20%	
Mach No.	Error in Nose Pressure	Error in Surface Pressure	Error in Nose Pressure	Error in Surface Pressure
2	7.6%	3.0%	15.2%	6.0%
3	5.9%	2.7%	11.8%	5.4%
4	5.8%	2.7%	11.6%	5.4%
5	7.1%	2.9%	14.2%	5.8%
6	13.6%	3.1%	27.2%	7.4%

TABLE II

RELATIVE ERROR TOLERABLE IN MEASURED SURFACE PRESSURE TO ATTAIN INDICATED ACCURACIES IN COMPUTED AMBIENT TEMPERATURES

		Relative Error in Ambient Temperature	
	Mach No.	10%	20%
Fig. 2	2	2.9%	5.8%
	4	2.3%	4.6%
Fig. 5a	2	3.1%	6.2%
	4	0.5%	1.0%
Fig. 5b	2	0.4%	0.8%
	4	1.1%	2.2%
Fig. 6	2	4.5%	9.6%
	4	2.5%	5.0%

CHAPTER V

THEORETICAL DISCUSSIONS

B. Geometric Factors Underlying Coincidence Counting with Geiger Counters

by

Homer E. Newell, Jr. and Eleanor Pressly

1. Introduction. The intensity of cosmic radiation near the earth's surface shows a marked variation with zenith angle. Numerous investigations into the subject have revealed a close resemblance to a cosine squared law[1-3], and for the most part calculations of coincidence rates to be expected in Geiger counter telescopes have been based upon such a law.

At the altitudes attained by the V-2 rocket, however, cosmic radiation is presumably isotropic. Approximate relationships between intensity of radiation in such an isotropic region and coincidence rates with a pair of counters are derived below. Only cases in which the counter axes are parallel are considered. The formulas depend upon the sizes and separations of the counters in that they contain diameters, lengths, and distance between axes. In actuality the appropriate quantities are probably not actual physical lengths and diameters of the counter envelopes, but rather a set of effective lengths and diameters corresponding to the operating characteristics of the counters. The effective dimensions for insertion into the formulas may be obtained by suitable calibration of the counters.

The degree of approximation to true counting rates is only incompletely considered. More detailed study of this matter is under way, and findings will appear at a later date.

2. The Case of Identical Counters: The Counters Separated. Fig. 1 shows two orthogonal projections of a pair of counters which are placed as they might be for the recording of twofold coincidences. The counters are right circular cylinders of the dimensions shown. One is placed directly above the other and the two have the same orientation. The arrows vv denote the vertical direction. Lines LL, L'L', MM, and M'M' are the traces of planes orthogonal to the respective plane of projection. These four planes together form the boundary of a prismatic tube the direction of which in space may be specified by the angles α and β shown in the figure.

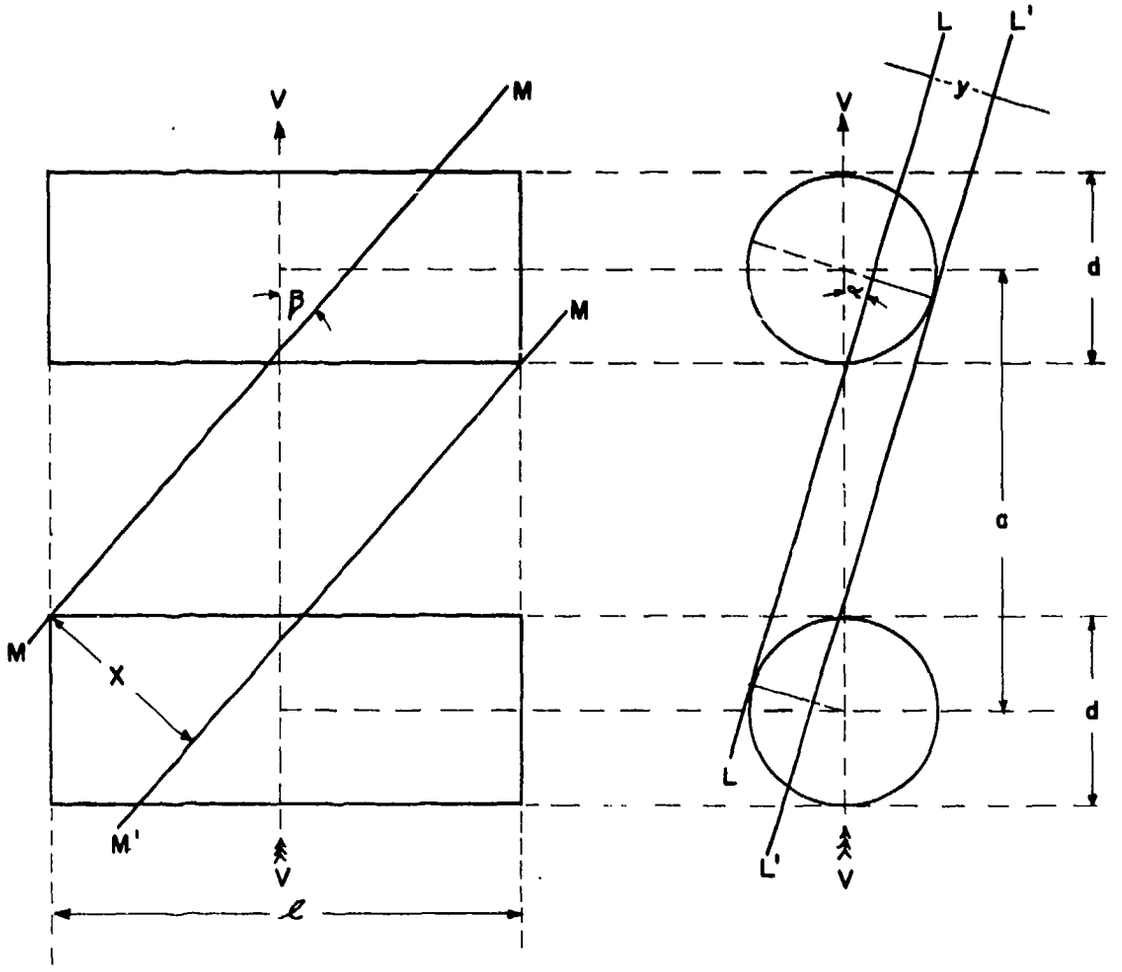

ORTHOGONAL PROJECTIONS OF THE COUNTER ARRAYS
FOR THE SPECIAL CASE CONSIDERED IN THE TEXT

CH. V SEC. B FIG. 1

It is plain that rays coming from the direction $[\alpha,\beta]$ give rise to a coincidence only if they travel within the prismatic tube. A right section of this tube is a parallelogram as shown in Fig. 2. It is a simple matter to show that the distances between opposite sides are also the distances between MM and M'M' and between LL and L'L'. These distances are designated as x and y in both Fig. 1 and Fig. 2. Onto this right section the two counters have a common projected area σ, shown schematically in Fig. 2. It is the rays which cross σ which give rise to actual coincidences.

The number of coincidences per second caused by rays coming from a small solid angle $d\Sigma$ about the direction $[\alpha,\beta]$ is given by the relation

1.) $$dN_2 = I\sigma d\Sigma,$$

where the constant of proportionality I is the "intensity" of the radiation. All three quantities I, σ, and $d\Sigma$ in general depend upon α and β, and to obtain the total number N_2 of coincidences per second caused by rays coming from a specified solid angle it is necessary to integrate over Σ:

2.) $$N_2 = \iint_{\Sigma} I\sigma d\Sigma.$$

The discussion just given clearly applies in principle to the general case of counters of any specified shape and relative orientation and of differing sizes. The chief difficulty lies in actually carrying out the integration in 2.). It is also plain that the use of α and β as the parameters specifying the directions of the rays is not essential. They are chosen in the present case since they appear to be the most convenient for the cylindrical counters under consideration.

In order to carry out the integration required to evaluate N_2, it is necessary to obtain expressions for σ and $d\Sigma$ in terms of α and β. The solid angle $d\Sigma$ will be considered first.

The drawing of Fig. 3 shows the relation which exists between α and β and spherical polar coordinates θ and ϕ. It is known that

$$d\Sigma = \sin\theta \, d\theta \, d\phi.$$

It suffices, therefore, to transform this expression to one involving α and β.

The relation between α, β, θ, and ϕ is given by

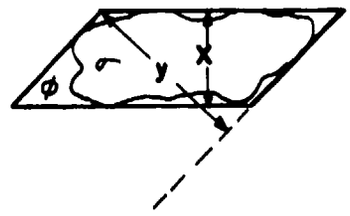

SCHEMATIC DRAWING OF TUBE CROSS SECTION

CH. V SEC. B FIG. 2

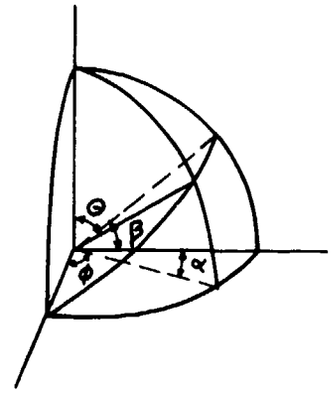

FIGURE SHOWING THE RELATION BETWEEN THE PARAMETERS α AND β AND SPHERICAL POLAR COORDINATES

CH. V SEC. B FIG. 3

$$\begin{cases} \theta = \operatorname{arcctn}(\cos\alpha \tan\beta), \\ \phi = \frac{\pi}{2} - \alpha. \end{cases}$$

Thus

$$J = \frac{\partial(\theta,\phi)}{\partial(\alpha,\beta)} = -\frac{\cos\alpha}{1 - \sin^2\alpha \sin^2\beta}.$$

Also

$$\sin\theta = \frac{\cos\beta}{(1 - \sin^2\alpha \sin^2\beta)^{1/2}}.$$

Hence finally:

3.) $$d\Sigma = \frac{\cos\alpha \cos\beta}{(1 - \sin^2\alpha \sin^2\beta)^{3/2}}\, d\alpha\, d\beta.$$

It is convenient to replace the area σ by that of the parallelogram in Fig. 2. In most cases the error introduced is small. From Fig. 2 it is plain that this area is given by

4.) $$\frac{xy}{\sin\phi}.$$

The value of $\sin\phi$ can be obtained with the use of Fig. 4. There OL is the trace of a plane normal to the yz-plane and corresponds to LL of Fig. 1, so that the unit vector $\underline{ON}$ normal to OL and lying in the yz-plane is also normal to the plane of which OL is the trace. A similar relationship exists between OM, $\underline{ON'}$, and the plane MM of Fig. 1. Now

$$\underline{ON} = \underline{j}\cos\alpha - \underline{k}\sin\alpha,$$

and

$$\underline{ON'} = \underline{i}\cos\beta - \underline{k}\sin\beta.$$

Hence

$$\cos\phi = \sin\alpha \sin\beta,$$

5.) $$\sin\phi = (1 - \sin^2\alpha \sin^2\beta)^{1/2}.$$

From Fig. 1, it may be seen that

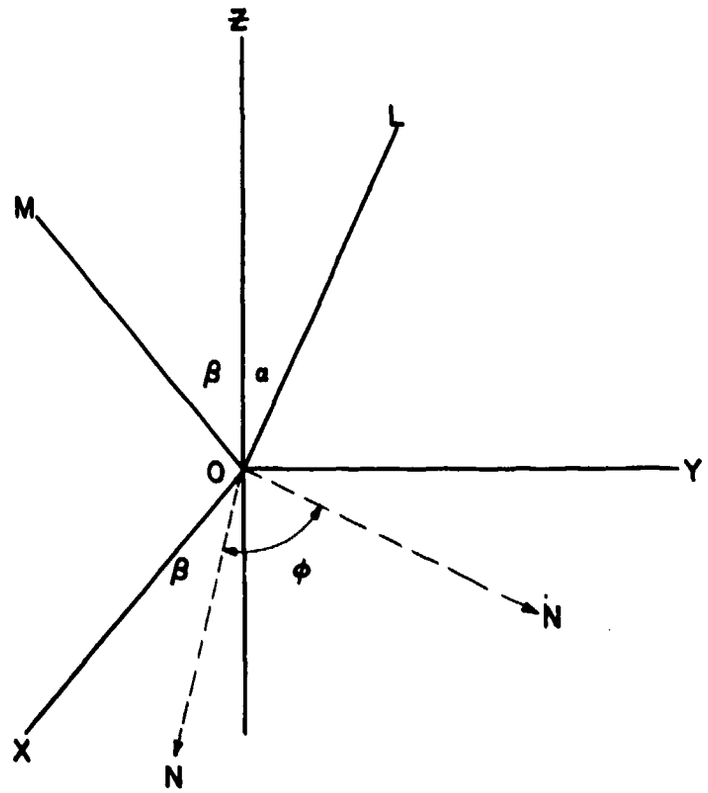

DRAWING FOR OBTAINING THE SINE OF THE POLAR ANGLE ϕ
IN TERMS OF THE PARAMETERS α AND β

CH. V SEC. B FIG. 4

$$x = \ell\cos\beta - (a - d)\sin\beta,$$
$$y = d - a\sin\alpha.$$

Thus, if only rays from a single hemisphere be considered,

6.) $$N_2 = 4I\int_0^{\beta_0}\int_0^{\alpha_0}(\ell\cos\beta-(a-d)\sin\beta)(d-a\sin\alpha)(1-\sin^2\alpha\cdot\sin^2\beta)^{-2}\cos\alpha\cos\beta\, d\alpha\, d\beta$$

where the limits of integration, α_0 and β_0, are to be determined from Fig. 1. The integration is straightforward, though tedious, and leads to

$$\begin{aligned}\frac{N_2}{2I} &= \ell d\,\frac{\cos\alpha_0}{\sin\alpha_0}\tan^{-1}(\cos\alpha_0\tan\beta_0) - \frac{\ell d}{\sin\alpha_0}\beta_0 \\ &+ \left[\frac{\ell d\cos\beta_0}{2} - \frac{(a-d)d\sin\beta_0}{2}\right]\log\frac{1+\sin\alpha_0\sin\beta_0}{1-\sin\alpha_0\sin\beta_0} \\ &- \frac{(a-d)d}{2\sin\alpha_0}\log(1-\sin^2\alpha_0\sin^2\beta_0) \\ &+ \ell d\sin\alpha_0\sin\beta_0\left[1 + \left(\frac{1}{9}\sin^2\alpha_0 + \frac{1}{6}\right)\sin^2\beta_0\right. \\ &+ \left.\left(\frac{1}{25}\sin^4\alpha_0 + \frac{1}{30}\sin^2\alpha_0 + \frac{3}{40}\right)\sin^4\beta_0 + \cdots\right].\end{aligned}$$

It can be seen from Fig. 1 that:

7a.) $$\begin{cases}\sin\alpha_0 = \dfrac{d}{a}, \\ \cos\alpha_0 = \sqrt{1-\dfrac{d^2}{a^2}}, \\ \tan\alpha_0 = \dfrac{d}{a}\Big/\sqrt{1-\dfrac{d^2}{a^2}},\end{cases}$$

7b.) $$\begin{cases}\sin\beta_0 = \ell/\sqrt{\ell^2+(a-d)^2} = \dfrac{\ell}{a-d}\left[1+\left(\dfrac{\ell}{a-d}\right)^2\right]^{-1/2}, \\ \cos\beta_0 = (a-d)/\sqrt{\ell^2+(a-d)^2} = \left[1+\left(\dfrac{\ell}{a-d}\right)^2\right]^{-1/2}, \\ \tan\beta_0 = \ell/(a-d).\end{cases}$$

Using these relations, expanding in terms of a^{-1}, and retaining only terms up to a^{-4}:

8.) $$\frac{N_2}{2I} = \frac{\ell^2 d^2}{2a^2} + \frac{\ell^2 d^3}{2a^3} + \frac{\ell^2 d^4}{2a^4} - \frac{1}{6}\frac{\ell^4 d^2}{a^4}.$$

When a is large, 8.) reduces to

8'.) $$N_2 = \frac{\ell^2 d^2}{a^2} I,$$

which is very easily applied.

Counters Together. Formula 8.) is no longer applicable when a is too small, that is, when the counters are close. It is, however, possible to obtain a formula for N_2 in closed form corresponding to the case in which the counters are in contact, for which $a = d$. Such a relationship can be used to obtain a rough estimate of the value of a below which 8.) is no longer useable.

Suppose that Fig. 1 still applies except that the counters are in contact. Thus $a = d$, and the limits of integration in calculating N_2 are $\alpha_0 = \frac{\pi}{2}$ and $\beta_0 = \frac{\pi}{2}$. This gives, from 6.):

$$N_2 = 2I \int_0^{\frac{\pi}{2}} \left\{ \frac{\ell d}{2 \sin\beta} - \frac{\ell d}{2} \sin\beta \right\} \log \frac{1 + \sin\beta}{1 - \sin\beta} \, d\beta,$$

where again only rays from a single hemisphere are considered. Integrating:

9.) $$N_2 = (\pi - 2) \frac{\pi}{2} \ell d \, I.$$

3. Counters of Different Sizes. Suppose, now, that the counters under investigation differ in size, as in Fig. 5a. For the moment the shorter counter is also taken as the thinner one. It becomes necessary to break the integration of 2.) into separate parts. From Figs. 5a and 5b it may be seen that

$$x = d' \sin\beta + \ell' \cos\beta, \quad 0 \leq \beta \leq \beta_1,$$

$$x = \frac{\ell + \ell'}{2} \cos\beta - \left(a - \frac{d + d'}{2}\right) \sin\beta, \quad \beta_1 \leq \beta \leq \beta_0,$$

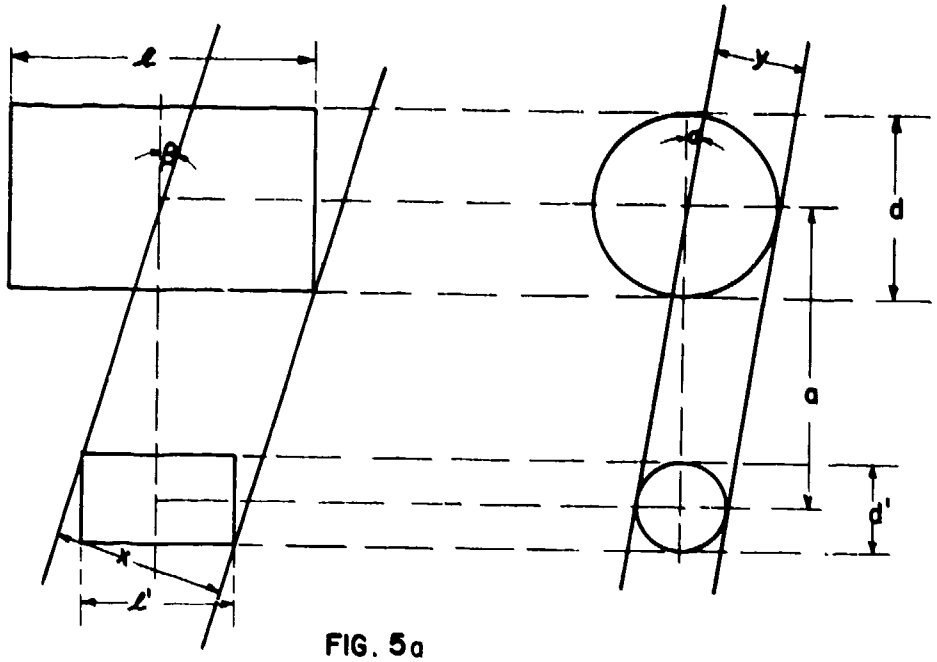

FIG. 5a

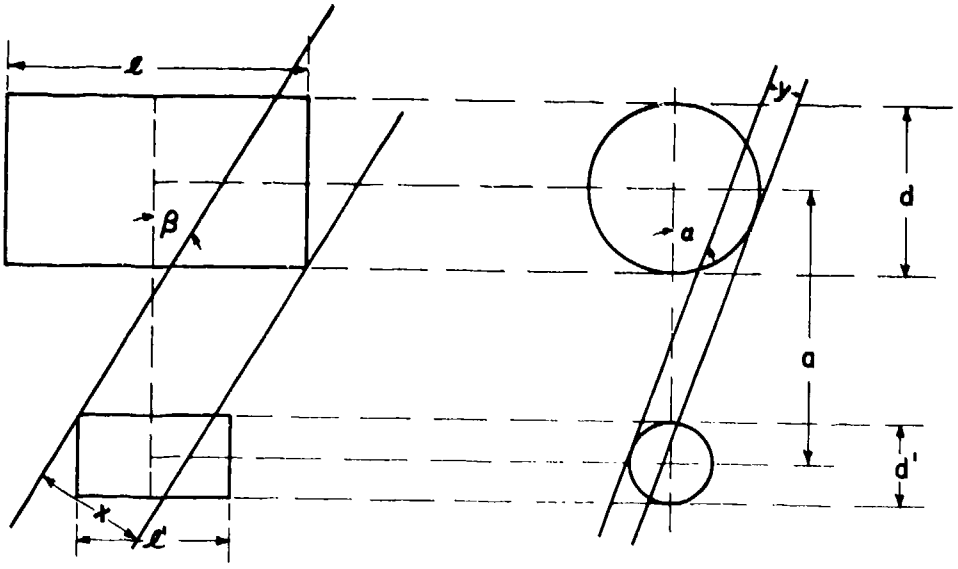

FIG. 5b

ORTHOGONAL PROJECTIONS OF THE COUNTER ARRAYS
FOR THE GENERAL CASE CONSIDERED IN THE TEXT

CH. V SEC. B FIG. 5

$$y = d' \quad , 0 \leq \alpha \leq \alpha_1,$$

$$y = \frac{d + d'}{2} - a \sin\alpha, \alpha_1 \leq \alpha \leq \alpha_0$$

where

$$\sin\alpha_1 = \frac{d - d'}{2a} ,$$

$$\sin\alpha_0 = \frac{d + d'}{2a} ,$$

$$\tan\beta_1 = \frac{\ell - \ell'}{2a - (d - d')} ,$$

and

$$\tan\beta_0 = \frac{\ell + \ell'}{2a - (d + d')} .$$

Hence, coincidences N_2 due to rays from a single hemisphere, are given by

$$\frac{N_2}{4I} = \int_0^{\beta_1}\int_0^{\alpha_1} \frac{(d' \sin\beta + \ell' \cos\beta)\, d' \cos\alpha \cos\beta}{(1 - \sin^2\alpha \sin^2\beta)^2}\, d\alpha\, d\beta$$

$$+ \int_0^{\beta_1}\int_{\alpha_1}^{\alpha_0} \frac{(d' \sin\beta + \ell' \cos\beta)\left(\frac{d + d'}{2} - a \sin\alpha\right) \cos\alpha \cos\beta}{(1 - \sin^2\alpha \sin^2\beta)^2}\, d\alpha\, d\beta$$

$$+ \int_{\beta_1}^{\beta_0}\int_0^{\alpha_1} \frac{\left\{\frac{\ell + \ell'}{2} \cos\beta - \left(a - \frac{d + d'}{2}\right)\sin\beta\right\} d' \cos\alpha \cos\beta}{(1 - \sin^2\alpha \sin^2\beta)^2}\, d\alpha\, d\beta$$

$$+ \int_{\beta_1}^{\beta_0}\int_{\alpha_1}^{\alpha_0} \frac{\left\{\frac{\ell + \ell'}{2} \cos\beta - \left(a - \frac{d + d'}{2}\right)\sin\beta\right\}\left\{\frac{d + d'}{2} - a \sin\alpha\right\} \cos\alpha \cos\beta}{(1 - \sin^2\alpha \sin^2\beta)^2}\, d\alpha\, d\beta .$$

After integration:

$$
\begin{aligned}
\frac{N_2}{4I} = {} & \frac{a}{4}\left(a - \frac{d-d'}{2}\right)\left\{\log\left(1 - \sin^2\alpha_0 \sin^2\beta_1\right) - \log\left(1 - \sin^2\alpha_1 \sin^2\beta_1\right)\right\} \\
& - \frac{a}{4}\left(a - \frac{d+d'}{2}\right)\left\{\log\left(1 - \sin^2\alpha_0 \sin^2\beta_0\right) - \log\left(1 - \sin^2\alpha_1 \sin^2\beta_0\right)\right\} \\
& + \frac{a}{2}\,\frac{\ell-\ell'}{2}\left(\cos\alpha_0 \tan^{-1}\frac{\operatorname{ctn}\beta_1}{\cos\alpha_0} - \cos\alpha_1 \tan^{-1}\frac{\operatorname{ctn}\beta_1}{\cos\alpha_1} - \frac{\pi}{2}\left(\cos\alpha_0 - \cos\alpha_1\right)\right) \\
& - \frac{a}{2}\,\frac{\ell+\ell'}{2}\left(\cos\alpha_0 \tan^{-1}\frac{\operatorname{ctn}\beta_0}{\cos\alpha_0} - \cos\alpha_1 \tan^{-1}\frac{\operatorname{ctn}\beta_0}{\cos\alpha_1} - \frac{\pi}{2}\left(\cos\alpha_0 - \cos\alpha_1\right)\right) \\
& - \left(a - \frac{d-d'}{2}\right)\sin\beta_1\left(\frac{d-d'}{8}\log\frac{1+\sin\alpha_1\sin\beta_1}{1-\sin\alpha_1\sin\beta_1} - \frac{d+d'}{8}\log\frac{1+\sin\alpha_0\sin\beta_1}{1-\sin\alpha_0\sin\beta_1}\right) \\
& + \left(a - \frac{d+d'}{2}\right)\sin\beta_0\left(\frac{d-d'}{8}\log\frac{1+\sin\alpha_1\sin\beta_0}{1-\sin\alpha_1\sin\beta_0} - \frac{d+d'}{8}\log\frac{1+\sin\alpha_0\sin\beta_0}{1-\sin\alpha_0\sin\beta_0}\right) \\
& + \frac{\ell-\ell'}{2}\,\frac{d-d'}{8}\left\{2\sin\alpha_1\sin\beta_1\left[1 + \left(\frac{1}{9}\sin^2\alpha_1 + \frac{1}{6}\right)\sin^2\beta_1\right.\right. \\
& \qquad \left.\left. + \left(\frac{1}{25}\sin^4\alpha_1 + \frac{1}{30}\sin^2\alpha_1 + \frac{3}{40}\right)\sin^4\beta_1 + \cdots\right] + \cos\beta_1 \log\frac{1+\sin\alpha_1\sin\beta_1}{1-\sin\alpha_1\sin\beta_1}\right\} \\
& - \frac{\ell-\ell'}{2}\,\frac{d+d'}{8}\left\{2\sin\alpha_0\sin\beta_1\left[1 + \left(\frac{1}{9}\sin^2\alpha_0 + \frac{1}{6}\right)\sin^2\beta_1\right.\right. \\
& \qquad \left.\left. + \left(\frac{1}{25}\sin^4\alpha_0 + \frac{1}{30}\sin^2\alpha_0 + \frac{3}{40}\right)\sin^4\beta_1 + \cdots\right] + \cos\beta_1 \log\frac{1+\sin\alpha_0\sin\beta_1}{1-\sin\alpha_0\sin\beta_1}\right\} \\
& - \frac{\ell+\ell'}{2}\,\frac{d-d'}{8}\left\{2\sin\alpha_1\sin\beta_0\left[1 + \left(\frac{1}{9}\sin^2\alpha_1 + \frac{1}{6}\right)\sin^2\beta_0\right.\right. \\
& \qquad \left.\left. + \left(\frac{1}{25}\sin^4\alpha_1 + \frac{1}{30}\sin^2\alpha_1 + \frac{3}{40}\right)\sin^4\beta_0 + \cdots\right] + \cos\beta_0 \log\frac{1+\sin\alpha_1\sin\beta_0}{1-\sin\alpha_1\sin\beta_0}\right\} \\
& + \frac{\ell+\ell'}{2}\,\frac{d+d'}{8}\left\{2\sin\alpha_0\sin\beta_0\left[1 + \left(\frac{1}{9}\sin^2\alpha_0 + \frac{1}{6}\right)\sin^2\beta_0\right.\right. \\
& \qquad \left.\left. + \left(\frac{1}{25}\sin^4\alpha_0 + \frac{1}{30}\sin^2\alpha_0 + \frac{3}{40}\right)\sin^4\beta_0 + \cdots\right] + \cos\beta_0 \log\frac{1+\sin\alpha_0\sin\beta_0}{1-\sin\alpha_0\sin\beta_0}\right\}
\end{aligned}
$$

Replacing α_1, α_0, β_1, and β_0 by their expressions in terms of the dimensions and separation of the counters, expanding in powers of a^{-1}, and retaining terms only as far as a^{-4}:

$$10.)\qquad \frac{N_2}{2I} = \frac{\ell\ell' dd'}{2a^2} + \frac{dd'}{8a^3}\left\{ d'\,(\ell^2 + \ell'^2) + 2\,d\ell\ell' \right\}$$

$$+ \frac{dd'}{8a^4}\left\{ \ell\ell'(d^2 + d'^2) + dd'(\ell^2 + \ell'^2) - \frac{\ell\ell' dd'}{12a^4}(\ell^2 + \ell'^2). \right.$$

Formula 10.) applies to the case in which

$$\ell > \ell' ,$$

$$d > d' .$$

It is however, a simple matter to show that it also applies when

$$\ell > \ell' ,$$

$$d < d'$$

By letting $d = d'$, $\ell = \ell'$, one again obtains 8.).

4. Counting Rates in a Single Counter. It is often convenient to compare coincidences in a telescope with the number of counts registered by a single counter. For this purpose a formula giving the counts N_1 in a single counter caused by radiation from one hemisphere in an isotropic region is provided here. N_1 is given very simply as 1/2 of πI times the surface area of the counter. Thus

$$N_1 = \frac{1}{2}\pi^2 \ell d \left[1 + \frac{d}{2\ell}\right] I.$$

Here again I, d, and ℓ are the intensity of radiation and the effective diameter and length of the counter.

5. Summary. The following is a summary of the formulas obtained above.

Let two Geiger counters be oriented with their axes parallel, and with the line of centers perpendicular to the axes. Let the separation of the axes be a. Let the effective lengths and diameters be ℓ and d for one counter, and ℓ' and d' for the other. Suppose that

$$\begin{cases} \ell > \ell' , \\ d > d' . \end{cases}$$

or that

$$\begin{cases} \ell > \ell' , \\ d < d' . \end{cases}$$

Then the number N_2 of coincidences per unit time caused in the counters by radiation from one hemisphere of an isotropic field of intensity I, is given approximately by

10'.) $$N_2 = \left[\frac{\ell\ell' dd'}{a^2} \quad \frac{dd'}{4a^3}\left\{ d'(\ell^2 + \ell'^2) + 2\, d\ell\ell' \right\} \right.$$

$$\left. + \frac{dd'}{4a^4}\left\{ \ell\ell'(d^2 + d'^2) + dd'(\ell^2 + \ell'^2) \right\} - \frac{\ell\ell' dd'}{6a^4}(\ell^2 + \ell'^2) \right] I.$$

When a is large, N_2 is given by

10".) $$N_2 = \frac{dd'\ell\ell'}{a^2} \; I.$$

If the counters are exactly alike, so that $\ell = \ell'$, $d = d'$,

then

8".) $$N_2 = \left[\frac{\ell^2 d^2}{a^2} + \frac{\ell^2 d^3}{a^3} + \frac{\ell^2 d^4}{a^4} - \frac{\ell^4 d^2}{3a^4} \right] I ,$$

and for large a

8'.) $$N_2 = \frac{\ell^2 d^2}{a^2} \; I.$$

The goodness of approximation of all of these formulas decreases with a. In the case of similar counters in contact, however, a good approximation to N_2 is given by

9.) $$N_2 = (\pi - 2)\frac{\pi}{2}\ell d \; I.$$

Finally, for comparison purposes, the counts N_1 per unit time caused in a single counter by radiation from one hemisphere of an isotropic field of intensity I is given by

$$N_1 = \frac{1}{2} \pi^2 \ell d \left[1 + \frac{d}{2\ell} \right] I.$$

REFERENCES

1. GREISEN, K.: The Intensities of the Hard and Soft Components of Cosmic Rays as Functions of Altitude and Zenith Angle, Phys. Rev., Vol. 61, pp 212-221, March 1 and 15, 1942.

2. JOHNSON, T.H.: Comparison of the Angular Distributions of the Cosmic Radiation at Elevations 6280 feet and 620 feet, Phys. Rev., Vol. 43, pp 307-310, March 1, 1933.

3. SKOBELZYN, D.: Repartition Angulaire des Rayons Ultrapenetrants (Rayons Cosmiques), Comptes Rendus, Vol. 194, pp 118-121, Jan. 4, 1932.

CHAPTER VI

FUTURE RESEARCH

by

E. H. Krause

Because of the important results already obtained in the study of the upper atmosphere by means of rockets, and especially because of the highly successful experiment conducted on October 10, elaborate plans are being made to continue the experiments over an extended period of time. It appears now, according to word from Army Ordnance that 50 V-2's in all will be fired. At the present rate of firings this extends the V-2 program into the middle of 1948. Subsequently the HASR-2 rocket, now being built by the Glenn L. Martin Company for the Naval Research Laboratory, should extend the program at least to January, 1950. In addition five XASR-2 rockets are at present being constructed by the Aerojet Corporation and should become available next spring. It is planned to use them during the two year period beginning with the summer of 1947.

The XASR-2 has a payload of 68 kilograms (150 pounds), and a maximum altitude of 90 kilometers (about 300,000 feet). Because of its small size it will probably be employed for conducting single experiments in cosmic rays, spectroscopy or atmospheric physics. No ionosphere experiments will be conducted in this rocket since it does not reach a sufficiently high altitude.

The HASR-2 rocket is being built by Martin on an ONR-NRL contract. It is still in the design stage. The rocket is expected to reach an altitude of 150 kilometers (about 500,000 feet) with a payload of 225 kilograms (about 500 pounds) or alternatively an altitude of 225 kilometers (about 750,000 feet) with a payload of 45 kilograms (about 100 pounds). Its motor, being built by Reaction Motors, Inc., will use alcohol and oxygen as fuel and oxidizer, and is expected to develop a thrust of 9,000 kilograms (about 20,000 pounds). The length of the rocket is to be about 13.5 meters (44.5 feet), and the diameter, about 80 cm. (32 inches). The use of this rocket for high altitude research will differ considerably from the use of the V-2, the payload being about one-third that of the V-2. Moreover, the warhead will be of an airplane type reinforced steel rather than the heavy solid steel used in the V-2. Also, in contrast to the V-2, there will not be a large amount of space in the center of the body between fuel tanks, or between the tanks and combustion chamber. Complete details will be published in another report when the design has reached a more advanced stage.

Research in cosmic rays will continue. The most elaborate experiment yet tried on this subject will be attempted on December 5, and a still more elaborate experiment is being planned for the January 9 missile.

The taking of solar spectrograms is continuing, utilizing a grating spectrograph. Work on the sweeping photocell method, which was developed to enable the telemetering of the spectrographic informa- to the ground, has been virtually completed. However, because of the successful recovery of a spectrographic film after the October 10 firing, the use of this instrument in the near future is not contemplated. The photocell method was developed primarily because the film was not recovered in the early flights. Recovery of a spectrograph film yields a much larger amount of information that does the photocell, the reasonable success in recovery should make the film method the superior one. It should be possible in the not too distant future to obtain solar spectra from an altitude of 170 kilometers. Only malperformance of the equipment limited the altitude to 88 kilometers in the October 10 experiment.

The effort in atmospheric physics is presently directed toward improving Pirani gages and extending pressure measurements to higher altitudes through the use of ionization gages and Philips gages. The main emphasis is being placed on pressure measurements, since these can be taken with greater reliability and have more meaning than either temperature or composition measurements. It is felt, on the basis of work already performed, that good pressure data, and possibly also temperature data, should be obtained to an altitude of 170 kilometers some time during the next year.

The ionosphere experiments have been delayed in the past partly due to inadequate antennas, or antennas having unknown characteristics. Pattern studies of the various ionosphere antennas are currently being made through the use of models. It is now considered that drag antennas can be made mechanically satisfactory; nevertheless, tuning them present great difficulties. They, therefore, will probably not be used in the next series of firings. The method of measurement described in the first report will continue to be used.

Recovery methods involving parachute and drag mechanisms are being temporarily abandoned in favor of recovery by direct attachment to the missile. As has already been pointed out, the parachute and drag mechanisms used in the October 10 and October 24 firings were never found, although apparently they were successfully ejected. This difficulty in locating a recovery device after it has landed is one of the fundamental shortcomings of such a recovery method. There are, of course, certain techniques such as the use of a radio beacon, which

might prove successful in marking the landing spot, and which still remain to be tried. It is felt, however, that the success of recovery of the V-2 body has been good enough to minimize the need for other recovery methods at this time. The use of parachutes and drag mechanisms for the sole purpose of slowing descent is not particularly worth while since the slowed descent is confined primarily to the region in which it is normally possible to take data with balloons.

Telemetering will continue to undergo improvement. The present system, although it has been producing fairly good results, is not as yet completely satisfactory. Power is to be increased still further. Circularly polarized antennas are to be added on the end of the missile during some of the flights within the next month. Higher gain antennas are being built in order to decrease the amount of power required in the rocket and thereby to reduce the number of batteries. Better synchronization methods are under study.

Photographs from the high altitudes will be attempted again in the December 5 flight, and probably in subsequent flights. Considerably better cameras are under consideration for this purpose. In addition to pictures of the ground, it may be possible by these photographic techniques to obtain information on missile aspect, air turbulence, shock waves, and general rocket motion.

In general it is becoming clear that the number of experiments which can be performed in the V-2 is increasing due to the success of the first experiments. Already the V-2 has provided the most important contribution in many years to the fields of solar spectroscopy, cosmic rays, and upper atmosphere physics.

APPENDIX

Table of Critical Values

The material in the following table has been in frequent demand in the work of the Rocket-Sonde Section. The data are available in other places, but the form of tabulation employed here appears to be of considerable aid in facilitating reference.

The values of most constants are for pure elements. However, in some cases 0.01% of impurities (Te for example) changes a resistance by a factor of two or more and the thermoelectric power from a large positive value to a negative value. For this reason values of the resistances of semi-conductors are quite variable depending upon the impurities. For good conductors the temperature coefficient of resistance is as much as 30% low for commercial metals compared to pure metals. Thermoelectric power varies greatly, and the value given in the table is only the most probable value for the metal listed.

Two metals can in general form an alloy if the corresponding ratios $\frac{A}{D}$ do not differ by more than 30%.

An impure metal (or alloy) has a higher resistance and a lower temperature coefficient of resistance than the pure metal (or the pure metal constituent of the alloy). The only known exception is Bi with a slight impurity of Te. Other metals, however, which approach semi-conductors in resistance are also probable exceptions.

APPENDIX

TABLE OF CRITICAL VALUES

1	2 Atomic Weight	3 Density gm/cm³	4 D|P	5 Melting pt. °C	6 Boiling pt. °C	7 Relative Hardness	8 Youngs Modulus (lb/in²) x 10⁶	9 Breaking Strength (lb/in²) x 10³	10 Reflectivity λ (microns) 6	2	10	11 Specific Resistance x 10⁶	12 ΔR/R ΔT at 0°C x 10³	13 K Thermo-elec. Power in microvolts	14 Specific Heat Conduction watts/deg. cm/cm²	15 Specific Heat Joules/deg/cm²	16 L ΔT/ΔT Thermal Expansion x 10⁶	17 Volts °E	18 φ Work Function of Metal	19 Ionization Potential	20 Valence
1S H	1	.08	11.5	-259	-252				%	%	%							0		13.5	1
Li	7	.5	14	186	1220	.6						8.6	4.7	14	.7	1.7		3.0		5.4	1
Na	23	.95	24	97	880	0.4						4.3	5.4	-4	1.3	1.2	62	2.7		5.1	1
K	39	.9	43	62	760	0.5						6.0	5.8	-11	1.	.7		2.9		4.3	1
(Cu)	64	8.9	7	1083	2300	2.9	18	32 40	72	95.5		1.7	3.8	3	4.0	3.4	17	-.3		7.7	1,2
Rb	85	1.5	59	38	700	0.3						12	6	-5		.5	86	2.9		4.2	1
(Ag)	108	10.5	10	960	1950	2.6	11	40 44-9	92.7	97	99	1.6	3 4	3	4.2	2.4	19	-.8		7.5	1
Cs	133	1.9	70	29	670	0.2						19				.4			1.81	3.9	1
(Au)	197	19	10.4	1063	2600	2.5-3	11	25 38				2.4		2.9	3.1		14	-1.4		9.2	1,3
6P Be	9.0	1.8	5	1350	(1500)	3						5.5	14. 7.		1.6	3.1	12	1.7		9.3	2
Mg	24	1.7	14	651	1110	2.3	6	15-19 25-31	73	77		4.6		-0.2	1.6	1.7	26	2.4		7.6	2
Zn	65	7.1	9	419	907	2.5	11-14.8	17-43	57.5	94	98	6.0		3.0	1.1	2.8	26	.8		9.4	2
Cd	112	8.6	13	320	767	2.0	10	12		87	98	7.5	3.8		.9	2.0	29	.4		9.0	2
Hg	201	13.5	15	-40	357	1.5			70			96		-8.8	.08	1.9		-.8		10	1,2
5P B	11	2.5	4	2000	2550	9.5										3.2				8.2	3
Al	27	2.7	10	660	1800	2.7	10	8 34		85	97	2.8		-.47	2.0	2.5	25.5	1.7		6.0	3
Ga	70	5.9	12	30	1600	1.5						53	3.			2.0				6.0	2,3
In	115	7.3	15	155	1450	1.2						8.4		2.4			42	.3		5.8	3
Tl	204	12	17	303	1650	1.2						18	1	1.6	0.4	1.5	30	.3		6.1	1,3
4P C	12	2.2 3.5	4	73500	4200	10			23.5	35	55	10^3		11		1.7	1.2 5.4 7.9		4.0	11	2,4
Si	28	2.4	11	1420	2600	7.0			32	28	28	60		-408	.8	1.7	7.6			8.1	4
Ge	73	5.5	13	958	2700	6.2						10^5		300		1.7				8.1	4
Sn	119	7.3 5.25	17	231	2260	1.6	5.7-7.8	10 4		61	84	11.5		07 .23	.7	1.7	27	.1		7.3	2,4
Pb	207	11	19	327	1620	1.5	2.1-2.4	2 3				22			.4	1.5	29	.1		7.4	2,4
3P N	14	1.0	14	-209 -120	-195															14	3,5
P	31	1.8 2.4	19	44	280	6		35 40								1.4	124			11	3,5
As	75	5.7	13	500	615	3.5						35	4	0		1.9	4	-.3		10.5	3,5
Sb	122	6.6	19	630	1380	3.1	11	1.5	53	60	72	42		36	.2	1.4	12	-.1		8.5	3,5
Bi	209	9.8	21	271	1450	2-						120		-44 -74	.08	1.2	13	-.2		8.0	3,5
2P O	16	1.4	11	-218	-180													(-.4)		13.5	2
S	32	2.0	16	112	444	2.0											64	.5		10.3	2,4,6
Se	79	4.5	16	220	688	2.0											37			9.7	2,4,6
Te	128	6.2	20	452	1390	2.3			49	52	78	4.10^5			.06	1.3	2 17	.8		9.0	2,4,6
Po	(210)			(1800)														-.4			
1P F	19	1.3	15	-223	-187													-1.9		17	1
Cl	35	(1.9)	18	-101	-35													-1.4		13	1,3,5,7
Br	80	3.1	26	-7	59													-1.1		12	1,3,5,7
I	127	4.9	26	113	184											1.1	84	-.5		11	1,3,5,7

* ELECTROMOTIVE FORCE RELATIVE TO HYDROGEN.

APPENDIX

TABLE OF CRITICAL VALUES (Continued)

1	2	3	4	5	6	7	8	9	10			11	12	13	14	15	16	17	18	19	20
	Atomic Weight	Density gm/cm³	A/D	Melting pt. °C	Boiling pt. °C	Relative Hardness	Young's Modulus (lb/in²) x 10⁶	Breaking Strength (lb/in²) x 10³	Reflectivity λ (microns) 6	2	10	Specific Resistance x 10⁶	ΔR/R at 0°C x 10³	K Thermo-elec. Power in microvolts	Specific Heat Conduction Watts/deg cm/cm²	Specific Heat Joules/deg/cm²	Thermal Expansion ΔL/L ΔT x 10⁶	Volts* E	Work Function of Metal φ	Ionization Potential	Valence
1P F	19	1.3	15	-223	-187													-1.9		17	1
Cl	35	(1.9)	18	-101	-35													-1.4		13	1,3,5,7
Br	80	3.1	26	-7	59													-1.1		12	1,3,5,7
I	127	4.9	26	113	184											1.1	84	-.5		11	1,3,5,7
10d Ca	40	1.5	26	810	1170	1.5		8.5				4.6	3.6	-8		1.0		2.9	2.6	6.1	2
Sr	88	2.5	34	800	1150	1.8						25						2.9		5.7	2
Rd	226	(5)	45	960	1140															5.2	2
9d Sc	45	(2.5)	18	1200	2400	2.0														6.7	3
Y	89	5.5	16	1490	(2500)															6.5	3
Ac	(227)																				
8d Ti	48	4.5	11	1800	3000	4.0						3.2	3.5			2.0				6.8	3,4
Zr	91	6.4	14	1900	2900	4.5						164	1.1			1.7			4.5	6.9	4
Hf	179	13.3	13	2200	3200							32							5.09		4
Th	232	11.5	21	1845	3000			80				11-18 1.9				1.4	12		3.35		4
7d V	51	5.7	8	1710	3000				58	69	92					2.7				6.7	3,5
Cb	93	8.4	11	1950	2900																3,5
Td	181	16.6	11	2850	4100	7	27	132	45	90	94	15	3.3		.5	2.6	6		3.5		5
Pa	231																				
6d Cr	52	6.5	8	1615	2200	9.0				63	93	2.6				3.0		.55		6.7	2,3,6
Mo				(2300)																	
W	184	19	10	3370	5900	7.0	51	597	51	85	95.5	5.5	4.5	2	1.6	2.7	4		4.5	8.1	6
U	238	18.7	13	4850												2.2		1.4			4,6
5d Mn	55	7.4	7.4	1267	1900	5.5						110 23.5	6.3			3.4	23	1.1		7.4	2,3,4,6,7
Mo				(2300)																	
Re	186	20.5	9	3400								18.9				3.0					
4d Fe	56	7.9	7	1535	3000	4.5	29	15 113	57.5	78	94	10	6.8	-51 16	.64	4.0	9.1	.4		7.8	2,3
Ru	102	12.2	8.4	2450	2700	6.5						7.6				3.1	10			7.7	3,4,6,8
Os	190	22.5	8	2700	5300	7.0						8.9 60				2.9	7			(8.7)	2,3,4,8
3d Co	59	8.7	7	1480	3000	5		35 100		72	97	10	5.5	-11		3.6	12	.3		7.8	2,3
Rh	103	12.4	8	1985	2500	6	42		77	91	94	4.7	4.4		1.9	3.1	8			7.7	3
Ir	193	22.4	9	2300	4800	6.2	7			87	96	6.1	3.7 4.1		.6	3.0	6				3,4
2d Ni	59	8.9 8.6	7	1455	2900	5	30	50 170		83	86	7.8	5.4 6.3	-18	.58	3.8	13	.2	2.77	7.6	2,3
Pd	107	12.2	9	1553	2200	4.4	17	54		85	96	11	3.6 6.7	-7	.71	2.8	12	-.8		8.3	2,4
Pt	195	21.3	9	1773	4300	4.3	25	35 48		80	93 95	10	3.5	-3 -7	.70	2.8	9.0	-.9	5.0(avg)	8.9	2,4
Cu	64	8.9	7	1083	2300	2.9	18	32 40				1.7		2.7			17			7.7	1,2
He	4	.13		-272	-269															24	0
Ne	20	(1.0)		-249	-246															21	0
A	40	1.65		-189	-186															16	0
Kr	84	(2)		-169	-152															14	0
Xe	131	(2.7)		-140	-109															12	0
Rn	222	(4)		-71	-62															11	0

* ELECTROMOTIVE FORCE RELATIVE TO HYDROGEN.

DISTRIBUTION

No. of copies	
(13)	ONR-Planning Division; Program Subdivision; Armament and GM Section; Scientific Subdivision; Geophysics Section; Electronics Section; Physics Section; Publication Liaison; Scientific Subdivision; Tech. Information Section(4 copies).
(1)	ONR-SDC, Sands Point, Port Washington.
(17)	CNO-OP-05; OP-06; OP-03; OP-503; OP-601; OP-413; OP-413C; OP-04/06; OP-100F; OP-57(5 copies);CinCLantFlt; CinCPacFlt.
(13)	BuAer-Aer-E-18; Aer-E1; Aer-E1-35; Aer-SI-50DAS(2 copies); Aer-PA; Aer-TD-4(6 copies).
(9)	BuOrd-Adlf; Ple; Re; Rea; Re-9(4 copies).
(8)	BuShips-Code 330; Code 900; Code 910; Code 918-L.O. Watson Labs; Code 920; Code 938(2 copies).
(2)	PG School-Annapolis.
(1)	Naval Observatory.
(1)	NGF Washington.
(1)	NGF-Optical Shop.
(6)	MarCorps-Military Sec. G-3; Div. Plans & Pol; G-3, Spec. Weapons(2 copies); MarCorps School, Quantico, (3 copies).
(7)	OinC BOEU-NBS, Att: Dr. J.H.Dellinger; Dr. I.O.Gardner; Dr. W.F.Meggers; Dr. Newburn Smith; Dr. H.Diamond; Dr. H. C. Dryden.
(1)	NEL-San Diego.
(5)	NORTLO-MIT, Att: Dr. D.C.Stockbarger; Dr. G.R.Harrison; Dr. Z. Kopal.
(2)	NOL-Washington.
(1)	NOTS-Inyokern.
(1)	NOTU-WSPG.
(1)	NPG-Dahlgren.
(4)	NavOrdDev.U.-APL, Att: Dr. Hafstad; Dr. Van Allen; Dr. Tatel; Dr. Hopfield.
(3)	NMTC-Pt. Mugu.
(4)	NRL Field Group-WSPG.
(1)	SNLO-USNELO-Ft. Monmouth.
(1)	BAGR-ED, 90 Church St., N.Y.
(1)	BAGR-WD, 624 Van Nuys Bldg., Los Angeles.
(1)	BAGR-Wright Field.
(1)	NATC-Patuxent River, Md.
(1)	NAES-Philadelphia.
(1)	NAOTS-Chincoteague, Va.
(2)	ComOpDevFor-FPO, N.Y.

DISTRIBUTION (Cont'd)

No. of copies	
(1)	NAM Center-Philadelphia.
(2)	NAMU-Johnsville.
(1)	DTMB-Washington.
(1)	ASO-Philadelphia.
(1)	USNA-Head, Ord. & Gun., Annapolis
(1)	NAF-Philadelphia.
(1)	Sec. of War-Washington.
(3)	HQ-AAF-Office of Air Com.
(32)	HQ-AAF-AC/AS-4; AC/AS-3(AF66M); OACS Guided Missile Branch; DRE-3(5 copies); Wright Field (22 copies).
(2)	AMC-Watson Labs,CFS, Cambridge.
(1)	AWS-R & D Div., Langley Field.
(10)	Ch/ORD-Rocket Dev. Div.; Sub Office (Rockets) CIT(1 copy); Sub Office (Rockets) Ft. Bliss(2 copies).
(3)	AOTS-WSPG.
(2)	ABL-Aberdeen, Att: Col. Simon, BRL; Dr. Johnson.
(8)	OCSigO-Eng. & Tech Ser; SIGET; SIGID; BIGEE; SIGGG; Eng. Div.; SIGOP(2 copies).
(3)	ESL-Belmar, N.J., Att: Dr. M.J.E.Golay.
(5)	SCEL-Bradley Beach, Att: Lt. Col. Zahl; CSL, Redbank; Eatontown; Via: SNLO, Fort Monmouth, N.J.
(1)	WDSS-Res. & Dev. Div., Att: Col. Trichel.
(2)	Chief of Chemical Corps-Washington.
(1)	Chief GM Br., Tech. Command-Edgewood Arsenal, Md.
(1)	PGC-Eglin Field, Fla.
(1)	Antiaircraft Artillery School-Ft. Bliss, Tex.
(1)	Frankford Arsenal-Philadelphia.
(1)	Wendover Field, Wendover, Utah.
(5)	AGF-Ft. Monroe, Va; Board No. 1, Ft. Baker, Cal.; Board No. 1, Ft. Bragg(2 copies); Board No. 3.
(2)	US Mil.A.-West Pt.
(1)	Air Tactical School, Air Un.-Tyndall Field, Fla.
(1)	JCS-GM Committee
(8)	JRDB(3 copies); JRDB-GM Committee(5 copies)
(1)	Army Forces Staff College-Norfolk.
(2)	Weather Bureau.
(7)	NACA-Langley Field (3 copies); Washington (4 copies).
(3)	UCLA-Att: Dr. Joseph Kaplan.
(2)	Cal Tech-Att: Dr. Millikan; Dr. Malina.
(1)	U. of Cal.
(1)	Carnegie Inst.-Att: Dr. Merle A. Tuve.
(1)	Carnegie Tech-Att: Mr. B. R. Teare.

DISTRIBUTION (Cont'd)

No. of copies	
(1)	U. of Chicago-Att: Prof. Marcel Schein.
(1)	Cornell Aero. Lab-Att: Dr. C.C.Furnas.
(1)	Harvard Observatory-Climax, Att: Dr. Walter O. Roberts.
(3)	Harvard Observatory-Cambridge, Att: Dr. Shapley; Dr. Menzel; Dr. Whipple.
(2)	Harvard U-Att: Prof. Theo. Syman; Prof. H.R. Mimno.
(1)	U. of Ill.-Att: Mr. H.E.Cunningham, Sec'y.
(4)	Johns Hopkins U-Att: Dr. G.H. Dieke; Dr. A.H.Pfund; Dr. John Strong; Dr. R.W.Wood.
(4)	MIT, GMC-Project Meteor Office, Chairman.
(2)	MIT, GMC-Cambridge, Chairman.
(5)	U. of Mich-Att: Dr. Dow; Dr. Nichols; Mr. Robert T. May; Mr. M. B. Small; Dr. A.M. Kuethe.
(1)	Mt. Wilson Observatory-Att: Dr. H.D.Babcock.
(1)	NMCAMA-Att: Dr. Gardner.
(1)	N.Y.U.
(2)	Ohio State U-Att: Dr. George Sinclair; Mr. Thomas E. Davies.
(2)	Penn State U-Att: Haller, Raymond and Brown.
(1)	U. of Penn.
(2)	U. of Pitts.-Att: Dr. A.J.Worthing; Mr. E. O. Holbrook.
(1)	Polytech. Inst. of Brooklyn.
(5)	Princeton U-Att: Project SQUID(3 copies); Dr. Wheeler; Mr. J.F. Brinster.
(1)	Purdue U-Att: Mr. G.S. Meikel.
(1)	U. of Rochester-Att: Dr. Brian O'Brien.
(1)	U. of Southern Cal.
(1)	U. of Texas-Att: Dr. C.P.Boner.
(2)	U. of Va.-Att: Prof. L.G.Hoxton, Via: Naval Ord. Officer.
(1)	U. of Wisconsin-Att: Dr. Gregory Breit.
(1)	AIL-Mineola, Att: Mr. Skifter.
(2)	BAR, Pasadena, Cal. for Aerojet, Att: Dr. Zwicky.
(3)	SINM, Boston, Mass. for Baird Asso., Cambridge.
(2)	BAR, Buffalo for Bell Aircraft, Niagara Falls, Att: Mr. R. H. Stanley.
(1)	Bell Aircraft, Niagara Falls, Att: Mr. B. Hamlin.
(2)	Bell Telephone Labs., Att: Dr. H.W. Bode; Dr. W.A. MacNair.
(2)	Bendix Avia. Corp.-Att: Dr. Harner Selvidge.
(3)	BAR-Boeing Aircraft-Att: Dr. Stealman; Mr. E.V. Mock.
(1)	Boeing Aircraft-Att: Mr. R. H. Nelson.
(2)	BAR-Chance-Vought-Att: Mr. P.S.Baker.
(2)	Dev. Contract Officer-Consolidated Vultee, Daingerfield, Texas.

DISTRIBUTION (Cont'd)

No. of copies	
(2)	BAR-Consolidated Vultee, Downey, Cal.,Att: Mr. C. R. Irvine.
(1)	Consolidated Vultee, Downey, Cal., Att: Mr. W. H. Robinson.
(2)	BAR-Curtiss Wright Corp., Att: Mr. Bruce Easton.
(1)	Curtiss Wright Corp., Att: Mr. R. Darby.
(4)	BAR-Douglas Aircraft-Att: Dr. Klemperer, Mr. R.L. McKay; Mr. E. H. Heinemann.
(2)	Douglas Aircraft-Att: Mr. R.E. Raymond; Mr. E.F.Burton.
(2)	BAR-Fairchild Engine & Aircraft Corp., Att: Mr. J.A.Slonin.
(2)	NAMU, Johnsville, Pa. for Franklin Inst. Labs-Att: Mr. R. H. McClarren.
(8)	Dev.Contract Officer for Gen. Elec. Co., Schenectady-Att: Mr. J.W.Frick; Dr. D.F.Green(2 copies) Dr. K. H. Kingdon; Mr. G. K. Megerian(2 copies).
(4)	Gen. Electric Co., Schenectady, Att: Dr. R.W.Porter(2 copies); Mr. S.G.Schuler, Jr.; Mr. Phillip Class.
(1)	Ord. Adv. Committee on GM-Gen'l. Radio Co., Cambridge-Att: Dr. H.B.Richmond.
(2)	SINM-Gen'l. Textile Mills-Att: Mr. L.P. Freider.
(5)	BAR-Glenn L. Martin Co., Att: Mr. Goddard; Mr. Vorhees, Mr. Routh; Mr. Ebel.
(1)	Glenn L. Martin Co., Att: Mr. Bergen.
(2)	BAR-Goodyear Aircraft Corp-Att: Dr. Carl Arnstein.
(1)	Goodyear Aircraft Corp-Att: Mr. A.J. Peterson.
(2)	BAR-Grumman Aircraft, Bethpage, L.I., N.Y., Att: Mr. Wm. T. Schwendler.
(2)	SINM-Harshaw Chemical Co., Att: Dr. H. O. Kremers.
(2)	BAR, El Segundo, Cal. for Hughes Aircraft Corp, Att: Mr. R. E. Hopper.
(1)	Hughes Aircraft Corp., Att: Mr. D. H. Evans.
(3)	O-in-C, Cal Tech-Jet Propulsion Lab (2 copies).
(2)	BAR-Kaiser Fleetwings, Inc. Att: Mr. Carl Deganahl.
(2)	INM-Kellex Corp.
(2)	INM-M.W.Kellogg.
(1)	M. W. Kellogg, Att: Dr. Messerly.
(3)	INM-Kodak, Att: Dr. B. H. Carroll; Dr. Herbert Trotter.
(2)	BAR-Lockheed Aircraft Corp.
(2)	BAR-McDonnel Aircraft Corp., Att: Mr. H.A.Steel.
(1)	McDonnell Aircraft Corp., Att: Mr. G. V. Covington.
(4)	BAR-North Amer. Avia., Att: Dr. Wm. Bollay; Mr. R.H.Rice Mr. D. H. Mason.
(1)	Northrop Aircraft, Inc.
(1)	Radio Corp., Att: Mr. A. W. Vance.

DISTRIBUTION (Cont'd)

No. of copies	
(5)	INM-Raytheon-Att: Dr. Edelfsen; Mr. H.T.Ashworth; Mr. H. Grant; Mr. R. C. Saunders.
(2)	BARR-Reaction Motors-Att: Mr. Nesbitt.
(1)	Republic Avia. Corp., Att: Dr. Wm. O'Donnell.
(1)	Ryan Aero. Co., Att: Mr. B.T.Salmon.
(2)	INM, Baltimore for S.W. Marshall Co., Washington, D.C.
(2)	INM-Sperry Gyroscope Co., Great Neck, L.I., N.Y.
(1)	Sperry Gyroscope Co., Garden City, N.Y. Att: Mr. G.E.White.
(3)	BAR-United Aircraft Corp., Att: Mr. John G. Lee; Mr. F.W. Caldwell.
(2)	BAR, Downey, Cal. for Willys-Overland Motors, Inc., Att: Mr. Joe Talley.
(2)	BAR-Wright Aero. Corp., Woodridge, N.J.
(4)	CNO-OP-32-for distribution to BAM(2 copies) BSCO(2 copies).

o.

TITLE: Upper Atmosphere Research Report II

ATI- 4267

REVISION (None)

ORIG. AGENCY NO. Rpt R-3030

PUBLISHING AGENCY NO. (Same)

AUTHOR(S) : Newell, H. E. Jr.; Siry, J. W.
ORIG. AGENCY : Office of Naval Research, Naval Research Laboratory, Washington, D. C.
PUBLISHED BY : (Same)

DATE	DOC. CLASS.	COUNTRY	LANGUAGE	PAGES	ILLUSTRATIONS
Dec' 46	Unclass.	U.S.	English	165	photos, tables, diagrs, graphs

ABSTRACT:

Research in connection with V-2 firings. Telemetering system improvements and location of experimental equipment in missile. Instrument ejection and recovery. Results obtained in solar spectroscopy and pressure-temperature studies. Cosmic ray auxiliary electronics and recorder described. Biological experiments discussed. Pertinent theoretical discussions and outline for future research.

DISTRIBUTION: Copies of this report obtainable from CADO

DIVISION: Meteorology (30)
SECTION: Upper Air Research (3)

SUBJECT HEADINGS: Atmosphere, Upper - Research (12398); Missiles, Guided - Test vehicle use (83829.3)

ATI SHEET NO.: R-30-3-12

Central Air Documents Office
Wright-Patterson Air Force Base, Dayton, Ohio

AIR TECHNICAL INDEX

Recd 10/27/2000

Naval Research Laboratory
Technical Library
Research Reports Section

DATE: October 10, 2000

FROM: Mary Templeman, Code 5227

TO: **Code 7600 Dr Gursky**

CC: Tina Smallwood, Code 1221.1

SUBJ: Review of NRL Reports

Dear Sir/Madam:

1. Please review NRL Reports R-3030, R-3031, R-3120, R-3139, and R-3358 for:

- ☑ Possible Distribution Statement
- ☐ Possible Change in Classification

Thank you,

Mary Templeman

Mary Templeman
(202)767-3425
maryt@library.nrl.navy.mil

The subject report can be:

- ☒ Changed to Distribution A (Unlimited)
- ☐ Changed to Classification _____
- ☐ Other:

Signature 10 Oct 2000 Date